HIV-1 Engages a Dynein-Dynactin-BICD2 Complex for Infection and Transport to the Nucleus

By

Stephanie K. Carnes

Dissertation

Submitted to the Faculty of the

Graduate School of Vanderbilt University in

partial fulfillment of the requirements for the

degree of

DOCTOR OF PHILOSOPHY

in

Microbiology and Immunology

May 10, 2019

Nashville, Tennessee

Approved:

Borden Lacy, Ph.D.

Christopher Aiken, Ph.D.

Lauren Jackson, Ph.D.

Matthew Tyska, Ph.D.

To Mom and Dad, thank you for your support, prayers, and constant encouragement. To my husband, Stephen, thank you for helping me chase my dreams and loving me unconditionally. Thank you for holding down the fort when life gets tough, spending far too much time in lab with me, and reminding me of my capabilities and passion for science. To baby Parker, thank you for the giggles, smiles, and showing us what life is truly about.

ACKNOWLEDGEMENTS

This PhD would not have been possible without the dedication and support of my friends, family, and colleagues. I would like to thank my advisor, Chris Aiken, for his mentorship, guidance, and encouragement throughout this process. You challenged me to think critically and work hard. You provided the resources and time to train me into an independent researcher and cared for my success not only in the lab, but in life. My committee members also provided invaluable insight and training for my project and in my career, and I am grateful for the time you each dedicated. I also thank the professors in the PMI department and the IGP for their didactic training. And to the PMI staff, thank you for always making the "details" run smoothly- be it room reservations, paperwork, or getting lab equipment fixed.

I couldn't have asked for a better lab environment to spend my time in. My current and past lab mates have made work enjoyable and I have loved getting to know each and every one of you. Thank you especially for all the training, celebrating the victories with me, and consoling me during the inevitable defeats. And to the Aiken Lab breakroom couch- you may have been gross, but you served us well. Many a pregnant nap will be remembered on your frayed fabric.

To the Indiana University friends that stuck with me, and the new Vanderbilt friends I made here, thank you for always supporting me and reminding me of my worth. Thank you for reminding me there is more to life than work, and that the journey is more fun with people you care about beside you. And to my Central Christian family, thank you for your prayers and encouragement along the way. Stumbling across your church wasn't an accident. And finally, and most importantly, my Lord for giving me the skills, strength, and community to succeed. With God, all things are possible. Matthew 19:26

TABLE OF CONTENTS

Page

LIST OF TABLES

LIST OF FIGURES

LIST OF ABBREVIATIONS

AIDS	Acquired Immune Deficiency Syndrome
ART	Antiretroviral Therapies
ATP	Adenosine Triphosphate
BICD2	Bicaudal D 2
BME	2-Mercaptoethanol
BSA	Bovine serum albumin
CA	capsid protein, p24
CBV	Ciliobrevin D
CCR5	CC chemokine receptor 5
CD4+	Protein marker on surface of HIV-1 target cells
CsA	Cyclosporin A
CTD	Carboxy-terminal end
CypA	Cyclophilin A
CXCR4	CX chemokine receptor 4
DMEM	Dulbecco's modified Eagle's medium
DMSO	Dimethyl sulfoxide
dNTP	Deoxynucleotide
DNA	Deoxyribonucleic acid
EFV	Efavirenz
ELISA	Enzyme-linked immunosorbent assay
EM	Electron microscopy
Env	envelope glycoprotein
Gag	group specific antigen

GFP	Green fluorescent protein
gp120	Envelope glycoprotein
HIV-1	Human Immunodeficiency Virus type 1
IN	integrase
Kb	kilobases
LTR	long terminal repeat
MA	matrix protein, p17
MAP	Microtubule Associated Protein
MLV	Murine leukemia virus
MT	microtubule
MTOC	microtubule organizing center
NaCl	Sodium chloride
NC	nucleocapsid protein, p7
Nef	Negative factor
Nup	Nucleoporin
NTD	Amino-terminal end
PAGE	polyacrylamide gel electroporesis
PBS	phosphate-buffered saline
PCR	polymerase chain reaction
PIC	pre-integration complex
qPCR	Quantitative PCR
RNA	Ribonucleic acid
RT	reverse transcriptase
RTC	reverse transcription complex
SDS	sodium dodecyl sulfate
Tat	HIV transactivator of transcription

TRIM	Tripartite motif
TRIMCypA	Tripartite motif fused with cyclophilin A
Vif	Viral infectivity factor
VSV	Vesicular stomatitis virus
VSV-G	Vesicular Stomatitis V glycoprotein

CHAPTER I

BACKGROUND AND RESEARCH OBJECTIVES

Viruses can be thought of as one of both the simplest and most complex entities in nature. At their most basic level, viruses contain a genome and a surrounding protein shell. This simplicity also leads to their complexity- because they contain so few components, viruses depend heavily on the cell for their own replication, leading to an intricate network of usurped pathways in the cell. Viruses are obligate parasites, meaning they cannot reproduce without utilizing the host machinery. Understanding the ways in which viruses hijack these cellular systems can lead to opportunities to target and thwart viral infection through therapeutic design. In this dissertation, I describe my investigations into the ability of Human Immunodeficiency Virus type 1 (HIV-1) to commandeer one such cellular system, active dynein transport along microtubules, for its infection.

A global health crisis

HIV-1 is a virus that attacks the host immune system, eventually leading to Acquired Immune Deficiency Syndrome (AIDS) and opportunistic infections [14-17]. While antiretroviral therapies (ART) have greatly improved longevity and quality of life for many patients, no practical cure currently exists. According to UNAIDS, in 2018, 36.9 million people worldwide were living with HIV/AIDS, with 5,000 new infections occurring daily [18]. This health burden emphasizes the need for an in-depth understanding of this virus and for new therapeutics.

Transmission of HIV-1 occurs through sexual, perinatal, and percutaneous routes. After

traversing the epithelial layer, the virus encounters dendritic cells, is phagocytosed, and is brought to the peripheral lymph nodes. The dendritic cells then encounter CD4+ T cells and release the captured HIV-1 particles while promoting the activation of T cells. The transmitted virus can continue replicating in the CD4+ T cell population, leading to eventual T cell death and immune suppression [19].

There are three stages of an HIV infection: acute infection, clinical latency, and AIDS (Figure 1-1)[7]. Acute infection corresponds to the first 2-4 weeks of infection, with many people developing a flu-like illness characterized by fever, swollen glands, sore throat, muscle aches, and headache [20]. During acute infection, viral replication is high, leading to high viral titers in the body, and causing the CD4 population of cells to decrease rapidly. Over time, the immune system can bring the viral titer back down to a "viral set point" which is maintained. CD4 T cells begin to rebound at this point, but the population may not fully recover. Although the immune response can reduce viral levels, HIV-1 infection cannot be entirely cleared by the immune system [20]. Therefore, HIV-1 infection is lifelong.

After acute infection, the disease progresses to the "clinical latency" stage in which a person is still infected but may not be showing symptoms. Viral replication is still occurring at low levels. This stage can be maintained for an average of 10 years without ART treatment. With ART treatment, some patients never progress to AIDS. AIDS occurs when the population of CD4 cells falls below 200 cells/mm^3 of blood or when an opportunistic illness has developed. Symptoms of AIDS may include prolonged fevers, sweats, swollen lymph nodes, weakness, weight loss, and diarrhea. The development of AIDS is often associated with pneumocystis pneumonia, cachexia (HIV wasting syndrome), esophageal candidiasis, and recurrent respiratory tract infections. People with AIDS are also more susceptible to certain cancers, including

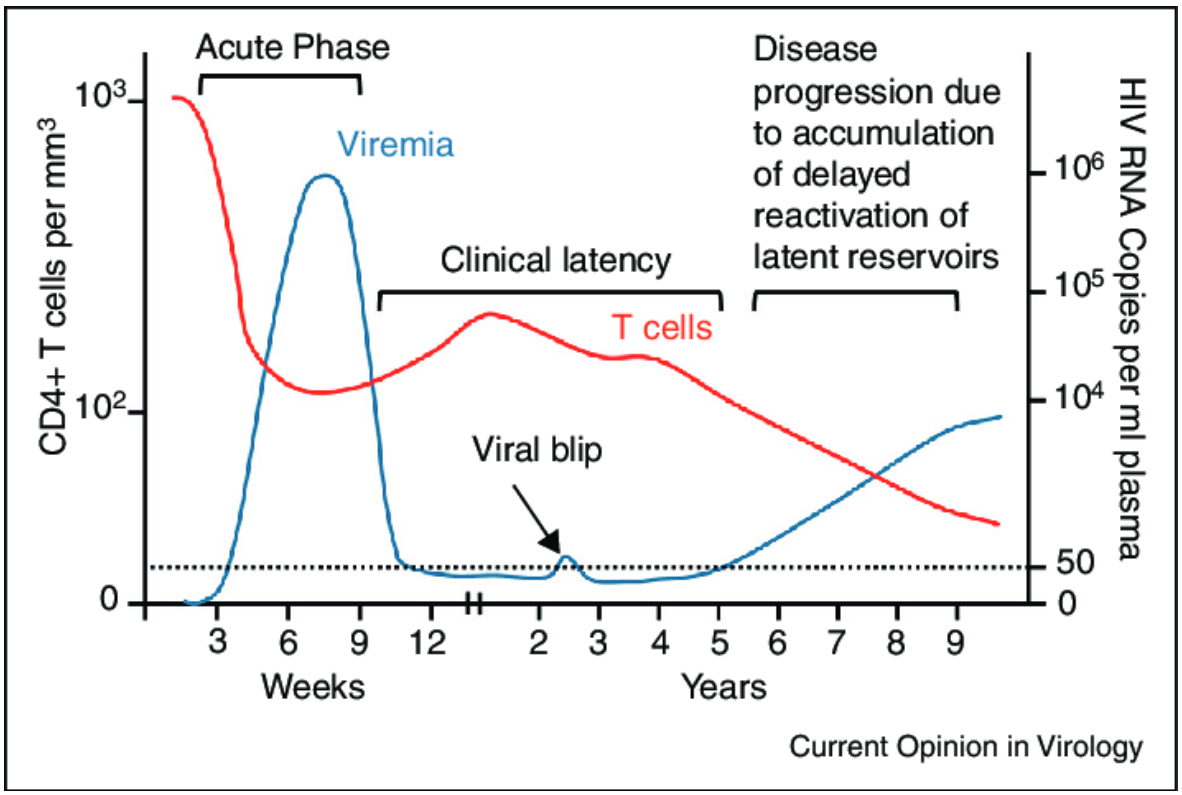

Figure 1-1. Disease progression during HIV infection. In the acute phase, the viral load is high and CD4 T cell counts begin to decrease. During the clinical latency phase, a "set point" is reached where viral levels are low and T cell populations begin to recover. Eventually, disease progression continues to AIDS, which can result in death if left untreated. Reprinted from Selinger *et. al. Curr Op. Vir.* (2013) [7]

Kaposi's sarcoma, Burkitt's lymphoma, and cervical cancer. Life expectancy without treatment is typically 1-3 years. With effective ART treatment, however, progression to AIDS can be prevented [20].

HIV-1 structure and life cycle

HIV-1 has unique structural and life cycle features that set it apart from other viruses. Structurally, HIV-1 is enveloped by a viral lipid membrane and has an interior capsid shell containing the genetic material and associated proteins (Figure 1-2). The envelope protein (Env) is transcribed as a polyprotein and is processed into gp41 and gp120 which form trimers protruding through the lipid membrane. The polyprotein Gag is processed into the structural proteins matrix (MA), capsid (CA), nucleocapsid (NC), and p6 [21]. MA associates with the plasma membrane and targets viral proteins and RNA to the site of assembly for incorporation into the budding virion. After budding, maturation by proteolytic cleavage enables CA to form a fullerene cone shape called the capsid, unique to lentiviruses. There are about 1500 molecules of CA in the capsid which align into repeating hexamer subunits. To generate the distinctive curvature of the cone, 12 pentamers are present in specific locations at the ends of the cone [22-26].

Within the capsid, two positive-sense single-stranded copies of viral RNA are present. Also present are the proteins reverse transcriptase and integrase, which are important for viral replication. HIV-1, other members of the *Retroviridae* family, and the *Hepadnaviridae* family are unique among viruses due to their dogma-breaking replication strategy. Retroviruses utilize the enzyme reverse transcriptase to transcribe their single-stranded RNA genome into DNA readable by host cellular machinery. This DNA can then be integrated into the host genome

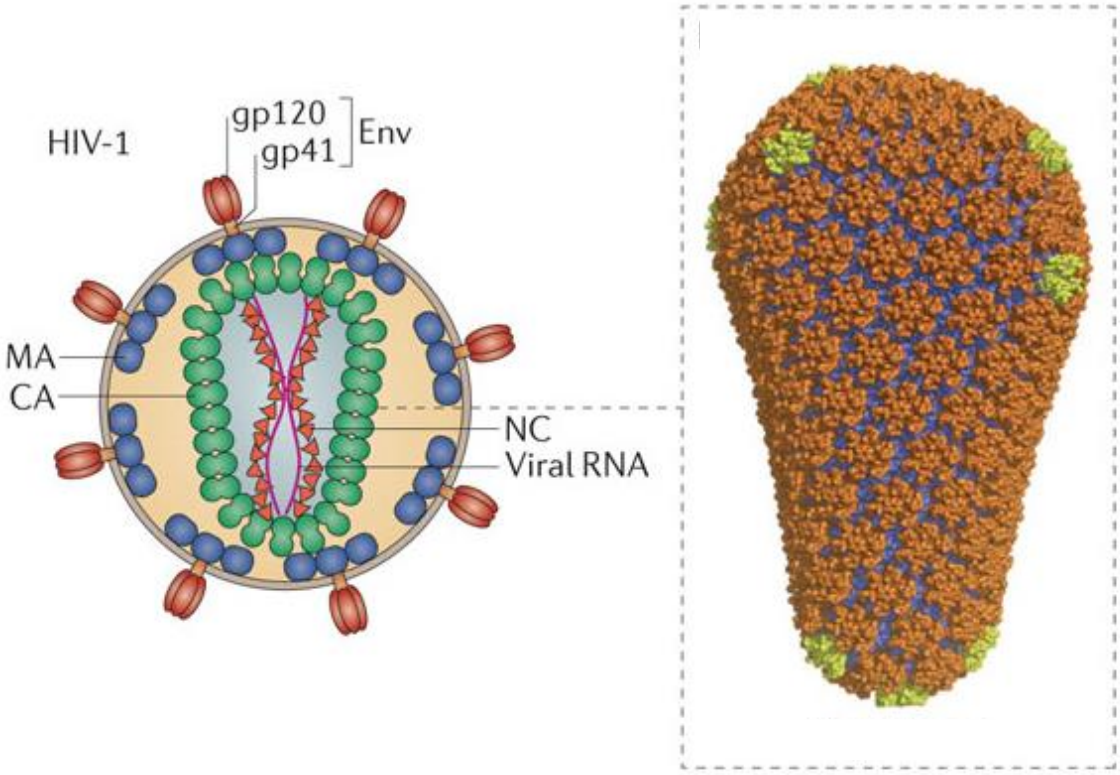

Figure 1-2. Schematic representation of the HIV-1 virion. The virion is composed of a viral envelope (Env) surrounding structural proteins MA, CA, and NC. The CA protein assembles into a repeating hexameric lattice with interspersed pentamers to give a fullerene conical shape. Within the cone are two single-stranded RNA copies of viral genome, reverse transcriptase, integrase, and other RNA-associated proteins. Adapted from Pornillos *et. al.*, *Nature* (2011) and Campbell and Hope *Nat. Rev. Micro.* (2015) [4, 5]

through the actions of integrase. After integration, viral replication can actively occur, or viral latency, in which replication occurs at a low steady-state level. HIV-1 also encodes additional accessory proteins: vif, vpr, vpu, and nef. These proteins aid in infection through various mechanisms, either directly, or through effects on host cell machinery or immunity [27-29].

The HIV-1 life cycle can be separated into early events: those happening before integration, and late events: those happening post-integration (Figure 1-3). HIV-1 infection begins at the plasma membrane, where the Env glycoprotein binds to the CD4 receptor and the chemokine co-receptor CCR5 or CXCR4, resulting in a rearrangement of the Env trimers and fusion of the viral and cellular membranes [30-32]. Fusion releases the viral core into the cytoplasm of the cell, at which point necessary early events can be completed.

Reverse transcription is the process by which the viral RNA is converted to double-stranded DNA. Reverse transcription begins soon after cell entry and the resulting complex is referred to as the reverse transcription complex (RTC) [33]. The process of uncoating occurs concurrently with reverse transcription. Uncoating is the disassembly of the viral capsid. Uncoating occurs in a two-step process, with an initial disassembly occurring rapidly (~30 min) after fusion, and a slower, secondary break-down occurring during transit to the nucleus [34, 35]. After reverse transcription completion and uncoating begins to occur, the particle is termed the preintegration complex (PIC). Some CA stays associated with the PIC at least until nuclear entry [35].

A unique aspect of HIV-1 and other lentiviruses is their ability to infect non-dividing cells. Non-mitotic cells have an intact nuclear envelope so transport into the nucleus must occur through nuclear pores. Lentiviruses are too large to passively go through nuclear pores. Due to

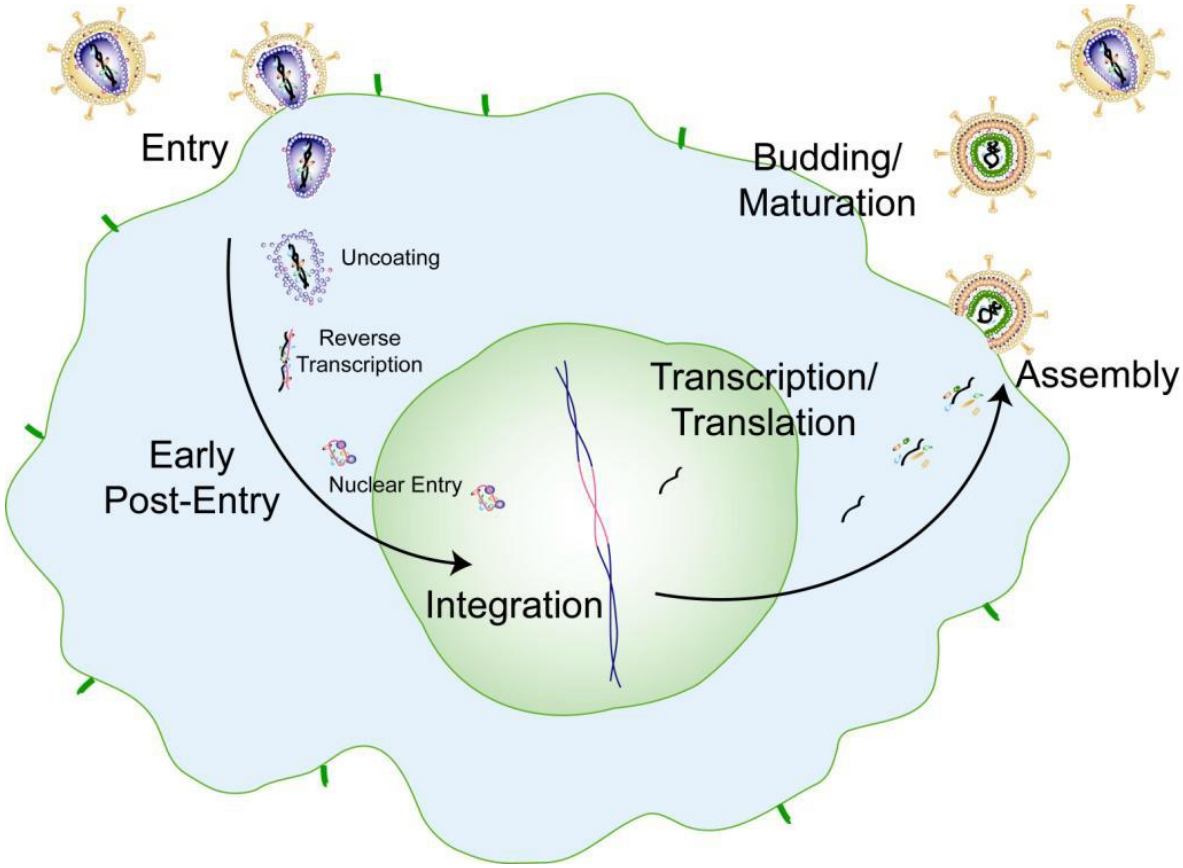

Figure 1-3. The HIV-1 life cycle. HIV binds to the cell membrane through interactions with CD4, and CCR5 or CXCR4. After fusion, the core undergoes uncoating concurrently with reverse transcription. Nuclear import can then occur, followed by integration into the host genome. Newly transcribed proteins and polyproteins aggregate at assembly sites on the plasma membrane and bud from the producer cell, resulting in immature virions. Maturation of the virus occurs after the viral protease cleaves gag and the HIV-1 core assembles. Drawing prepared by David Dismuke.

this, HIV-1 utilizes the nuclear pore complex for entry into the nucleus. Integrase and host DNA repair proteins then direct the integration of the newly formed viral DNA into the host genome for replication [36].

The late events of the HIV-1 life cycle are centered around new particle production. As replication occurs, the viral proteins Tat, Rev, and Nef are expressed first from the integrated DNA and aid in transcription, nuclear export of the HIV-1 transcripts, and downregulation of immune response, respectively. After the Env protein is produced, it is post-translationally modified and proteolytically processed into gp41 and gp120. During assembly, Gag associates with the plasma membrane at specialized microdomains and directs the clustering of Env there [37]. The NC subunit of Gag interacts with the RNA transcripts, ensuring they are recruited into the forming particle. Once a critical concentration of Gag is reached, the proteins form a spherical structure, and budding from the host membrane can occur. After budding, the viral protease cleaves Gag in a process known as maturation, and the HIV-1 capsid can assemble around the genome in its mature, fullerene structure [37].

The microtubule network and active transport

Viruses, including HIV-1, are adept at hijacking microtubules (MTs) for their intracellular transport. The MT network is the dynamic and complex arrangement of microtubules within a cell. MTs are part of the cell cytoskeleton, which gives the cell structure, shape, and in some cell types, polarity. MTs are made up of repeating alpha and beta tubulin heterodimers, which nucleate from gamma tubulin at centrosomes. Since MTs emanate from centrosomes near the nucleus, this area is often called the MT Organizing Center (MTOC). Due to the repeating heterodimer structure of microtubules, they are polarized, with the negative end

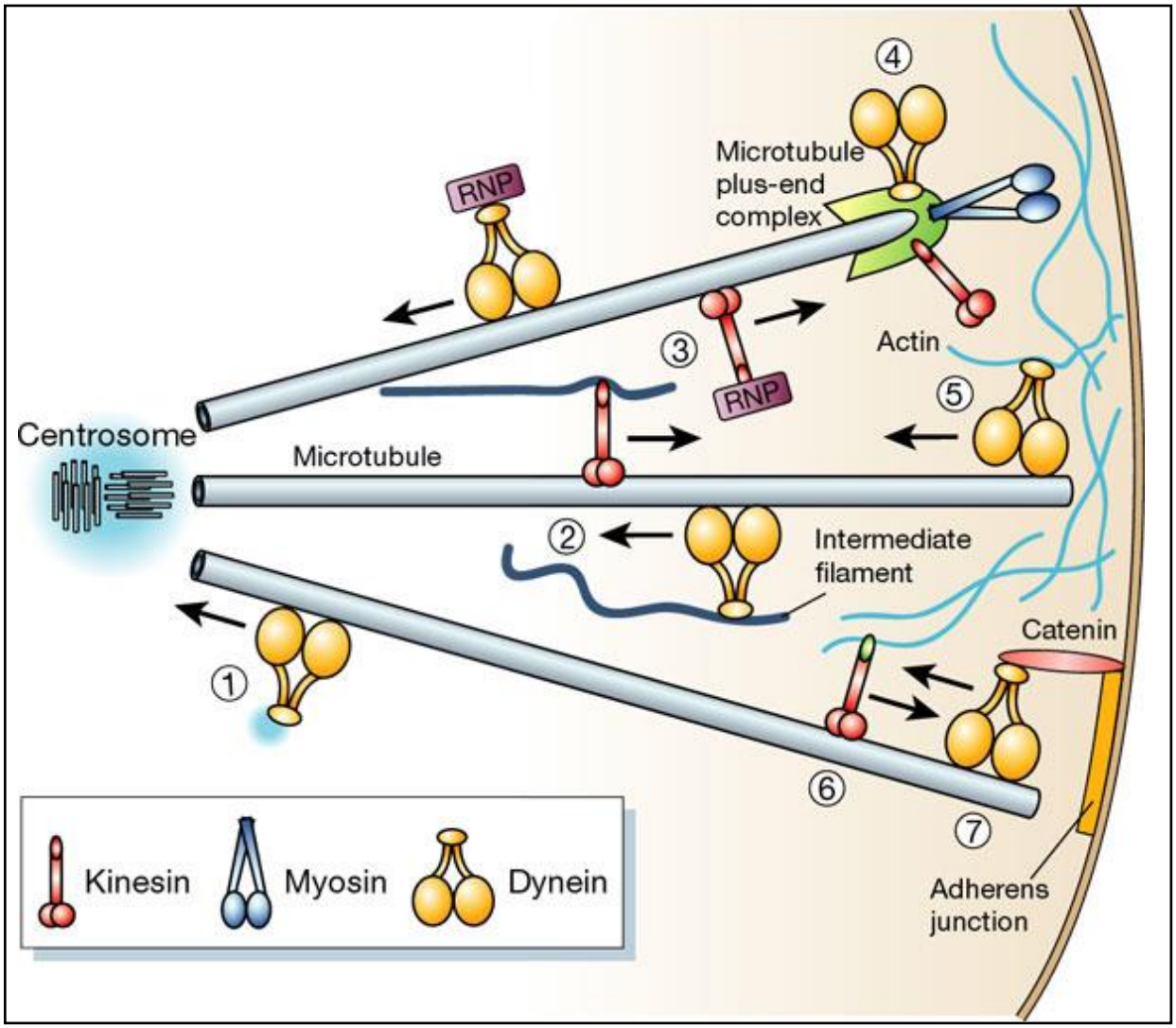

Figure 1-4. The microtubule network and motors. Motor proteins have many transport-related roles within the cell. Some examples are depicted. 1. Retrograde transport of centrosomal components. 2. Anterograde and retrograde transport of intermediate filaments. 3. Anterograde and retrograde transport of ribonucleoprotein complexes. 4. Myosin, kinesin, and dynein interactions with the microtubule plus-end complex. 5. Anchorage of dynein at the actin-rich cell cortex. 6. Interaction of a kinesin-like protein with actin. 7. Caterin-mediated anchorage of dynein at adherens junctions. Reprinted from Schliwa and Woehlke *Nat. Insight. Rev.* (2003)[8]

located at the MTOC, and the positive end extending outward [38]. In a nonpolarized interphase cell, this MT polarity results in the positive end of MTs extending toward the cell periphery (Figure 1-4). The polarity of these tracks is important for cargo transport and the directionality of microtubule-associated proteins (MAPs), as discussed below.

Although most MTs nucleate from centrosomes, MTs can emanate from kinetochores, the Golgi apparatus, the nuclear envelope, and other MTs, increasing the complexity of the overall network [39]. Adding to the complexity, MTs exhibit a phenomenon called dynamic instability, in which they undergo a series of growth and shrinkage events at their plus ends. Dynamic instability is influenced by microtubule-associated proteins (MAPs) and is marked by post-translational modifications [40, 41]. The adaptable structure of the microtubule network allows it to form the mitotic spindle, which is crucial for the search, capture, and separation of chromosomes during mitosis. The fine-tuned regulation of MT stability also influences cargo transport during interphase, as MT stabilization or depolymerization by drugs can both alter transport by molecular motor proteins [42, 43].

Intracellular cargo transport requires the actions of a subset of MAPs which contain motor function. Two types of motor complexes, dynein and kinesins, hydrolyze ATP to move along microtubules and transport cellular cargo, including vesicles, organelles, RNA, etc. In general, kinesins walk toward the positive end of microtubules (anterograde movement) to transport cargo, and dynein walks toward the negative end of microtubules (retrograde movement) [44, 45]. In non-dividing cells, cargo gets transported toward the nucleus predominantly by dynein and away from the nucleus by kinesins. Nonetheless, owing to the dynamics and branching of the microtubule network, both types of motors can be involved in the transport of a specific cargo.

Dynein, a large protein complex, transports vesicles and endosomes within the cytoplasm,

and it helps position organelles and the mitotic spindle during cell division [reviewed in [44, 46-48]]. In contrast to the single dynein complex, there are 15 different kinesin families, termed kinesin 1 to kinesin 14B, based on phylogenetic analyses. Kinesins are variable in form and function, but can bind vesicles, organelles, and other microtubules and function in microtubule plus end and minus end-directed transport [45].

Molecular motors must transport a variety of protein cargos to various destinations within the cell, raising the question of how specificity is achieved. Dynein and kinesins interact with numerous cargo-specific adaptor proteins, which connect the molecular motors to the various cargoes [49-51]. Adaptors can also activate the motors to move along microtubules: recent studies have confirmed this function for BICD2, Hook3, Spindly, and Rab11-FIP3 [52]. Many adaptors can perform cellular functions other than cargo transport, including nuclear and spindle positioning during mitosis. Kinesin and dynein motors can simultaneously bind to a single microtubule, and there is evidence for simultaneous binding of motors to a single cargo molecule, suggesting that the net transport of a particular cargo relies on coordination of its movement by opposing motors. Thus, regulation of transport appears to depend on regulation of motor activity by adaptors [53-55].

Viral usurpation of the microtubule network

In addition to transporting cellular cargoes, kinesin-1 and dynein inadvertently transport viruses for infection. Regardless of whether they replicate in the cytoplasm or nucleus, many viruses utilize the MT network and active transport to move to appropriate locations within the cell for replication [56]. Viruses can also use microtubule transport to localize virion components at the plasma membrane for assembly of viral progeny. For this bidirectional

transport, dynein and kinesin-1 both play roles in many cases [57].

Dynein is utilized by several viruses for transport towards the MTOC, including herpes simplex virus [58, 59], HIV-1 [60], circovirus [61], adenovirus [62-64], Zika virus [65], influenza A virus [66], and others. Interestingly, viruses use a variety of mechanisms to engage dynein. For example, adenovirus hexon capsid subunit interacts directly with dynein intermediate and light intermediate chains for transport [62] whereas herpes simplex virus utilizes both capsid and an internal tegument protein for binding to the dynein intermediate and light chains [59, 67-69]. Ecotropic Murine Leukemia Virus, by contrast, utilizes the dynein adaptor NudEL for infection [70]

In addition to transport after initial cell entry, dynein also plays a role in transport of some nascent virions. Following their exit from the nucleus, herpes simplex virus recruits both kinesin-1 and dynein to its capsid for transport to the site of envelopment, and then to the plasma membrane. The mechanism of dynein involvement in this process has not been fully elucidated, but dynein promotes both transport and envelopment [57].

Kinesin-1 also contributes to the transport of several viruses [57, 71]. Not surprisingly, kinesin-1 plays a major role in the transport of viral components for egress and assembly of nascent particles. For example, vaccinia virus utilizes kinesin-1 to transport its intracellular enveloped virus to the plasma membrane. Intracellular enveloped viruses are formed when mature virions become wrapped by a double membrane cisternae in the trans-golgi or from endosomal membranes [72, 73].

Interestingly, kinesin-1 may also play a role in early transport of virions after cell entry. For HIV-1, the bidirectional motility of dynein and kinesin-1 is important for overall retrograde transport to the nucleus. When kinesin-1 is knocked down, movement to the nucleus is impaired.

The kinesin-1 adaptor FEZ1 acts to bridge the HIV-1 capsid to the dynein complex for transport [51]. Other viruses, including vaccinia virus [74], and alpha herpesviruses on axons [75], have also been observed to move bidirectionally, suggesting that this phenomenon may be a conserved mechanism for viral transport.

Research objectives

HIV-1 depends on a series of events to productively infect cells and replicate. The microtubule network and its associated proteins are involved in several of the early steps in HIV-1 infection, including entry [76], reverse transcription [77-79], uncoating [78, 80-82], and transport to the nucleus [51, 60, 80, 82-85]. HIV-1 egress and assembly also utilize the microtubule network to efficiently assemble particles for budding and spread (reviewed in [86]). It was established over a decade ago that the microtubule network is involved in HIV-1 infection, but the specific transport machinery and mechanisms involved in the early stage of infection are not well understood. The ability of dynein to have specificity for different cargos in the cell led me to the hypothesis that HIV-1 would be utilizing a specific adaptor or subset of adaptors for transport.

I sought to identify the components of the dynein complex that are important for HIV-1 infection. I utilized an siRNA-based screen to determine which proteins in the dynein and dynactin complex are important. I also sought to identify the specific adaptor that HIV-1 utilizes for transport and infection. I identified a specific adaptor, BICD2, utilized by HIV-1 for transport by the dynein complex. Furthermore, I determined the mechanism of BICD2 as an adaptor for HIV-1 infection, specifically determining its role in transport, and bridging HIV-1 with the dynein complex. My work has established an understanding of the mechanism through

which HIV-1 is able to usurp the dynein transport pathway for its own infection.

CHAPTER II

THE DYNEIN-DYNACTIN-BICD2 COMPLEX IS IMPORTANT FOR HIV-1 INFECTION

A portion of this work was published in: Carnes SK, Zhou J, Aiken C. HIV-1 Engages a Dynein-Dynactin-BICD2 Complex for Infection and Transport to the Nucleus. 2018. *Journal of Virology*. 92 (20) e00358-18.

Introduction

Following cell penetration, HIV-1 must traverse the cytoplasm from the cell periphery to reach the nucleus. The process by which the virus is transported to the nucleus has not been thoroughly investigated. Genome-wide siRNA screens have revealed microtubule-associated proteins as necessary for HIV-1 infection [85, 87-89]. Recent studies suggest that the cellular transport of HIV-1 depends on the microtubule network and on the molecular motor proteins dynein and kinesin [51, 83, 84, 90, 91].

Dynein is a microtubule motor complex that utilizes ATP to walk along microtubules and move cargo toward the negative end of microtubules, toward the cell nucleus. Dynein functions in vesicle and endosomal transport and helps position organelles and the mitotic spindle during cell division [reviewed in [44, 46-48]]. The dynein complex consists of two copies of the heavy chain (DYNC1H1 cytoplasmic and DYNC2H1 flagella), which contains the ATPase activity required for movement; two intermediate chains (DYNC1I1, DYNC1I2) and two light-intermediate chains (DYNC1LI1, DYNC1LI2) that stabilize the structure of the complex (Figure 2-1, Table 2-1)[10]. The complex also contains multiple copies of various light chains (DYNLT1, DYNLT3, DYNLRB1, DYNLRB2, DYNLL1/2) that link dynein to other proteins and to cargo. Previous studies have indicated that dynein light chain 2 in yeast may be involved in HIV-1 integrase

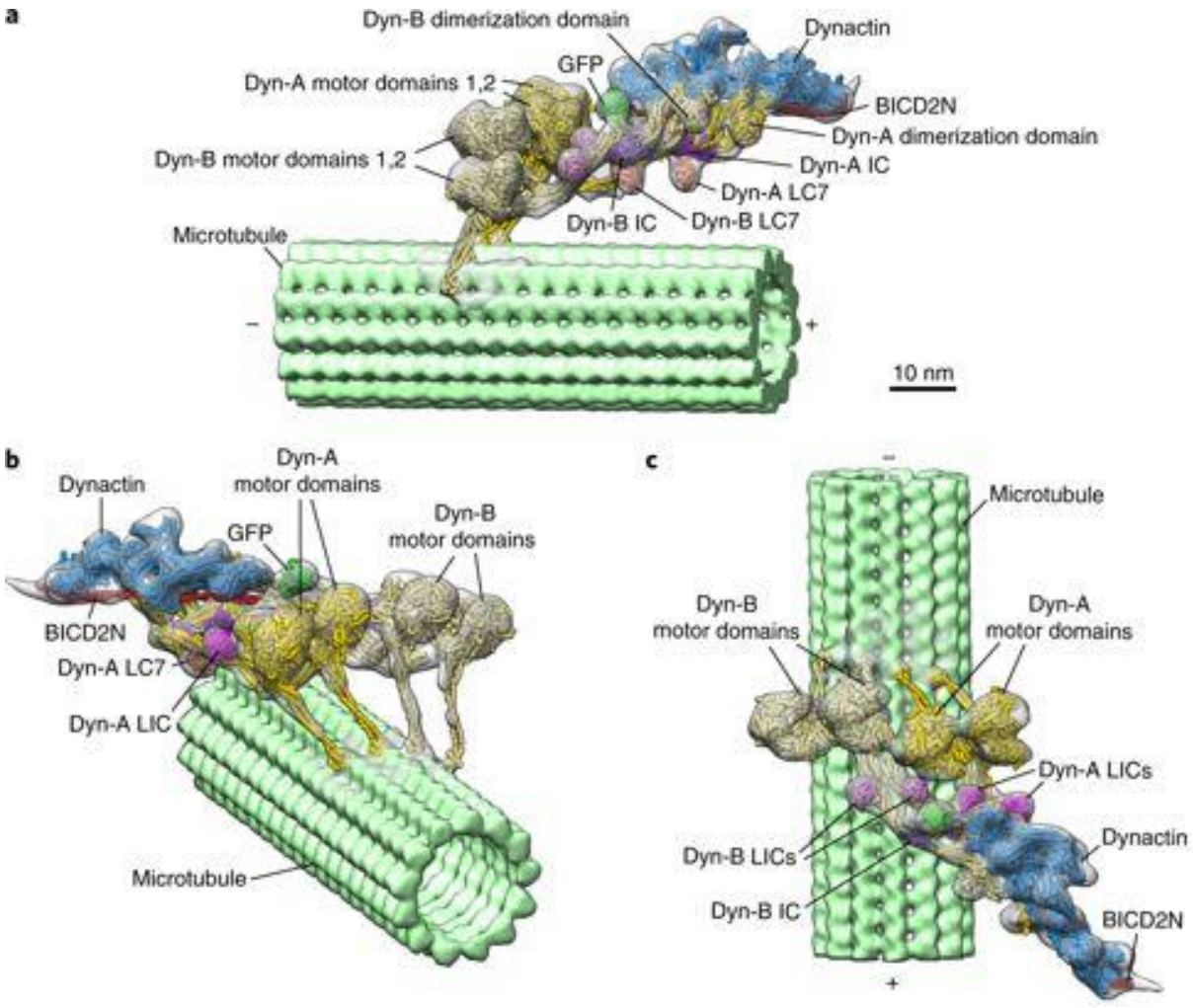

Figure 2-1. The dynein-dynactin-adaptor complex. 3D organization of the MT-bound dynein–dynactin–BICD2N complex. (A-C) Three views of the subtomogram average (gray transparent density) of the MT–DDB complex are shown, with fitted atomic models of dynein dimer-1 (Dyn-A, yellow), dynein dimer-2 (Dyn-B, light yellow), dynactin (blue), BICD2N (red), associated chains (purple, salmon, and magenta), and the BICD2N GFP tag (green) and a microtubule model (light green). Reprinted from Grotjahn *et al.* (2018) [10]

Table 2-1: Dynein and Dynactin Components in HIV-1 Infection			
Dynein and Dynactin Component	**Known Function**	**Previous HIV-1 findings**	**Expected siRNA effect**
Dynein Heavy Chain DYNC1H1 DYNC2H1	ATPase Activity Required for *in vitro* motility [93, 94]	Important for transport, uncoating, reverse transcription [81, 83, 95]	Decrease HIV infection and transport to the nucleus
Dynein Intermediate Chain DYNC1I1 DYNC1I2	Regulatory, cytoskeletal assembly [96]	None	Unknown
Dynein Light Intermediate Chain DYNC1LI1 DYNC1LI2 DYNC2LI2	Dynein recruitment to endosomes, spindle bipolarity [97-100]	Vpr interacts with DYNC1L1 [101]	Unknown
Dynein Light Chain DYNLL1 (LC8) DYNLRB1 (LC7) DYNLRB2 (LC7) DYNLT1 (TCTEX1) DYNLT3	Cargo binding, spindle assembly [102, 103]	Uncoating, reverse transcription, integrase interacts with DYNLL1 [77, 92]	Decrease uncoating, reverse transcription, infection
Dynactin Complex DCTN1 DCTN2 DCTN3 DCTN4 DCTN5 DCTN6 ACTR1A (Arp1) CapZ ACTR10	Activates dynein, increases processivity [50, 104]	Uncoating, inhibits viral production [81, 84, 95, 105]	Decrease uncoating, transport, infection

transport [92] and that DYNLL1 may interact with HIV-1 capsid and affect HIV-1 reverse transcription [77].

Dynein interacts with dynactin, another multi-subunit adaptor complex that links dynein to cargo and acts as a regulator for movement (Figure 2-1, Table 2-1). Engagement of dynactin increases dynein's processivity while walking along microtubules [104, 106-110]. The dynactin complex has at five components, including: (1) an Arp1 backbone (ACTR1A) [111, 112]; (2) a p150 side-arm (DCTN1) that aids in microtubule processivity [104, 107]; (3) a shoulder complex (DCTN2/DCTN3) that attaches the side-arm to the backbone and binds additional interacting proteins [113-115]; (4) a pointed end complex (DCTN4, DCTN5, DCTN6) that binds the nuclear envelope prior to mitosis [116]; and (5) a barbed end complex (CAPZA and CAPZB) that aids in structure stabilization [111]. The function of each of these components depends on interactions with the other components. By contrast to dynein, dynactin proteins do not function redundantly. Together, the five components interact to form the dynactin complex. Although there is compelling evidence that HIV-1 infection depends on dynein-dependent transport, the role of dynactin and of dynein adaptors in infection is not well understood.

Owing to the variety of protein cargoes that require cellular motors for movement, the cell faces the problem of cargo specificity. To solve this problem, dynein interacts with numerous cargo-specific adaptor proteins (Figure 2-1). Adaptors link cargo to the dynein complex, allowing the proper transport of cargo to the proper locations in the cell. Adaptor proteins also link dynein to dynactin [50, 117, 118], resulting in dynein activation and processive walking along microtubules. Some dynein adaptors also act in specific cellular functions through their interactions with dynein, playing roles in interphase transport and organelle and microtubule positioning before and during mitosis [119-125]. The number of known dynein adaptor proteins has expanded in recent years, with new adaptors being discovered and new functions being assigned for previously known adaptors (Table 2-2) [reviewed in [49]]. Some of the best-characterized adaptors are LIS1, NUDE, and NUDEL, which form complexes between

Table 2-2: Adaptors and MAPs in HIV-1 Infection			
Adaptor/MAP Gene	**Known Function**	**Previous HIV-1 Findings**	**Expected siRNA effect**
PAFAH1B1 (Lis1)	Nuclear and spindle positioning, organelle and mRNA transport [120, 121]	Inhibition of PP2A by Lis1 increases Tat-mediated transcription [126]	Decrease HIV-1 infection (depletion mimics dynein depletion)
NDE1 (NUDE)	Microtubule organization, dynein regulation, transport [121]	None	Unknown
NDEL1 (NUDEL)	Cytoskeletal organization, transport [120, 121]	None	Unknown
BICD1 BICD2	Activates dynein; vesicle transport, nuclear positioning, microtubule organization [119, 122, 127]	Genome-wide screen; depletion reduces infection [89]	Decrease infection
RAB6a	Linkage to vesicles; transport in both retrograde and anterograde [128, 129]	Knockdown inhibits HIV-1 replication Involved in membrane fusion by gp120/gp41 [87]	Decrease infection
KNTC1 (Rod) ZW10 ZWILCH	Chromosome segregation [123, 124]	None	Unknown
SPDL1 (Spindly)	Spindle Regulation, mitotic checkpoints [123]	None	Unknown
CLIP1 CLIP2	Recruits Lis1 to MT plus ends; recruitment of dynein; links endocytic vesicles to microtubules [130-132]	None	Unknown
SPTBN4 SPTAN1	Links plasma membrane to actin; cargo binding activation at plus ends of MTs [133, 134]	Cleaved by HIV-1 protease [135] Knockdown inhibits HIV-1 replication [87]	Unknown

Table 2-2 cont'd: Adaptors and MAPs in HIV-1 Infection			
Adaptor/MAP Gene	**Known Function**	**Previous HIV-1 Findings**	**Expected siRNA effect**
SPF27 (BCAS2, NUM1)	Receptor for dynein at plus ends of MTs [136]	None	Unknown
SEC23A/B SEC24A/B/C/D	Cargo binding in COPII coat [137, 138]	None	Unknown
RILP RAB7A RAB7B	Regulation of late endocytic traffic [128, 129]	Rab7 and RILP direct endosome-associated Gag towards to the MTOC [139]	Unknown
MAPK8IP3 (JIP3)	Links dynein to endosomes [140, 141]	None	Unknown
CCDC155 (KASH5) SUN1	Forms a transluminal linker from the nucleus to the cytoskeleton [142], associates with dynactin [143]	Gp160 physical interaction with SUN1 and Sad1 [101] Sun1 regulates HIV-1 nuclear import [144]	Unknown
RAB11FIP3	Transport vesicles, links dynein to Rab11 positive endosomes [145]	Nef alters endosomal trafficking Lck and Rac1 [146]	Unknown
HOOK1 HOOK2 HOOK3	Links dynein to early endosomes, organelles [125, 147, 148]	None	Unknown
MAP1A MAP1S MAP1B	Microtubule assembly and stability, endocytic vesicle trafficking [149]	MAP1A and MAP1S activate HIV-1 transport [85]	Decrease infection and transport
TBCB (CKAP1)	Regulates cytoskeletal dynamics, EB1 [150]	Interacts with HIV-1 cores in primary human macrophages [85]	Unknown
KPNA2	Nuclear import, transport [151]	Interactions with several HIV proteins, may assist in nuclear import of PIC [152-154]	Unknown

Table 2-2, cont'd: Adaptors and MAPs in HIV-1 Infection			
Adaptor/MAP Gene	**Known Function**	**Previous HIV-1 Findings**	**Expected siRNA effect**
TTL	Posttranslational modifications of tubulin [155]	None	Decrease HIV-1 infection and transport based on Naghavi et al.
AGTPBP1	Nuclear localization; detyrosinates MTs [156] after tyrosination occurs by TTL	None	Increase HIV-1 infection and transport based on Naghavi et al.
WIPF2 (WIRE)	Actin cytoskeleton organization [157]	Interacts with HIV-1 cores in primary human macrophages [85]	Unknown
FEZ1	Cargo transport as kinesin adaptor [158]	Depletion inhibits infection, no net movement to nucleus [51, 159, 160]	Decrease in HIV-1 infection and transport
ARF6	Vesicle transport, actin remodeling [161]	Knockdown enhances HIV-1 replication in human acute monocytic leukemia cells [162]	Increase in HIV-1 infection
PCNT	Centrosome and cytoskeleton regulation, cell cycle checkpoint[163-165]	Vpr causes accumulation of centrosome-structures in perinuclear region [166]	Unknown
LAMTOR2	Late endosomal transport [167, 168]	Knockdown inhibits HIV replication [89]	Potential decrease in infection
MAPRE1 (EB1) MAPRE2	Localizes to plus ends of MTs, regulates MT stability [169-171]	EB1-mediated MT stabilization enhances HIV-1 infection [84]	Decrease in HIV infection and transport
CLASP1 CLASP2	Regulate MT dynamics, endosomal targeting [172, 173]	None	Unknown
BLOC1S6	Interacellular vesicle transport [174]	None	Unknown
CSPP1	Spindle organization, cell cycle checkpoint [175]	Knockdown inhibits HIV-1 replication [87]	Potential decrease in infection

themselves and dynein to function in nuclear and spindle positioning, and in organelle and mRNA transport. The adaptors ROD-ZW10-Zwilch and Spindly also interact with dynein to aid in docking dynein and other dynein adaptors to the kinetochores. Bicaudal D has been shown to be important for organelle and mRNA transport.

Because HIV-1 infection depends on efficient traversal of the cytoplasm to the nucleus, I hypothesized that the virus exploits one or more specific adaptor proteins and the dynactin complex for dynein-dependent transport. I designed an siRNA-based screen to test whether components of dynein, dynactin, and known and hypothetical adaptors facilitate HIV-1 infection. I show that HIV-1 infection and nuclear import is facilitated by the dynactin backbone and shoulder complex (ACTR1A, DCTN2/DCTN3) and the dynein adaptor BICD2. I also found that Murine Leukemia Virus and Simian Immunodeficiency Virus are similarly dependent on the dynein-dynactin-BICD2 complex for infection. This comprehensive analysis of dynein transport components leads to a further understanding of the key players involved in HIV-1 transport.

Results

Dynein perturbation reduces HIV-1 infection

Previous studies have suggested that dynein plays a role in HIV-1 intracellular transit, which may be important for infection [51, 83]. To determine if dynein is important for HIV-1 infection, I utilized a small molecule dynein ATPase inhibitor ciliobrevin D (CBV) to perturb dynein-based transport in the cell [176] (Figure 2-2). TZM-bl cells were pretreated in the presence of increasing concentrations of CBV and then inoculated with HIV R9 (A), HIV-GFP (VSVG pseudotyped) (B), or HIV NL43-GFP (C). The extent of infection was analyzed by the expression of a luciferase reporter gene in the cells upon infection by HIV-1. HIV-GFP and HIV

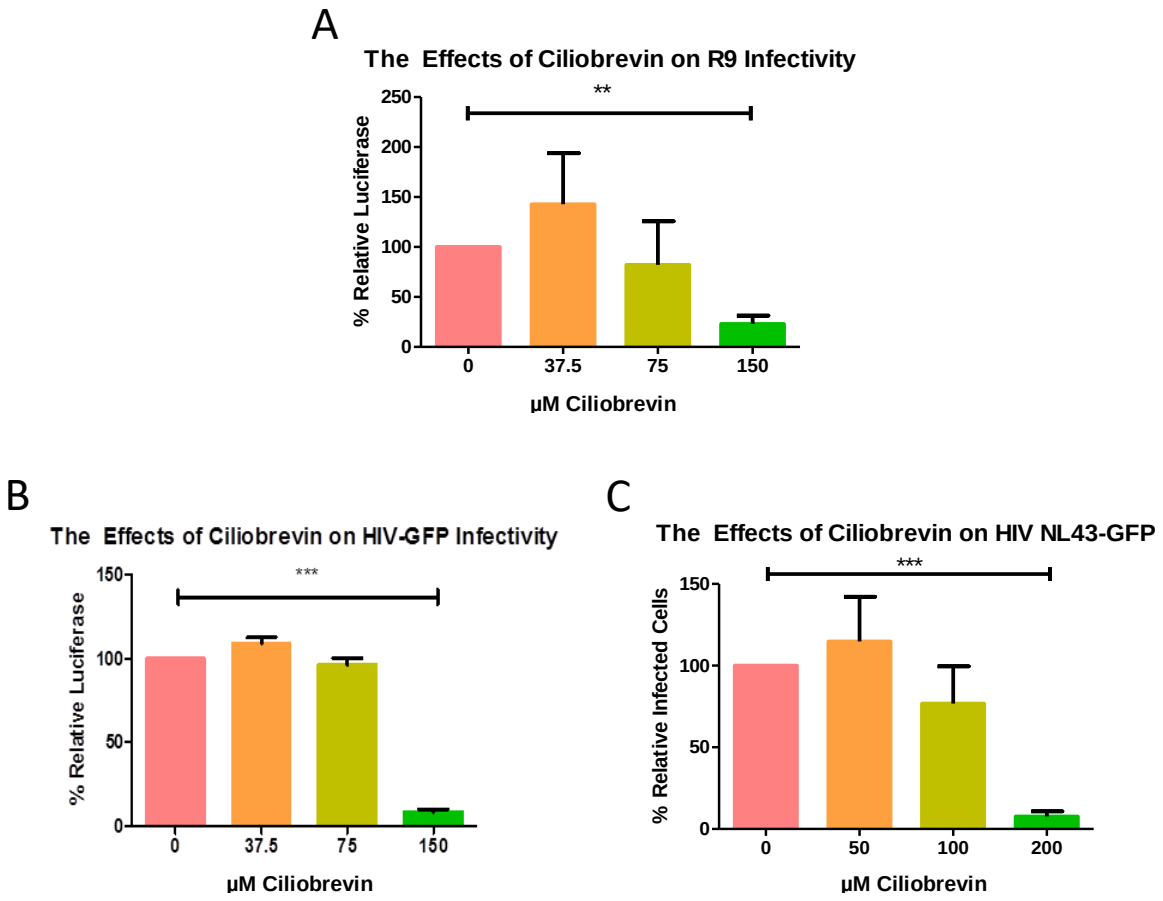

Figure 2-2. Dynein perturbation reduces HIV-1 infection. TZM-bl cells were pretreated with the dynein inhibitor Ciliobrevin D for 1 hour, then inoculated with indicated HIV strains. Infectivity after 48 hours was determined by flow cytometry or total luciferase emission. ***p<0.001, **p<0.01

NL43-GFP both encode GFP in the place of Nef, and extent of infection can be observed by fluorescence intensity within the cells. These viruses were analyzed by flow cytometry. For all viruses tested, I observed a marked decrease in infection in the presence of increasing concentrations of ciliobrevin D, suggesting that dynein is important for HIV-1 infection (Figure 2-2).

Dynein heavy chain and dynactin component depletion inhibits HIV-1 infection

The results from the ciliobrevin experiment in Figure 2-2 suggested that dynein is important for HIV-1 infection. However, this approach inhibited the dynein complex as a whole, and did not reveal the specific components of the dynein complex, or the associated dynactin complex, that are important for infection. A systematic analysis of the components of dynein and the associated dynactin complex required for HIV-1 infection had not been reported.

Therefore, to determine the contribution of dynein and dynactin to HIV-1 infection, I analyzed the effects of depleting components of the dynein and dynactin complex on cell permissiveness to HIV-1 infection. TZM-bl cells were transfected with pooled siRNAs specific to individual genes of the dynein or dynactin complex, or a nontargeting siRNA control, then inoculated with the GFP-encoding HIV-1 reporter virus NL43-GFP (Figure 2-3 and 2-4). An siRNA targeting of the HIV-1 cell receptor CD4 was used as a positive control for reduction in HIV-1 infection. Effects on expression of the targeted mRNAs were analyzed by quantitative RT-PCR (Figure 2-3B and 2-4B).

The dynein complex is composed of two heavy chains (cytoplasmic DYNC1H1 or ciliary DYNC2H1), two intermediate chains (DYNC1I1, DYNC1I2), two light intermediate chains (DYNC1LI1, DYNC1LI2), and multiple sets of light chains (DYNLT1, DYNRB1, DYNRB2,

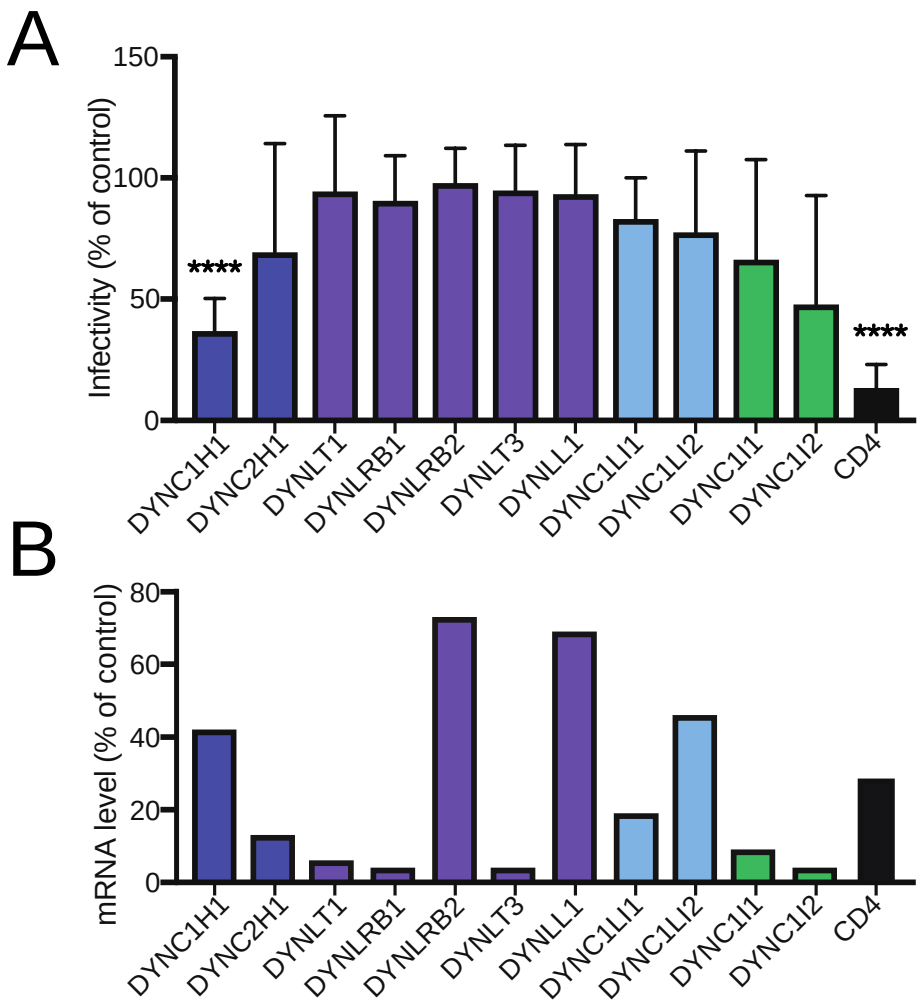

Figure 2-3. Depletion of DYNC1H1 inhibits HIV-1 infection. TZM-bl cells were pretreated with indicated pooled siRNAs and then inoculated with GFP-expressing HIV-1 (A) or harvested for knockdown efficiency by qPCR analysis (B). Infection was assessed by flow cytometry for GFP expression. The values shown represent the extent of infection relative to nontargeting siRNA treatment (A). Infection results are the means of three independent determinations. Error bars represent standard deviations. Statistical significance was calculated by a Student t test for each siRNA treatment compared to nontargeting control siRNA treatment. (**, P <0.01; ***, P <0.001; ****, P< 0.0001). mRNA analyses are from a single experiment.

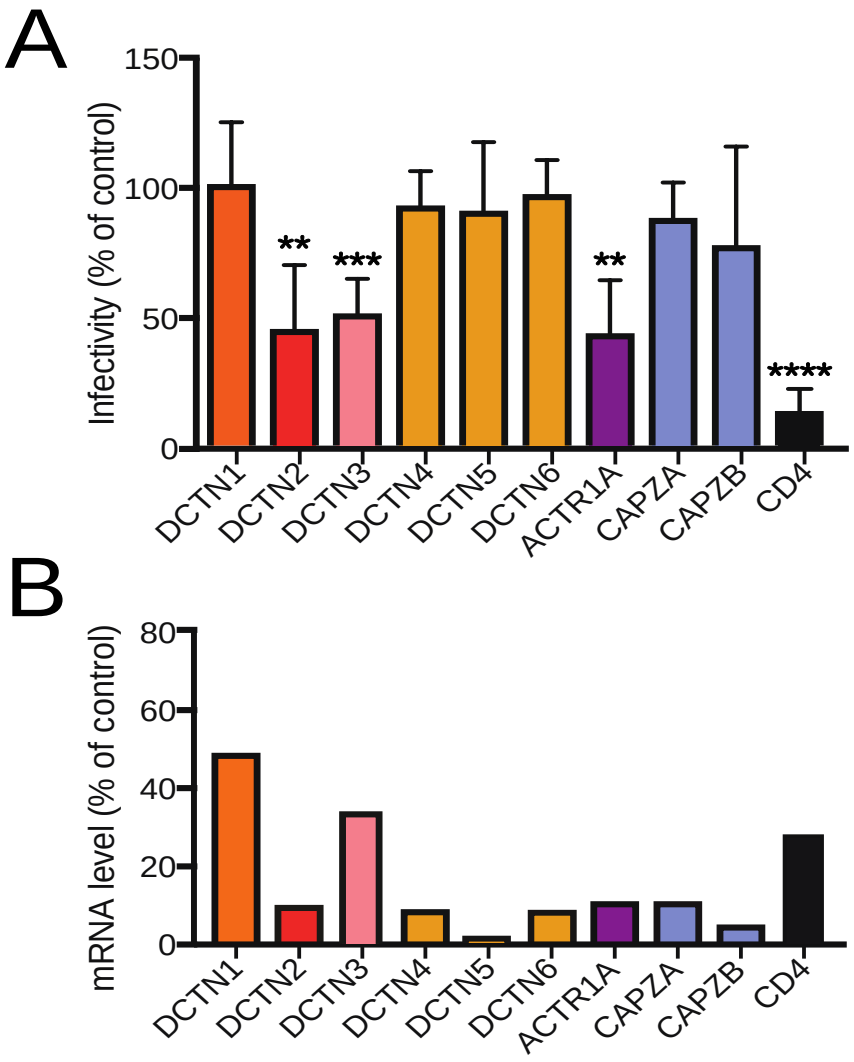

Figure 2-4. Depletion of some dynactin components inhibits HIV-1 infection. TZM-bl cells were pretreated with indicated pooled siRNAs and then inoculated with GFP-expressing HIV-1 (A) or harvested for knockdown efficiency by qPCR analysis (B). Infection was assessed by flow cytometry for GFP expression. The values shown represent the extent of infection relative to nontargeting siRNA treatment (A). Infection results are the means of three independent determinations. Error bars represent standard deviations. Statistical significance was calculated by a Student t test for each siRNA treatment compared to nontargeting control siRNA treatment. (**, P< 0.01; ***, P <0.001; ****, P <0.0001). mRNA analyses are from a single experiment.

DYNLT3, DYNLL1) (Figure 2-3). The various chains in dynein and dynactin can exhibit functional redundancy. I observed that depletion of the dynein heavy chain significantly reduced the extent of HIV-1 infection, consistent with previous reports [51, 83]. By contrast, I observed no significant effect of depleting other dynein components on HIV-1 infection, despite efficient knockdown of most of these components as assessed by mRNA quantification (Figure 2-3). As expected, depletion of cellular CD4 markedly reduced cell permissiveness to HIV-1.

The dynactin complex associates with dynein, increasing the processivity of dynein movement along microtubules [106]. Dynactin can also act as an adaptor for some cargoes. The dynactin complex is composed of the p150 sidearm (DCTN1), dynamitin/shoulder (DCTN2, DCTN3), pointed-end complex (DCTN4, DCTN5, DCTN6), Arp1 rod (ACTR1A), and the barbed end complex (CAPZA and CAPZB) (Figure 2-4). Depletion of DCTN2, DCTN3, and ACTR1A resulted in decreased HIV-1 infection, consistent with a role for the dynactin complex in HIV-1 infection.

To validate these results, I tested the effects of individual siRNAs from the four siRNA pools in Figures 2-3 and 2-4 that showed a significant effect on HIV-1 infection (Figure 2-5). Each single siRNA also significantly reduced the extent of infection of TZM-bl cells ($p<0.0001$ for all samples), thus confirming the results of the pooled siRNAs. Depletion of the corresponding mRNAs was confirmed by RT-PCR (Figure 2-5B). The observation that each of the individual siRNAs had a similar effect as the pooled siRNAs reduces the possibility of off-target effects being responsible for the observed outcome. In addition to RT-PCR analysis, protein depletion was confirmed by immunoblot analysis of extracts of cells transfected with each of two individual siRNAs for four targets for which antibodies were available. (Figure 2-5C). Collectively, the results in Figures 2-3, 2-4, and 2-5 indicate that HIV-1 infection depends

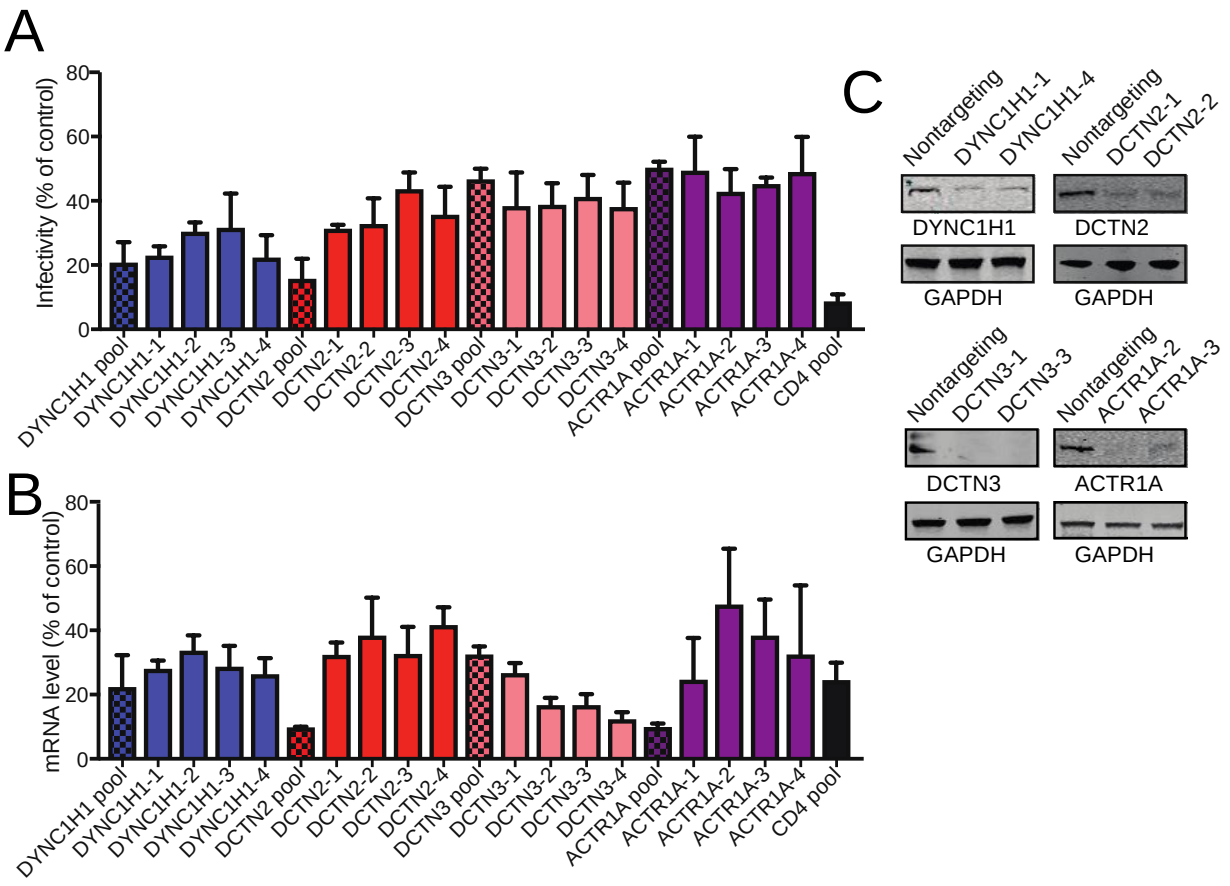

Figure 2-5. Individual siRNA depletion of DYNC1H1 and some dynactin components inhibits HIV-1 infection. TZM-bl cells were pretreated with indicated siRNAs and then inoculated with GFP-expressing HIV-1 (A) or harvested for knockdown efficiency by qPCR analysis (B). Infection was assessed by flow cytometry for GFP expression. The values shown represent the extent of infection relative to nontargeting siRNA treatment (A). Infection results are the means of three independent determinations. Error bars represent standard deviations. Statistical significance was calculated by a Student t test for each siRNA treatment compared to nontargeting control siRNA treatment. All samples had equal significance values (****, P <0.0001). mRNA analyses are from a single experiment. (C) Immunoblot analysis of the effects of two individual siRNAs for four targets on the corresponding target protein levels.

on the dynein heavy chain and on specific components of the dynactin complex.

Analysis of the effects of depletion of dynein adaptors on HIV-1 infection

Dynein adaptors are host proteins that link dynein to specific cargo and activate dynein movement along microtubules. I hypothesized that HIV-1 exploits one or more dynein adaptors for infection and transport to the nucleus. To identify dynein adaptors utilized during HIV-1 infection, I screened a panel of host proteins that I considered candidates for HIV dynein adaptors. These included known and putative dynein adaptors, including proteins with both dynein and HIV-1 interactions, and other host proteins that had previously been shown to be important for HIV-1 transport (Table 2-2). TZM-bl cells were treated with pooled siRNAs for 48 h, then challenged with HIV-1. Targets that had the most pronounced and reproducible effect on HIV-1 infection at 48h siRNA treatment were then analyzed under 72h siRNA treatment (Table 2-3, 2-4).

BICD2 depletion consistently reduced HIV-1 infection (Figure 2-6). To confirm that BICD2 depletion reduces cell permissiveness to HIV-1 infection, I repeated the experiments using individual siRNA duplexes present in the siRNA pool (Figure 2-6A). I observed that the individual siRNAs also reduced HIV-1 infection. Knockdown efficiency of the individual siRNAs was analyzed by RT-PCR (Figure 2-6B). To confirm that the siRNAs reduced BICD2 protein levels, I analyzed extracts of cells transfected with either of two of the individual siRNAs by immunoblotting (Figure 2-6C). I observed a marked decrease in BICD2 protein levels in the cell extracts transfected with either of the two BICD2 siRNAs.

Table 2-3: Infection and mRNA expression levels of siRNA targets

	48 hour siRNA treatment			72 hour siRNA treatment		
	Infectivity (% of nontargeting)		mRNA Expression (% of nontargeting)	Infectivity (% of nontargeting)		mRNA Expression (% of nontargeting)
	Expt 1	Expt 2		Expt 1	Expt 2	
BICD2	50	83	86	17	34	36
NDE1	117	114	70	20	62	8
SPTBN1	73	71	62	7	31	8
SEC24C	95	91	10	16	68	2
RAB11FIP3	94	102	91	11	73	64
HOOK3	97	93	58	88	36	50
MAP1A	107	111	83	35	100	50
MAP1S	115	137	56	28	103	5
WASF1	101	97	60	66	51	54
FEZ1	38	84	79	95	80	43
MAPRE1	118	110	66	72	38	22
MAPRE2	83	91	35	27	41	11
CSPP1	106	97	90	24	105	42
PAFAH1B1	73	80	98	97	68	11
NDEL1	96	73	20	102	64	8
BICD1	129	99	89	70	101	10
ZW10	106	102	42	65	105	19
CLIP1	116	86	16	144	124	20
BCAS2	82	87	58	84	103	12
SEC23A	125	68	54	76	87	15
SEC23B	120	129	42	111	105	10
SEC24A	145	116	44	111	119	19
RILP	133	99	32	68	97	6
RAB6A	9	51	61	22	60	27
RAB7A	92	125	90	98	110	10
MAPK8IP3	120	123	55	61	110	4
TBCB	124	126	74	56	122	2
KPNA2	117	122	19	107	110	5
TTL	116	124	63	56	127	13
SAP30BP	54	149	94	84	117	11
SPG20	112	127	76	68	129	14
PCNT	59	103	88	49	62	89
LAMTOR2	41	116	65	42	67	23

Table 2-3 cont.'d: Infection and mRNA expression levels of siRNA targets

	48 hour siRNA treatment			72 hour siRNA treatment		
	Infectivity (% of nontargeting)		mRNA Expression (% of nontargeting)	Infectivity (% of nontargeting)		mRNA Expression (% of nontargeting)
	Expt 1	Expt 2		Expt 1	Expt 2	
CLASP1	149	91	53	94	86	16
MID1IP1	106	113	20	173	138	14
MAP4	68	112	60	100	104	9
TTLL8	64	127	18	80	132	76

Table 2-4: Infection and mRNA expression levels of siRNA targets, poor knockdown

Adaptor Screen Infection Results, <80% Knockdown, <2 Fold Reduction of Infection

	48 hour siRNA treatment			72 hour siRNA treatment		
	Infectivity (% of nontargeting)		mRNA Expression (% of nontargeting)	Infectivity (% of nontargeting)		mRNA Expression (% of nontargeting)
	Expt 1	Expt 2		Expt 1	Expt 2	
KNTC1	101	97	82	104	102	57
ZWILCH	125	88	30	63	108	70
SPDL1	92	121	58	120	69	22
CLIP2	105	125	71	123	122	30
SPTBN4	109	111	78	68	118	46
SPTAN1	118	103	54	89	82	26
SEC24B	111	112	80	101	62	24
SEC24D	126	124	95	92	96	72
RAB7B	133	109	35	61	96	40
CCDC155	118	138	77	58	96	65
SUN1	102	94	86	113	105	21
HOOK1	121	108	51	146	116	37
HOOK2	124	82	47	109	126	25
MAP1B	105	117	95	114	120	76
AGTPBP1	133	105	90	92	115	22
WIPF2	117	109	65	61	89	23
ARF1	87	89	30	80	81	84

Table 2-4 cont.'d: Infection and mRNA expression levels of siRNA targets, poor knockdown						
Adaptor Screen Infection Results, <80% Knockdown, <2 Fold Reduction of Infection						
	48 hour siRNA treatment			72 hour siRNA treatment		
	Infectivity (% of nontargeting)		mRNA Expression (% of nontargeting)	Infectivity (% of nontargeting)		mRNA Expression (% of nontargeting)
	Expt 1	Expt 2		Expt 1	Expt 2	
ARF6	114	103	75	110	124	42
RUFY1	138	105	52	81	130	29
HDAC6	111	122	64	66	113	24
KAT7	103	96	72	112	75	32
CLASP2	118	99	95	149	116	42
BLOC1S6	116	100	92	78	95	22
FGD6	107	110	33	142	104	24

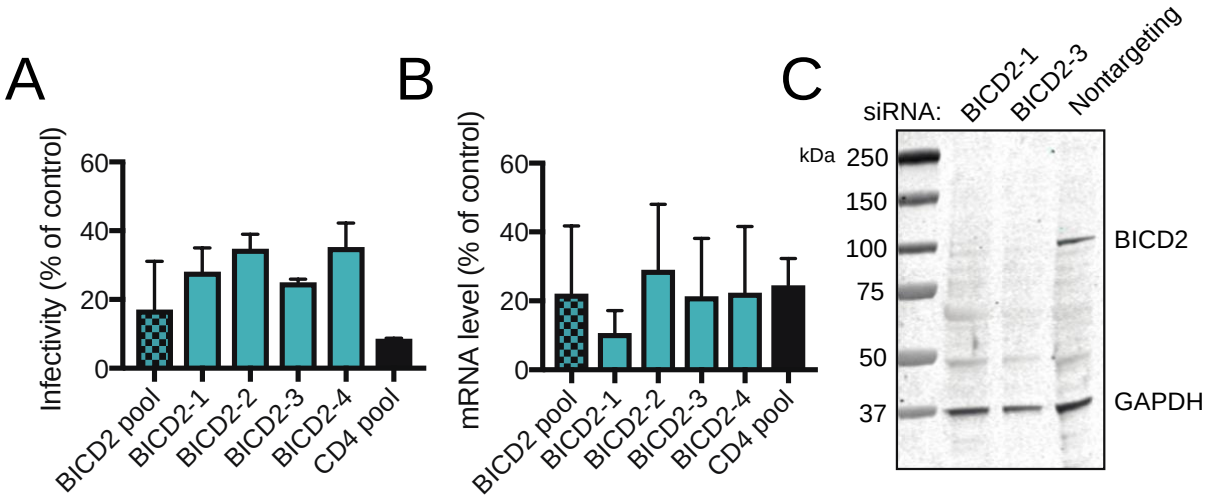

Figure 2-6. Analysis of the effects of depletion of dynein adaptors on HIV-1 infection. (A) TZM-bl cells were pretreated with BICD2 pooled siRNA or individual siRNAs and then inoculated with GFP-expressing HIV-1 (A) or harvested for knockdown efficiency by qPCR analysis (B). After infection with an HIV-1 reporter virus, the cells were fixed and analyzed by fluorescence-activated cell sorting for GFP expression, and the infectivity relative to nontargeting siRNA treatment was determined (A). The results shown are mean values from three independent determinations. Error bars represent standard deviations. Statistical significance was calculated by a Student's T test. All samples had equal significance values (****, P<00001). (C) Two of the single siRNAs were selected for BICD2 protein knockdown analysis by immunoblotting.

Depletion of components of the dynein-dynactin-BICD2 complex results in impaired HIV-1 nuclear import

After determining that the dynein-dynactin-BICD2 complex is important for HIV-1 infection, I asked which stage of HIV-1 infection the complex affects. Before infection occurs, HIV-1 must enter at the cell membrane, and traverse the cytoplasm to enter the nucleus for integration. During this period, the virus undergoes reverse transcription and partial uncoating [4]. I hypothesized that if the dynein-dynactin-BICD2 complex is important for transport of the virus to the nucleus, depletion of the components would result in reduced accumulation of HIV-1 DNA in the nucleus. After entry of HIV-1 into the nucleus, a fraction of the viral DNA is not integrated but instead forms 2-LTR circles within the nucleus, rendering 2-LTR circles a convenient PCR-based readout of nuclear entry. To determine if the dynein-dynactin-BICD2 complex is important for HIV-1 intracellular transit, I tested the effects of host proteins on the levels of accumulated 2-LTR circles. Two individual siRNAs were chosen for each gene of interest. TZM-bl cells were treated with siRNAs and subsequently challenged with GFP-expressing HIV-1 pseudotyped with VSV-G. 2-LTR circles were quantified, and the reduction relative to nontargeting control was determined. Efavirenz treatment, which blocks reverse transcription, and therefore downstream 2-LTR production, was used as a positive control. Depletion of the dynein heavy chain, dynactin components, and BICD2 each led to a reduction in HIV-1 2-LTR circles (Figure 2-7A), suggesting that HIV-1 does not efficiently reach the nucleus when components of the complex are depleted. Prior to nuclear entry, HIV-1 undergoes reverse transcription in the cytoplasm. Because formation of 2-LTR circles depends on viral DNA synthesis, a reduction in reverse transcription would be expected to result in a decreased level of 2-LTR circles. To test if depletion of the dynein-dynactin-BICD2 complex affects HIV-1

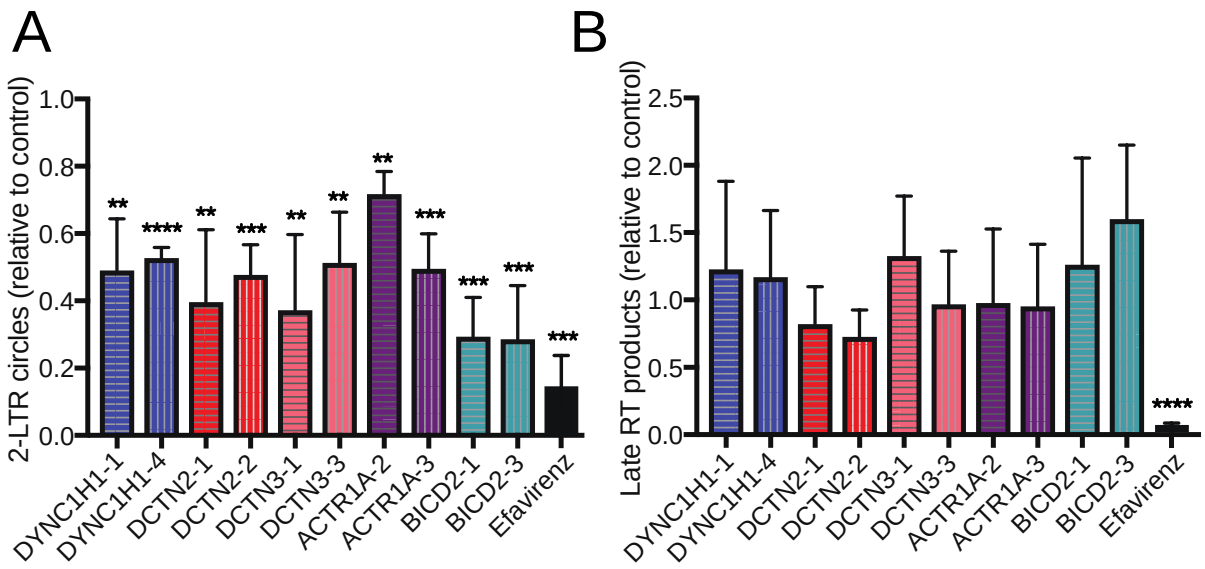

Figure 2-7. Analysis of HIV-1 DNA synthesis and nuclear entry in cells depleted for components of the dynein-dynactin-BICD2 complex. TZM-bl cells were pretreated with individual siRNA duplexes for 72h and then inoculated with GFP-expressing HIV-1 pseudotyped with VSVG. Cells were harvested for quantitative analysis of 2-LTR circles (A) and for analysis of second strand transfer reverse transcripts (B). The effects relative to nontargeting siRNA treatment are shown. The results shown are mean values from three independent determinations. Error bars represent standard deviations. Statistical significance was calculated by an unpaired parametric t test for each siRNA treatment versus nontargeting control siRNA treatment (**, P<0.01; ***, P<0.001; ****, P<0.0001). No significant effects of the siRNAs on late reverse transcripts were observed.

reverse transcription, I assayed late reverse transcription products by quantitative PCR using virus-specific primers (Figure 2-7B). Efavirenz treatment was used as a control to confirm that the assay signals resulted from *bona fide* reverse transcription vs. contaminating plasmid DNA. I observed no significant effect of siRNA treatment on the production of late RT products relative to the nontargeting siRNA control. My results are concordant with one, and differ with another, previous report of dynein heavy chain function in HIV-1 infection [78, 81]; they are also concordant with a recent study of the dependence of HIV-1 infection on BICD2 expression [82]. My data suggest that the reduction in HIV-1 infection by depletion of the dynein-dynactin-BICD2 complex results from intracellular transport and/or impaired nuclear entry.

The dynein-dynactin-BICD2 complex facilitates MLV and SIV infection

Previous studies of MLV infection have suggested that the dynein heavy chain, the dynein intermediate chain, the dynein light chain DYNLRB2, and the dynactin component DCTN2/p50/dynamitin are involved in MLV infection [70, 177]. Although I did not observe an effect of depletion of either dynein intermediate chain (DYNC1I1, DYNC1I2), or DYNLRB2 on HIV-1 infection, I did observe that the dynein heavy chain (DYNC1H1), and dynactin DCTN2 promote infection (Figure 2-3, 2-4, 2-5; Table 2-3). To determine whether the dependence of infection on these proteins extends to other retroviruses, I tested the effect of depletion of DYNC1H1, DCTN2, DCTN3, ACTR1A, and BICD2 (Figure 2-8, panels A-E, respectively) on cell permissiveness to MLV and SIV infection. To ensure that the viruses use a common mechanism for cell entry, I also employed GFP reporter particles that were pseudotyped with VSV-G. Interestingly, pseudotyping HIV-1 led to a decrease in the effects on infection compared to HIV-1 particles bearing native Env for all dynein-dynactin-BICD2 targets. The

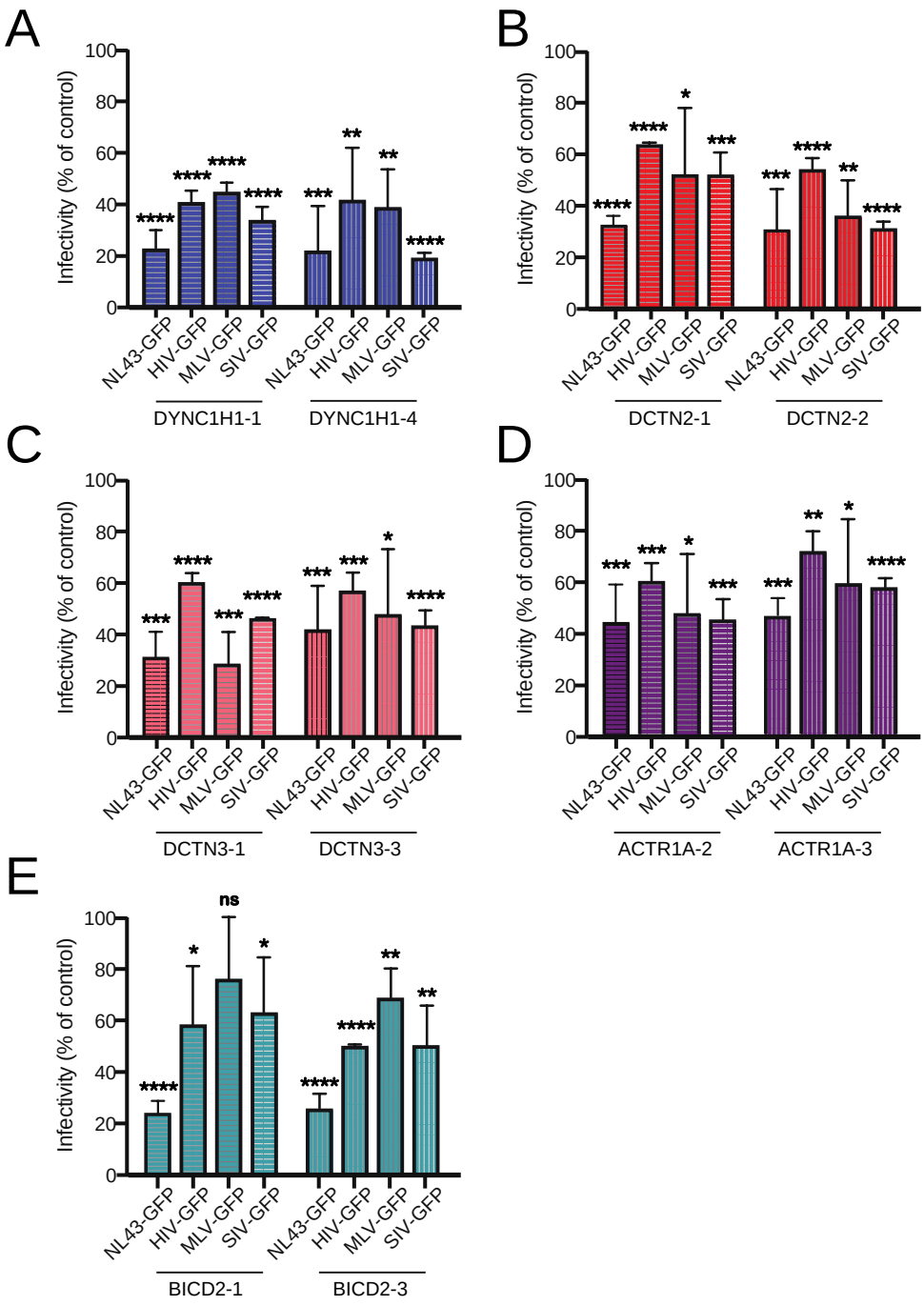

Figure 2-8 Effects of depletion of components of the dynein-dynactin-BICD2 complex on MLV and SIV infection. TZM-bl cells were pretreated with individual siRNA duplexes for 72h and then inoculated with (NL43-GFP), GFP-expressing HIV-1 pseudotyped with VSVG (HIV-GFP), murine leukemia virus (MLV-GFP), or simian immunodeficiency virus (SIV-GFP). Inoculated cells were fixed and analyzed by fluorescent-activated cell sorting for GFP expression, and the extent of infection relative to nontargeting siRNA was determined. The results shown are mean values from three independent determinations. Error bars represent standard deviations. Statistical significance was calculated by an unpaired parametric t test for each siRNA treatment versus nontargeting control siRNA treatment (**, P<0.01; ***, P<0.001; ****, P<0.0001).

observed effect of VSV-G pseudotyping is consistent with another study of the effects of BICD2 depletion on HIV-1 infection [82]. As with HIV-1, both MLV and SIV infection were reduced when DYNC1H1 (Figure 2-8A) and DCTN2 (Figure 2-8B) were depleted, consistent with a previous study of MLV [70]. Similar observations were obtained for the other dynactin components DCTN3 (Figure 2-8C) and ACTR1A (Figure 2-8D), which were not previously reported to play a role in MLV or SIV infection. I also observed that BICD2 depletion also reduced MLV and SIV infection, though the effect on MLV infection appeared to be less pronounced (Figure 2-8E). Together, my results suggest that the dynein-dynactin-BICD2 complex is exploited by both MLV and SIV for infection.

DYNC1H1 and BICD2 facilitate HIV-1 infection in multiple cell lines

To determine whether the dependence of HIV-1 infection on DYNC1H1 and BICD2 extends to other cell types, I tested the effect of depletion of DYNC1H1 and BICD2 on cell permissiveness to infection in Jurkat, A431-CD4, GHOST, and primary human fibroblast cultures. Cells were transfected with two individual siRNAs for DYNC1H1 and BICD2 for 72 h before challenge with HIV-1. For the infection assays, I employed GFP reporter particles that had either native HIV-1 envelope (NL43-GFP) or particles that were pseudotyped with VSV-G (HIV-GFP). DYNC1H1 and BICD2 depletion reduced HIV-1 infection in all of the cells (Figure 2-9A-D). Interestingly, pseudotyping HIV-1 did not lead to a decrease in the effects on infection compared to native HIV-1 env as was previously seen in TZM-bl cells. To confirm that DYNC1H1 and BICD2 were depleted in the siRNA-treated cells, I quantified mRNA levels by RT-PCR and protein levels by immunoblotting (Figure 2-9E-H). Together, my results suggest

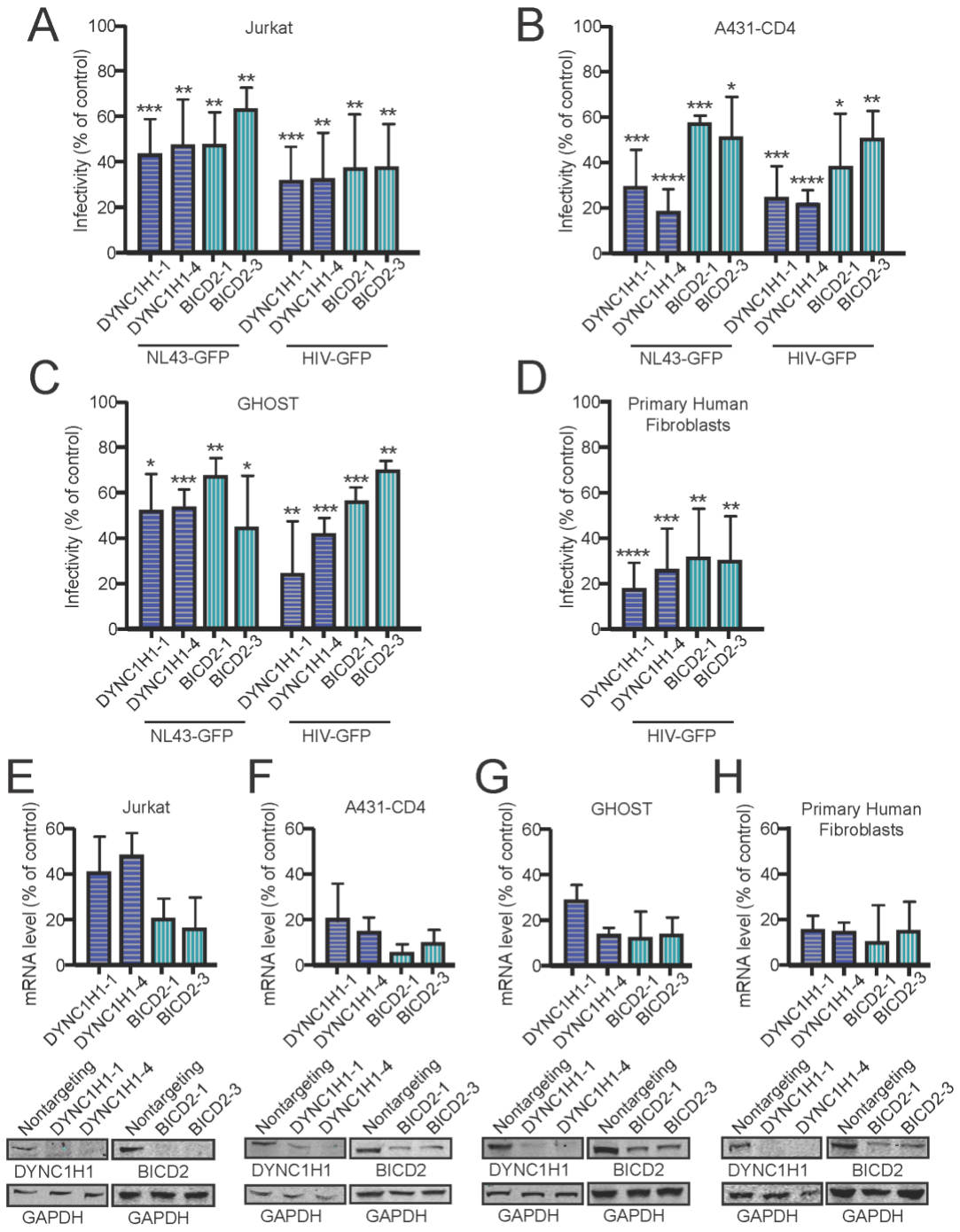

Figure 2-9 DYNC1H1 and BICD2 facilitate HIV-1 infection in various human cell lines. Cells were pretreated with individual siRNA duplexes and either inoculated with GFP-expressing HIV-1 (NL43-GFP) or VSVG pseudotyped HIV-1 (HIV-GFP) for infection analysis (A to D) or harvested for knockdown efficiency analysis by qPCR or immunoblotting (E to H). Inoculated cells were fixed and analyzed by fluorescence-activated cell sorting for GFP expression, and the extent of infection relative to nontargeting siRNA treatment was determined. The results shown are mean values from three independent determinations. Error bars represent standard deviations. Statistical significance was calculated by an unpaired parametric t test for each siRNA treatment versus nontargeting control siRNA treatment (**, P<0.01; ***, P<0.001; ****, P<0.0001).

that dynein and BICD2 facilitate HIV-1 for infection in a range of cell types, including the Jurkat T cell line.

Discussion

In this study, I performed a systematic analysis of the components of the dynein and dynactin complexes and of known dynein adaptors for their effects on HIV-1 infection. Consistent with earlier reports [51, 83], I observed that depletion of DYNC1H1 reduced cell permissiveness to HIV-1 infection. In addition to dynein heavy chain, depletion of the dynactin components DCTN2, DCTN3, and ACTR1A decreased cell permissiveness to HIV-1 infection, indicating that the dynactin complex also facilitates HIV-1 infection. Finally, I observed that BICD2 depletion reduced cell permissiveness to infection. My results suggest that a dynein-dynactin-BICD2 complex promotes HIV-1 infection (Figures 2-2 through 2-6).

Analysis of the stage at which infection is inhibited indicates that the dynein-dynactin-BICD2 complex promotes the intracellular transport of HIV-1 to the nuclear envelope. Depletion of DYNC1H1, dynactin components, and BICD2 each resulted in a decrease in the levels of nuclear HIV-1 DNA (2-LTR circles) without a reduction in viral DNA levels, suggesting that the virus is impaired at or prior to nuclear entry (Figure 2-7). While an effect of dynein depletion on reverse transcription was previously observed in one study [81], another study found the opposite [78]. My observation that dynein depletion reduced nuclear HIV-1 DNA without altering reverse transcription suggested that dynein accelerates HIV-1 transport to the nucleus, or nuclear entry itself.

I also observed that, relative to non-pseudotyped HIV-1, infection by HIV-1 particles pseudotyped by VSV-G was less affected by depletion of DYNC1H1, dynactin components, and

BICD2 in TZM-bl cells (Figure 2-8). Similar effects of pseudotyping on BICD2 dependence of HIV-1 were also observed in a recent study [82]. Cell entry by HIV-1 infection normally occurs via direct fusion at the plasma membrane; by contrast, HIV-1 (VSV-G) enters cells by endocytosis and requires the low pH of the endosome for fusion. I speculate that this alters the location at which the dynein machinery engages the virus, thereby reducing the requirement for the dynein-dynactin-BICD2 complex. Interestingly, however, this difference in the dependence of HIV-1 infection on dynein and BICD2 between pseudotyped and non-pseudotyped viruses was not observed in other cell lines tested (Figure 2-9), suggesting that this effect may be specific to TZM-bl cells.

In addition to HIV-1, infection by VSV-G-pseudotyped SIV and MLV was dependent on dynein, dynactin, and BICD2 (Figure 2-8), indicating that a common mechanism of dynein transport can be utilized by a variety of retroviruses. A previous report showed that infection by ecotropic but not amphotropic MLV depends on the adaptor NudEL [70], further suggesting that dynein adaptor utilization depends on the cell receptor and/or entry pathway utilized by the virus. The apparent broad dependence of diverse retroviruses on BICD2 suggests the possibility that convergent virus evolution adopted a common solution for engagement of the intracellular transport machinery. It will be interesting to determine whether nonprimate lentiviruses and avian retroviruses also utilize BICD2 for infection.

CHAPTER III

BICD2 BINDS THE HIV-1 CAPSID AND PROMOTES HIV-1 TRANSPORT TO THE NUCLEUS

A portion of this work was published in Carnes SK, Zhou J, Aiken C. HIV-1 Engages a Dynein-Dynactin-BICD2 Complex for Infection and Transport to the Nucleus. 2018. *Journal of Virology*. 92 (20) e00358-18.

Introduction

My results described in Chapter II indicate that HIV-1 infection depends on the dynein-dynactin-BICD2 complex. In cells, this complex is responsible for efficient intracytoplasmic transport of cargo. Adaptors, such as BICD2, are important for the activation of dynein movement along microtubules, and therefore active transport. Therefore, I hypothesized that this complex promotes HIV-1 infection by transporting the incoming viral core to the target cell nucleus. To analyze transport of HIV-1 in cells I utilized both fixed cell and live cell microscopy. These methods allowed me to determine the necessity of the dynein-dynactin-BICD2 complex for transport over a longer timescale (1-2 hours) and the necessity of the complex for the kinetics of movement.

Here, I show that HIV-1 is transported in short bursts that match kinetically to active transport by dynein. I also shown that siRNA depletion of the dynein heavy chain and BICD2 reduced virion transport toward the nucleus on longer time scales. Specifically, I observed that initiation of transport was thwarted. BICD2 depletion did not alter the particles that remained

mobile in terms of speed of movement or run length. However, the motile particles did have a net reduction in retrograde movement, suggesting they were not trafficked by dynein.

In order to act as an adaptor for dynein, BICD2 must bind both the dynein-dynactin complex, and the cargo it is transporting. This "bridge" between cargo and dynein activates transport. Therefore, I hypothesized that HIV-1 engages the dynein motor complex via BICD2 for intracellular transport. Specifically, I hypothesize that this engagement occurs through the HIV-1 capsid, as it acts as a shell around interior viral components, and remains associated with the viral PIC through transport to the nucleus.

There are two homologues of Bicaudal D: BICD1 and BICD2. Although both can serve similar functions in the cell, BICD2 is more abundant. In cultured mammalian cells, BICD2 promotes dynein-mediated transport from the ER to the Golgi and within the Golgi via its transport RAB6-positive endosomes. Also, prior to mitotic entry, BICD2 interacts with RANBP2 at the nuclear pores and recruits dynein and dynactin to ensure proper positioning of the nucleus [reviewed in [49]].

Structurally, BICD2 is a dimer with several regions that can form coiled coil domains and has an overall rod-like shape (Figure 3-1A) [111, 178]. The N-terminal region of BICD2 is responsible for binding dynein and dynactin [119, 122, 127], and promotes a stable ternary complex that activates processive minus-end directed motility. The C-terminal region of BICD2 is responsible for binding cargo, including interacting partners Rab6 and RANBP2 [179, 180]. The C-terminal may also be responsible for the autoinhibition of the protein when cargo is not bound (Figure 3-1B)[119, 122, 127, 181]. The C-terminal region binds to the N-terminal region until cargo is bound, at which time the N-terminal becomes available for binding with dynein and dynactin. This model is supported by the finding that mutation of the cargo-binding site in the C-

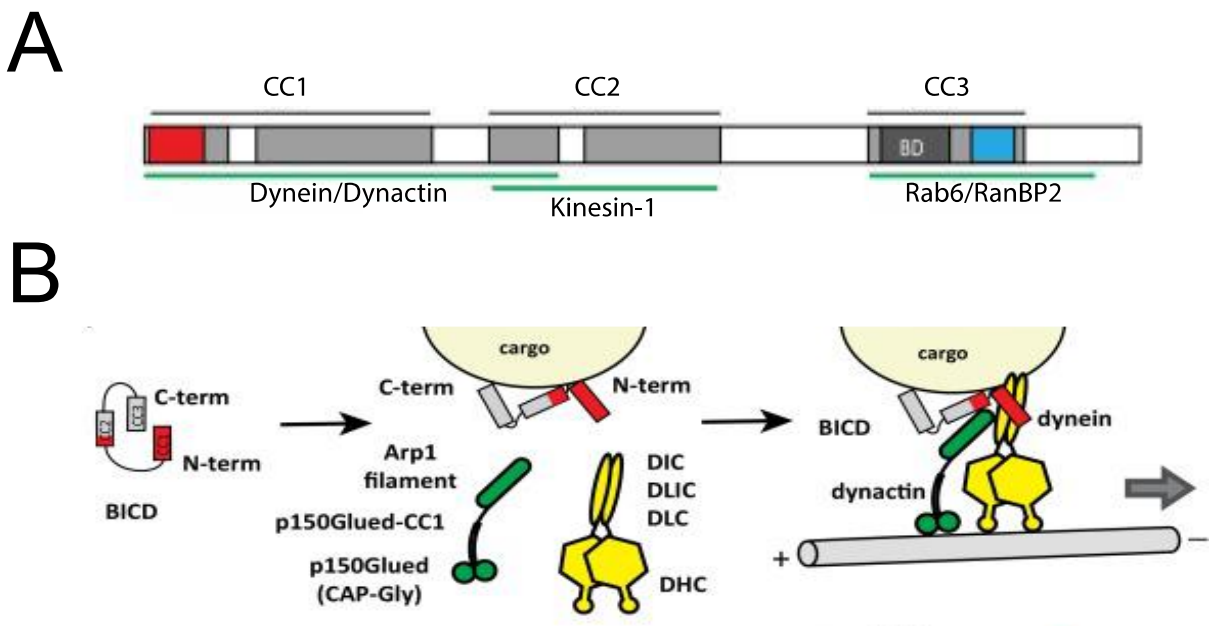

Figure 3-1 Schematic structure of BICD2. A. The structure of human BICD2 contains three regions of extensive coiled-coil structure (gray boxes), names CC1, CC2, and CC3. The N-terminal region, CC1 has a conserved region (red box) across *Drosophila melanogaster and Caenorhabditis elegans*. The CC3 region also has a conserved region (blue box) across these same organisms, and a conserved region (BD) specific to BICD1 and BICD2. The N-terminus can bind dynein and dynactin, the central region can bind kinesin-1, and the C-terminus can bind cargo, including Rab6 and RanBP2 (green lines). B. A model in which the C-terminal region of BICD2 interacts with the N-terminal region, autoinhibiting binding to the dynein complex. Cargo binding of the C-terminal domain relieves this inhibition, allowing the N-terminal region of BICD2 to bind to dynein (yellow) and dynactin (green). Adapted from Hoogenraad and Akhmanova, *Trends. Cell. Bio.* (2016) [12]

terminus reduces dynein association [182]. BICD2 is also able to bind kinesin-1 through its central coiled-coil region though, complicating the model [183]. It is unclear how autoinhibition would be relieved in this case. In these studies, I sought to determine if HIV-1 interacted with BICD2 for transport to the nucleus, and if so, what regions of BICD2 HIV-1 was binding. Biochemical studies revealed that dynein components and BICD2 associate with capsid-like assemblies of the HIV-1 CA protein in cell extracts and that purified recombinant BICD2 binds to CA assemblies *in vitro*. Association of dynein with CA assemblies was reduced upon immunodepletion of BICD2 from cell extracts. Our results demonstrate that BICD2 is a capsid-associated dynein adaptor utilized by HIV-1 for transport to the nucleus.

Results

HIV-1 is transported in short bursts

Although dynein was hypothesized to be the major HIV transporter toward the nucleus, studies had focused on the total distance transported in cells over a longer timeframe (2 hours)[83]. While this type of analysis suggests active transport, it doesn't analyze the kinetics of movement. To analyze transport kinetics of cargo transport, studies focus on the run length and velocity of events [118, 184]. For dynein, the average reported run length has been reported to be 1-5 µm, with an average velocity 0.09-1 µm/second. I analyzed the movements of HIV-1 over short timescales of 3 minutes at a time, and determined the run length and velocity of moving particles (Figure 3-2). From these results, I observed a distribution of run lengths from 0.25-5.25 µm, with the median being at 1 µm. This range of values suggests that particles are being transported by dynein. For the velocity, I observed a distribution of events from 0.1-2.25

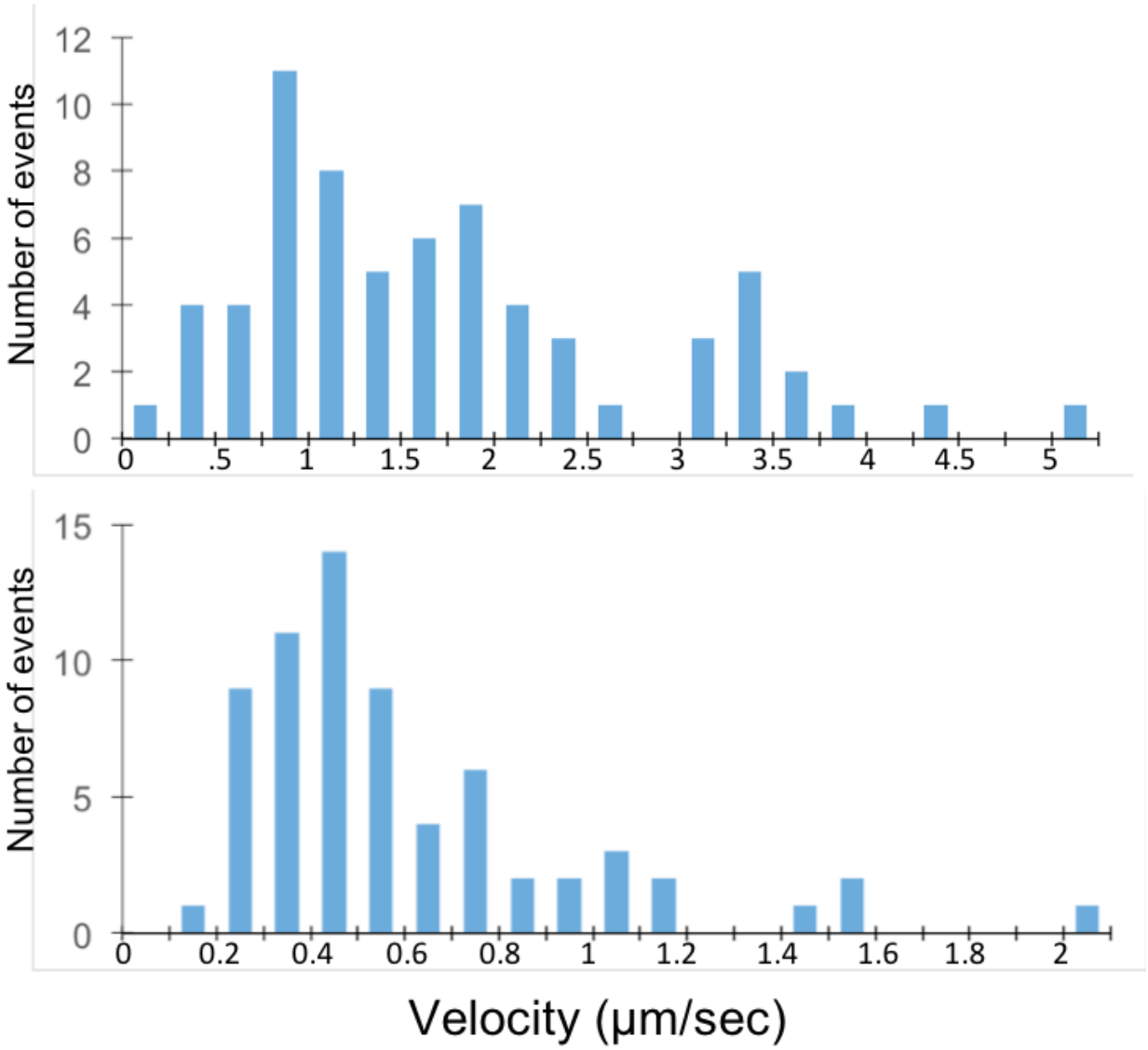

Figure 3-2 HIV-1 is transported in short bursts. TZM-bl cells were inoculated with HIV psedotyped with VSV-G, GFP-Vpr and moving particles imaged over the course of two hours. The distance and velocity were measured for 67 events. Imaging assistance by Stephen Norris.

μm/second, with the median at 0.5 μm/second. Interestingly, our result of distribution range is higher than the expected range of 0.09-1 μm/second, but the median is within the expected range. My analyses suggested that HIV-1 is transported in short bursts in the cytoplasm.

BICD2 promotes HIV-1 retrograde trafficking to the nucleus

By definition, a dynein adaptor engages both cargo and dynein and promotes intracellular transport[49]. To determine whether BICD2 promotes HIV-1 trafficking to the nucleus, I employed fluorescence deconvolution microscopy to analyze the intracellular location of HIV-1 cores in the target cell cytoplasm in BICD2-depleted cells and in control siRNA-treated cells (Figure 3-3). HIV-1 particles were generated containing two labels: the core-associated marker GFP-Vpr and the membrane label mCherry-S15 [185]. Upon fusion of the viral and cell membranes, the membrane-bound mCherry-S15 separates from the viral core, thus permitting identification of fused particles via loss of the mCherry associated fluorescent signal. The dynein heavy chain, DYNC1H1, was employed as a positive control, as previous studies have shown that depletion of this dynein component results in accumulation of HIV-1 particles at the cell periphery [51, 83], suggestive of impaired transport function.

Consistent with those reports, I observed a significant reduction in the average HIV-1 particle distance traveled toward the nucleus from the cell periphery in cells depleted of DYNC1H1 (Figure 3-3A and B left). BICD2 depletion also significantly increased the average HIV-1 distance from the nucleus (Figure 3-3A and B left), suggesting that BICD2 promotes HIV-1 movement to the nucleus. I also analyzed the fraction of HIV-1 particles that reached the nucleus within 1 hr in siRNA DYNC1H1- and BICD2-treated cells (Figure 3-3C). Consistent with a previous study [83], the fraction of fused HIV-1 particles that reached the nucleus in

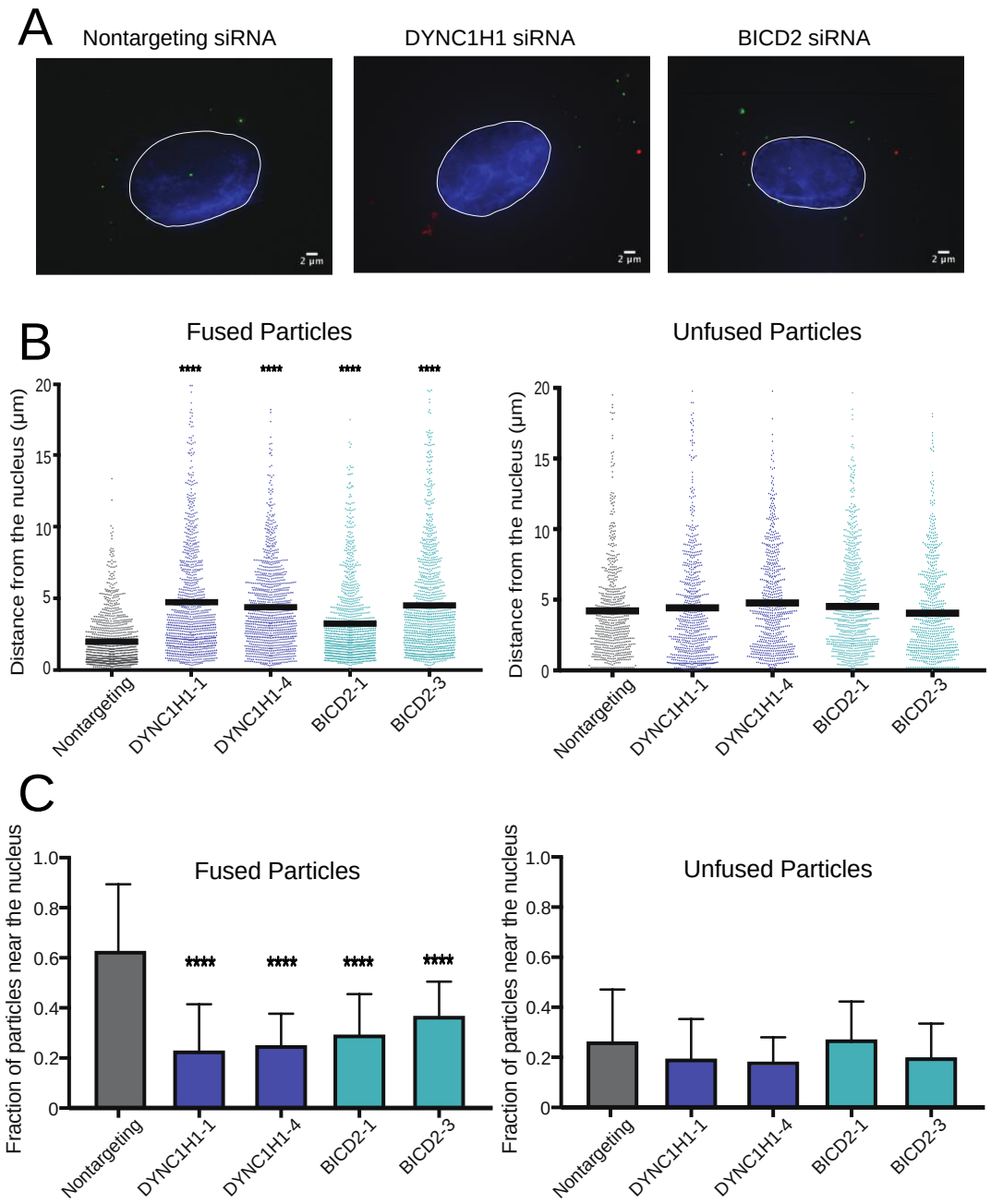

Figure 3-3 BICD2 promotes HIV-1 movement to the nucleus. TZM-bl cells wre pretreated with siRNAs and inoculated with VSV-G pseudotyped HIV-1 particles labeled with GFP-Vpr and S15-mCherry. (A) Representative images of cells. (B) Quantitative analysis of HIV-1 particle distance from the nucleus. Each dot represents the measurement of an individual HIV-1 particle. The results shown are from two independent experiements, each with >20 cells analyzed and >400 particles analyzed per condition. A one-way ANOVA was performed for statistical analysis, followed by a Dunnett's multiple-comparison test, and all treatment groups in the fused particle analysis exhibited P values of <0001. No treatment groups in the unfused particle analysis exhibited a significant difference compared to nontargeting control. (C) The average and standard deviation of the fraction of HIV-1 particles within 2 µm of the nucleus for each cell were analyzed. Analysis results for fused particles (left) and unfused particles (right) are shown. Significance was determined by one-way ANOVA, as in panel B.

DYNC1H1-depleted cells was significantly lower than that in control siRNA-transfected cells. Similarly, fewer particles reached the nucleus in BICD2-depleted vs. control cells (Fig. 3-3C left), consistent with a role of BICD2 in intracellular HIV-1 trafficking to the nucleus. For both analyses, movement of the unfused particles (Figure 3-3B and C, right panels) was unaffected by DYNC1H1 or BICD2 depletion compared to nontargeting control, indicating that the role of dynein and BICD2 in transport is specific to the fused viral core.

To test for a role of DYNC1H1 and BICD2 in the bi-directional motions of HIV-1 particles, I employed continuous imaging of live cells. Immediately before movies were captured, the mCherry-S15 signal was imaged. In subsequent analysis, those particles displaying mCherry signal were excluded from analysis. The velocity, net distance travelled, and directionality of individual virus particles were analyzed. In cells depleted of DYNC1H1 or BICD2, I observed a high fraction (30-40%) of nonmotile or slow-moving particles (less than 4 μm total distance over the 2.5-min imaging period), relative to control nontargeting siRNA-treated cells (~13%) (Figure 3-4A). Within the population of moving particles, I analyzed the net directionality of the particles. Particles moving toward the nucleus were classified as retrograde and particles moving away from the nucleus as anterograde. Depletion of DYNC1H1 or BICD2 resulted in a significantly lower fraction of HIV-1 retrograde particles vs control siRNA treatment (Figure 3-4B). These findings suggest that dynein and BICD2 are utilized to activate HIV-1 particle movement in the retrograde direction, consistent with BICD2's function as a dynein adaptor.

Quantification of HIV-1 intracellular velocity also revealed a reduction in DYNC1H1- or BICD2-depleted cells relative to control cells (Figure 3-4C), in agreement with a recent report [82]. However, when nonmotile particles (described in Figure 3-4A) were excluded from the

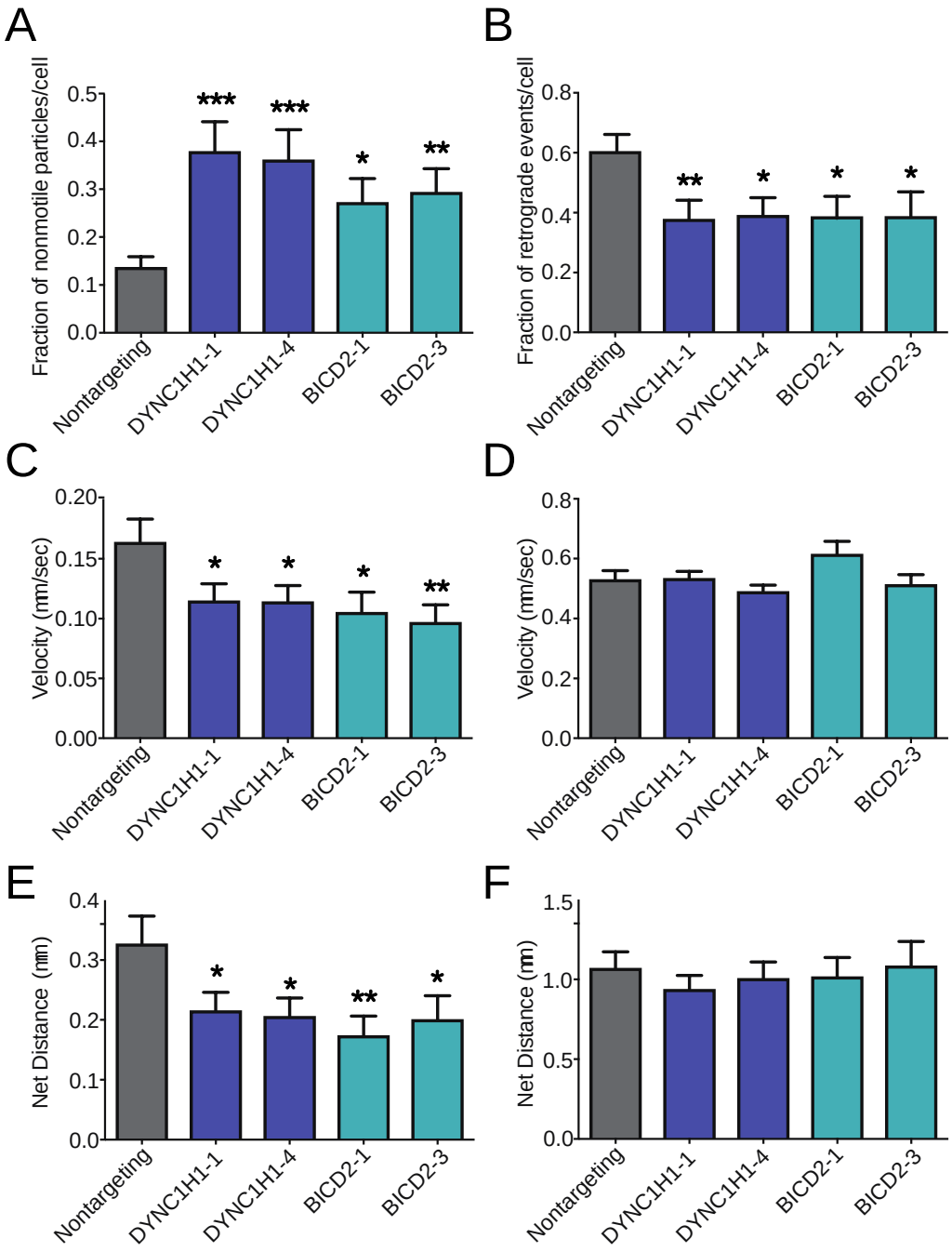

Figure 3-4 BICD2 promotes retrograde intracellular trafficking of HIV-1. TZM-bl cells wre pretreated with siRNAs and inoculated with VSV-G pseudotyped HIV-1 particles labeled with GFP-Vpr and S15-mCherry. (A) Fractin of nonmotile particles per cell. (B) Fraction of retrograde events per each cell for the motile population of particles. (C) Velocity of particle movement in the entire particle population. (D) Velocity of particle movement in the population of motile particles. (E) Net distance traveled in the entire particle population. (F) Net distance traveled in the population of motile particles. Results shown are from two independent experiments, each with >20 cells analyzed, and >400 particles analyzed per condition. Shown are the mean values and standard deviations of the particle events/cell for the cell population. Significance was determined by an unpaired parametric t test for each siRNA treatment relative to nontargeting control siRNA treatment (*, $p<0.05$; **, $p<0.01$; ***$p<0.001$; ****$p<0.0001$).

analysis, thus quantifying only moving particles, I observed that the effect of DYNC1H1 or BICD2 depletion on velocity was no longer significant (Figure 3-4D). Comparing the net distance of HIV-1 particle movement, I also observed a reduction in cells depleted of DYNC1H1 or BICD2 (Figure 3-4E). As with the velocity measurements, this difference was not detected when the nonmotile population of HIV-1 particles was excluded from the analysis (Figure 3-4F). Taken together, these results indicate that DYNC1H1 and BICD2 promote HIV-1 particle movement in the retrograde direction, likely by promoting the initiation of transport.

The HIV-1 capsid binds the dynein-dynactin complex

For HIV-1 to be transported to the nucleus by dynein, the virus should associate with the components of the dynein complex. The HIV-1 capsid encapsulates the internal core components, making it the most easily accessible component of HIV-1 for an interaction with dynein. The kinesin-1 adaptor FEZ1 also interacts with the HIV-1 capsid, suggesting that the capsid is important for molecular motor engagement [51]. Therefore, I hypothesized that dynein interacts with the HIV-1 capsid to facilitate viral intracellular transport.

To test this, I assayed the ability of dynein components in cell extracts to associate with assembled CA tubes *in vitro*. The CA protein assembles into a hexameric lattice structure that can be stabilized by engineered disulfide crosslinks at amino acid positions 14 and 45 in the CA protein or by linking CA to NC. These assemblies structurally resemble the native capsid lattice and are often used as surrogates in capsid-binding assays. I confirmed the tubular morphology of the assemblies by negative-stain electron microscopy (Figure 3-5A, CA; B, CA-NC). Assembled tubes can be readily pelleted by low speed centrifugation, thus facilitating the detection of proteins that associate with the HIV-1 capsid. To study capsid binding to dynein

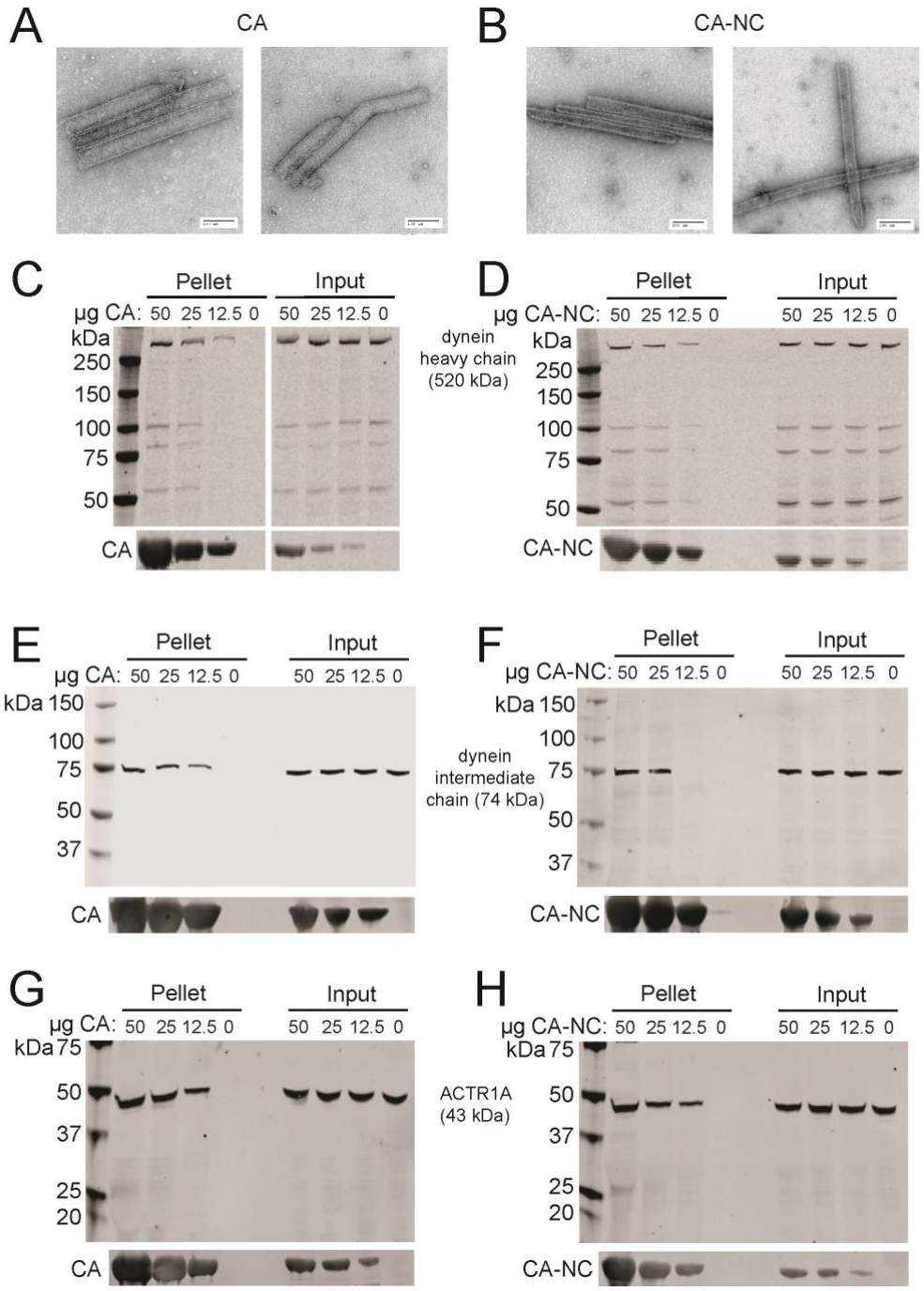

Figure 3-5 Association of dynein and dynactin with capsid-like HIV-1 assemblies *in vitro*. (A and B) Recombinant CA and CA-NC proteins were assembled into tubes and examined by negative-stain electron microscopy to confirm tubular assembly. CA tubes were incubated with 293T cell extracts. The reactions were then centrifuged, the pellets washed twice, and the pelleted proteins were analyzed by SDS-PAGE and immunoblotting. Blots were probed with antibodies to dynein heavy chain (C, CA; D, CA-NC), dynein intermediate chain (E, CA; F, CA-NC), and dynactin component ACTR1A (G, CA; H, CA-NC) or CA (C-H). Input samples corresponding to 10% of each reaction were removed prior to pelleting. Representative immunoblots from three independent experiments are shown.

and dynactin components, I incubated 293T cell extracts with various quantities of CA assemblies, pelleted the complexes, and analyzed the associated proteins by immunoblotting (Figure 3-5). I observed that dynein heavy chain (Figure 3-5C-D), dynein intermediate chain (Figure 3-5E-F), and dynactin component ACTR1A (Figure 3-5G-H) were all enriched in pellets from reactions containing CA tubes, suggesting that these dynein and dynactin components can associate with assembled HIV-1 capsids *in vitro*.

BICD2 binds the HIV-1 capsid via its CC1 and CC3 domains

My results indicated that the dynein complex can associate with the HIV-1 capsid *in vitro*. I hypothesized that the adaptor protein BICD2 binds to the HIV-1 capsid and functions as a capsid-specific dynein adaptor. To test this, CA (Figure 3-6A) and CA-NC (Figure 3-6B) tubes were incubated with cell extracts, pelleted, and proteins in the pelleted complexes were separated by SDS-PAGE and analyzed by immunoblotting with antibody to BICD2. I observed that cellular BICD2 associates with both CA and CA-NC tubes *in vitro* (Figure 3-6, panels A and B, respectively).

I next sought to identify the capsid-binding domain in BICD2. BICD2 contains two major domains: an N-terminal (NT) domain that links dynein to dynactin to activate processive movement, and a C-terminal (CT) domain that normally binds to cargo (Figure 3-7A) [119, 127, 182]. There are three regions in BICD2 containing coiled-coils: CC1 on the N-terminal end, a C-terminal region (CC3), and a central CC2 region that overlaps the NT and CT domains. To localize the region of BICD2 to which the HIV-1 capsid binds, I ectopically expressed full length BICD2 and portions corresponding to the individual NT and CT domains, and a region encoding only CC2 as N-terminal HA-tagged proteins in 293T cells. Cell extracts were prepared and

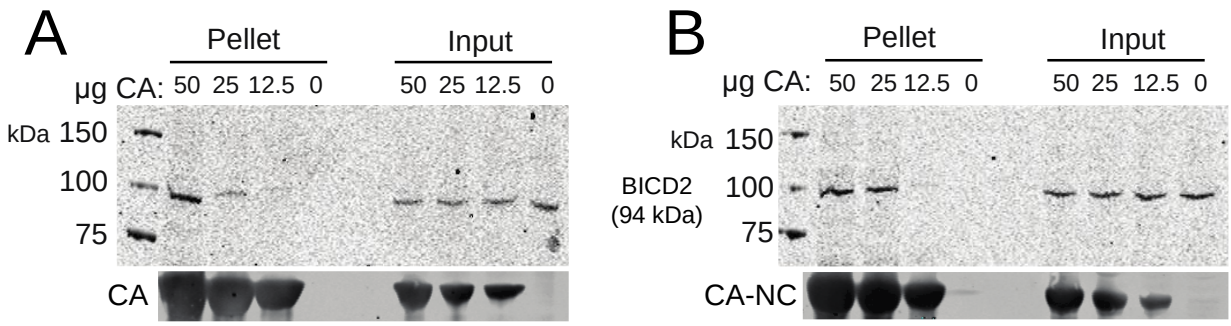

Figure 3-6 BICD2 binds to the HIV-1 capsid. Capsid-like protein assemblies were titrated and incubated with 293T cell extracts. The reactions were then centrifuged, and the pelleted material was washed once and subjected to immunoblot analysis. Endogenous cellular BICD2 was probed for interaction with CA (A, CA tubes; B, CA-NC tubes). Representative immunoblots from three independent experiments are shown.

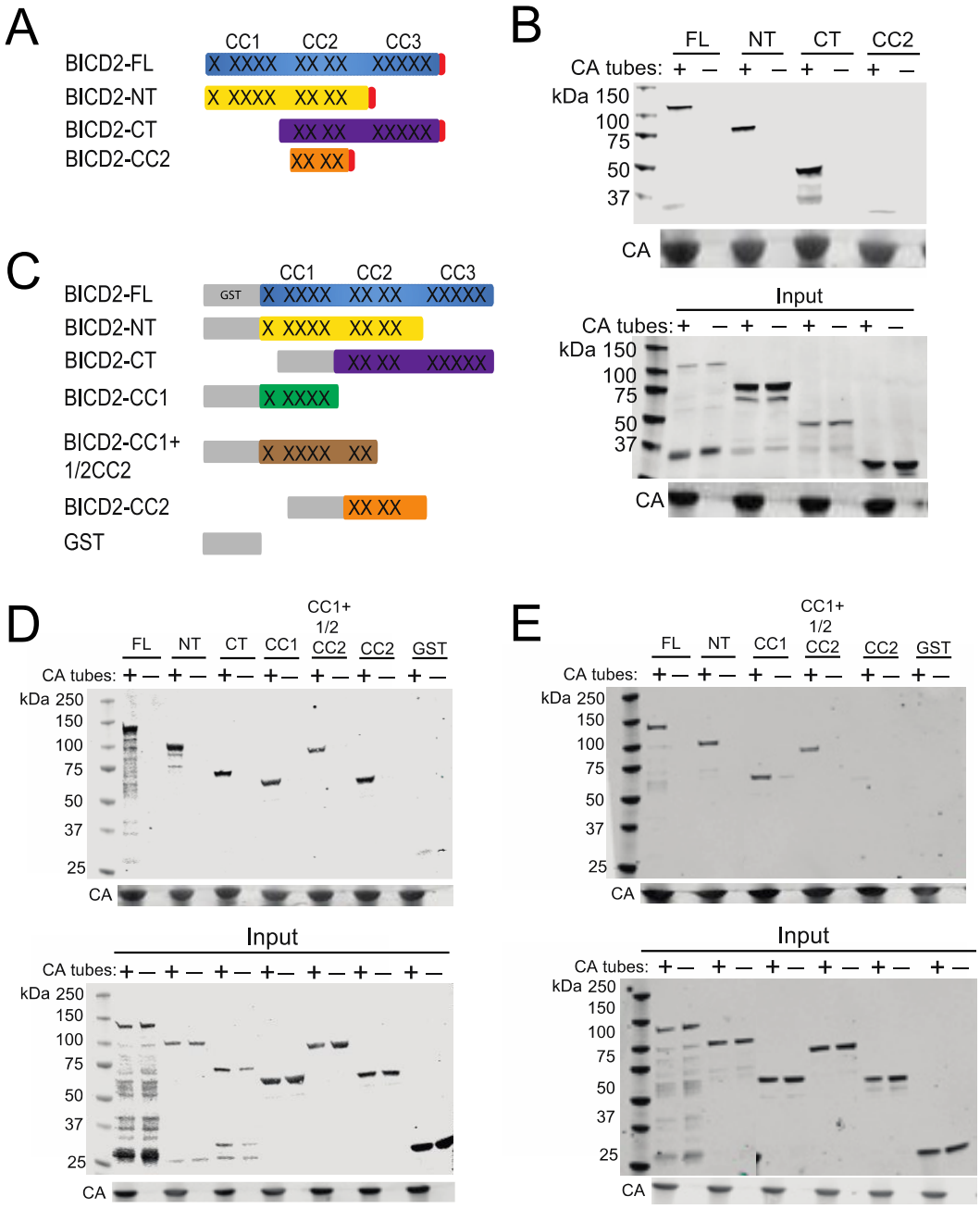

Figure 3-7 Analysis of BICD2 regions contributing to capsid binding. (A) Schematic representation of the HA-BICD2 constructs used in panel B. Coiled-coil regions of the protein are represented by x's. (B) BICD2-HA proteins were expressed in 293T cells and cell extracts were prepared and incubated with assembled CA tubes. Pelleted material was analyzed by immunoblotting. An antibody against HA was used to detect the proteins. (C) Schematic of GST-BICD2 fusion proteins used to study BICD2-capsid interactions. (D and E) Purified recombinant GST-BICD2 fusion proteins and GST were incubated with CA tubes, and then pelleted complexes were analyzed for association of the recombinant proteins by immunoblotting with antibody to GST. Binding reactions were performed with 150 mM NaCl (D) or 750 mM NaCl (E). Input samples corresponding to 10% of each reaction were removed prior to pelleting. Representative immunoblots from three independent experiments are shown.

utilized in CA tube binding assays (Figure 3-7B). Surprisingly, I observed that NT and CT domain fragments as well as the full-length BICD2 protein cosedimented with assembled CA, suggesting that both BICD2 domains can associate with the viral capsid. However, I observed less association of the protein containing only CC2 relative to the NT and CT proteins, consistent with recently published results [82]. These results suggest that BICD2 contains two capsid binding sites.

Direct binding of BICD2 to the HIV-1 capsid *in vitro*

The capsid-binding assays described above were performed with cell extracts; thus, it was possible that one or both BICD2 domains bound the CA tubes indirectly, e.g. via association with dynactin. To assess whether both domains can directly bind to CA tubes, I expressed and purified the recombinant N-terminal GST-BICD2 fusion proteins from *E. coli* and tested them for capsid binding *in vitro*. To further define the binding domain in the NT, I engineered an additional construct encoding only CC1, and another protein containing CC1 and approximately one half of CC2 (Figure 3-7C). I also made a GST-CC2 protein (Figure 3-7C).

Binding assays with the purified recombinant proteins revealed that, at physiological salt concentrations (150 mM NaCl), all of the GST-BICD2 fusion proteins copelleted with CA tubes, but the GST control protein did not (Figure 3-7D). The observed association of the GST-CC2 with CA tubes was surprising, as I had not detected binding with the CC2 in HA-lysates (Figure 3-7B). However, the GST-CC2 construct extended beyond the portion of the HA-CC2 (336-595 vs. 340-539, respectively). To examine the relative stability of the capsid associations of the recombinant proteins, I assayed binding of several of the GST-BICD2 fusions under elevated salt conditions (750 mM NaCl). Under these conditions, the capsid association of the GST-BICD2

CC1 and CC1-2 fusions was retained, but not that of the GST-CC2 protein (Figure 3-7E). Collectively, these results indicate that BICD2 can bind the HIV-1 capsid directly via both its N-terminal and C-terminal domains, likely utilizing the CC1 and CC3 coiled-coil regions.

BICD2 promotes the association of dynein with capsid-like HIV-1 assemblies *in vitro*

If HIV utilizes BICD2 as a dynein adaptor, BICD2 should link dynein to the viral capsid. To test this hypothesis, I analyzed the effects of BICD2 depletion on the binding of dynein present in cell extracts to capsid-like assemblies in vitro. I immunodepleted BICD2 from 293T cell extracts and incubated the extracts with CA (Figure 3-8A) or CA-NC (Figure 3-8B) tubes. The tubes were then pelleted, and proteins in the pelleted complexes were separated by SDS-PAGE and analyzed by immunoblotting. I observed reduced binding of the dynein intermediate chain (middle) in BICD2-depleted extracts to CA and CA-NC tubes, suggesting that BICD2 links the HIV-1 capsid to dynein. Analysis of the input samples demonstrated that BICD2 was effectively immunodepleted from the extracts, and that levels of dynein intermediate chain were unaltered by BICD2 depletion.

Discussion

In these analyses I sought to determine the mechanism of BICD2's action in HIV-1 infection. I performed two types of cell imaging analysis, the results of which indicate that the dynein-dynactin-BICD2 complex promotes intracytoplasmic movement to the nucleus (Figures 3-3 and 3-4). First, using fixed cell imaging, I showed that HIV-1 particles exhibit a greater average distance from the nuclear envelope in cells depleted of DYNC1H1 or BICD2. Second, my live imaging studies indicated that of the fraction of virus particles that exhibit movement

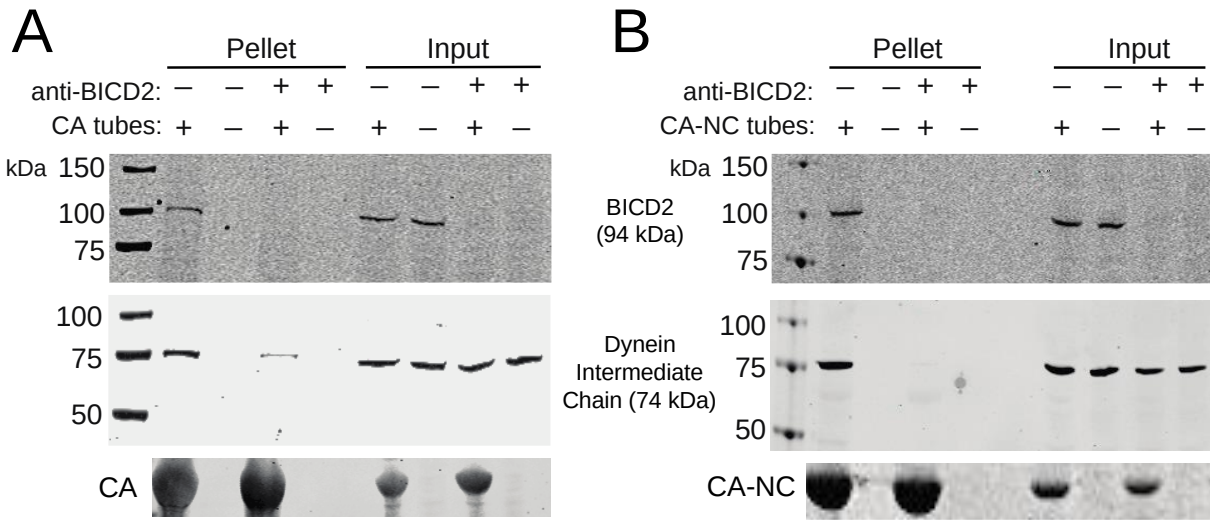

Figure 3-8 BICD2 facilitates association of dynein with capsid-like protein assemblies *in vitro*. (A and B) 293T lysates were immunodepleted for BICD2 before incubation with CA tubes (A, CA; B, CA-NC). The reactions were then centrifuged, the pellets washed once, and the proteins were separated by SDS-PAGE and analyzed by immunoblotting. Blots were probed with antibodies to BICD2 to test for depletion (top), dynein intermediate chain to test for binding (middle), and CA (bottom). Input samples corresponding to 10% of each reaction were removed prior to pelleting. Representative immunoblots from three independent experiments are shown.

within the cell was reduced in the depleted cells, and that particles that were moving exhibited reduced retrograde motion. Combined with the viral DNA analysis, these observations indicate that the failure of the virus to enter the nucleus can be mainly attributed to a trafficking defect vs. a specific impairment in nuclear import. Nonetheless, I have not excluded a direct effect of the dynein complex on HIV-1 nuclear entry.

My results indicate that BICD2 interacts directly with the viral capsid. I observed an association of native cellular BICD2 with CA assemblies in vitro, and recombinant purified BICD2 also bound to the assemblies. Using purified GST-BICD2 fusion proteins, I also observed that proteins containing only the N-terminal or C-terminal regions of BICD2 associated with HIV-1 capsid assemblies (Figures 3-6 and 3-7). The C-terminal region of BICD2 normally is responsible for cargo binding, while the N-terminal region engages dynein-dynactin. These two regions can interact with one another for autoinhibition, and previous models posit that BICD2 must interact with cargo before engaging the dynein-dynactin complex, thereby ensuring efficient tethering [122]. The presence of capsid binding sites in both the C-terminal and N-terminal of BICD2 suggests that the capsid may bind in a canonical manner to the BICD2 C-terminal site, but it can also bind in a non-canonical way to the BICD2 N-terminus. As the N-terminal site would not be available for binding naturally until cargo is bound, this suggests that the HIV-1 capsid must first hijack transport of a cellular cargo, and binds after the initial cargo releases the auto-inhibition of BICD2.

Dynein adaptors link specific cargo to the dynein-dynactin complex, resulting in dynein activation and its processive movement along microtubules. My data demonstrate that the adaptor protein BICD2 is important for HIV-1 infection. HIV-1 capsid-like assemblies bound to dynein chains, the dynactin component ACTR1A, and BICD2 in cell extracts (Figures 3-5, 3-6)

and to recombinant BICD2 *in vitro* (Figures 3-7). These observations suggested that BICD2 links the viral capsid to the dynein complex. Importantly, I also observed that immunodepletion of BICD2 in lysates reduced the binding of dynein intermediate chain to HIV-1 capsid-like assemblies (Figure 3-8). This result demonstrates that binding of dynein to the viral capsid depends on BICD2, suggesting that BICD2 tethers the viral core to dynein. BICD2 interacts directly with DCTN2/dynamitin [119, 122], and a current model proposes that dynactin links BICD2 to dynein and activates movement, thereby promoting cargo recruitment and transport. It will be of interest to characterize the interactions of additional dynein and dynactin components with HIV-1 capsid assemblies and to determine whether the associations depend on BICD2.

CHAPTER IV

CONCLUSIONS AND FUTURE DIRECTIONS

HIV-1 infection depends on the virus successfully reaching the nucleus for nuclear import and integration. To get there, HIV depends on the active transport of microtubule motor proteins dynein and kinesin-1[51, 60]. When I began this project, little was known about the key players in this transport, and even less about the mechanisms. I chose to focus on identifying the components of the dynein-dynactin-adaptor complex required for infection and transport. My first aim was to identify the components of the dynein-dynactin complex and the specific adaptor or adaptors required for infection. My second aim was to identify the mechanism for those components in HIV-1 infection. My work has accomplished these goals by determining the dynein heavy chain, components of the dynactin shoulder complex and Arp1 backbone, and BICD2 are the important players in HIV-1 infection.

The observations presented here suggest a model in which the HIV capsid binds BICD2, through either its N-terminal or C-terminal domain, thereby relieving the autoinhibition of BICD2. BICD2 can then bind the dynein-dynactin complex. The dynactin shoulder complex and ARP1 backbone have been shown to be important for linking BICD2 to dynein [111]. I found that this region of dynactin was important for HIV-1 infection, suggesting that BICD2 binding to dynein through this region is critical for infection. After HIV-1 capsid-BICD2 is linked to the dynein-dynactin complex, BICD2 can activate dynein movement in the retrograde direction. This transport is critical for HIV-1 to reach the nucleus for infection.

Although my data support the binding of BICD2 to the HIV-1 capsid, there is still much to be learned in this area. The finding that both the N-terminal and C-terminal regions of BICD2 can bind the capsid was surprising, as the N-terminal is canonically thought to bind dynein and dynactin, and the C-terminal cargo [12]. Since HIV-1 is a foreign cargo usurping the transport pathway, it may not act in canonical ways when it utilizes transport machinery.

For adaptor mediated transport, binding between the adaptor and cargo must occur [49]. Although I have seen that BICD2 is important for transport and binds the HIV-1 capsid, the link between the two observations has not yet been established. To do this, ideally, I would identify either a BICD2 or HIV capsid mutant that was unable to bind. I could then assess transport and infection defects in the presence of this mutant. In order to determine a BICD2 mutant, I will need to further define the specific region or regions on BICD2 that are important for the binding to the HIV-1 capsid. Smaller constructs can be designed and analyzed for their binding to the capsid until a region of several amino acids is determined. From there, specific site substitutions may lead to an inhibition of binding. This mutant could then be added back into BICD2 knock-down cells to determine if HIV-1 transport or infection was impaired. This will determine if the specific binding regions found *in vitro* contribute to the binding *in vivo*, and if those binding interactions are biologically relevant.

Identifying an HIV-1 capsid mutant that fails to bind BICD2 may prove to be less straightforward due to a loss of assembly and function with truncated versions of CA. The oligomeric state of CA required for binding BICD2 has not yet been determined. Several constructs of CA exist that allow for the formation of monomer, dimer, pentamer, and hexameric structures, in addition to the lattice tubes used in these assays. Binding assays with these proteins would reveal the type of binding occurring between the capsid and BICD2, which may

begin to inform where a capsid mutant would be. Additionally, structural-based analysis between BICD2 and the capsid may reveal specific amino acid interactions. Finally, there are several HIV-1 mutant viruses that have unexplained infection and/or nuclear import defects that need to be screened for their dependence on BICD2 for infection. If a mutant was found that was unaffected by BICD2 knockdown, it may suggest that it had an impairment to binding. The corresponding amino acid substitutions would then be engineered into the capsid tubes, and the binding assessed *in vitro*.

These proposed studies would link the binding of BICD2 to the HIV-1 capsid to transport and infection, therefore solidifying the role of BICD2 as an adaptor of HIV-1. Further determining the specific regions of interaction between BICD2 and HIV-1 capsid would be useful to not only understand the biology of the system, but also for therapeutic design. By disrupting the necessary binding interactions, transport can potentially be inhibited, reducing infection.

My findings indicate that the dynein-dynactin-BICD2 complex is required for transport to the nucleus. But are these the only components involved in the active transport of HIV-1? Several dynein adaptors can work in concert with other adaptors for their function. BICD2 can work with another adaptor Lis1 for transport [119]. In my initial studies, Lis1 was not important for HIV-1 infection, but BICD2 could be utilizing another unknown protein for its activity. To analyze the sufficiency of the dynein-dynactin-BICD2 complex for HIV-1 transport, a newly-developed reconstituted *in vitro* transport system could be used, in which the protein complexes are made recombinantly, and trafficking is reconstituted on microtubules attached to coverslips [118]. This approach would allow determination of all of the cellular components that are necessary for transport.

BICD2 is also known to bind Rab6a for vesicle transport, making it another viable target for a transport requirement [186]. Interestingly, my results for HIV-1 dependence on Rab6a were varied, with a range of infectivity from 9-60% depending on the knockdown conditions. Rab6a could be providing a direct binding partner to HIV-1 through the capsid or another viral protein, or may be serving in another role for transport. The importance of Rab6a in infection may also indicate that HIV-1 transport is piggy-backing on another cellular cargo transport in the cell, specifically Rab6a-based vesicle transport. HIV-1 piggy-backing on another cargo's transport would allow the virus to circumvent the need to relieve BICD2 autoinhibition and activation of the dynein complex. It may also explain how HIV-1 can utilize the N-terminal region of BICD2: i.e., if the C-terminal region is being utilized by Rab6a-vesicle binding, HIV-1 may need to utilize an unblocked region.

To determine if Rab6a is involved in HIV-1 transport, fixed and live cell imaging can be done to determine HIV-1 total movement and transport kinetics in cells depleted of Rab6a. Additionally, capsid binding analysis can be done to determine if Rab6a is able to bind from lysates indirectly, or recombinant protein directly. This will begin to determine the role of Rab6a in transport, and if HIV is binding Rab6a or piggybacking off other cargo transport. If these analyses suggest that piggybacking is occurring, other vesicle markers can be utilized in the cell to determine if HIV-1 localizes to vesicles during transport.

In addition to dynein being important for HIV-1 transport, recent studies have implicated kinesin-1 as being involved. Kinesin-1 interacts with the HIV-1 capsid through the adaptor FEZ1, and is important for overall retrograde movement to the nucleus, and infection [51]. This finding is surprising since kinesin-1 transport is in the anterograde direction, or towards the cell periphery in non-dividing cells. My research, and that of others, have determined that HIV-1 is

transported in short bursts, and that these events are often in "non-productive" directions, or making oscillatory movements [51, 83]. This phenotype may be due to the complexity of the microtubule network, or it may be important for HIV-1 transport. How the mechanism of bidirectional transport affects HIV-1 infection is not well understood. Along these lines, the way in which kinesin-1 and dynein work together for transport of HIV-1 is also poorly understood. Are they both bound simultaneously to the virion? Is there communication occurring between the motors, or is a tug-of-war ensuing? These questions are currently being answered in the motor transport field for cellular cargo, with findings supporting both models. The currently favored model suggests that some communication is occurring between the motors to activate each motor at specified times, potentially through the influence of adaptors [53, 54]. However, it is unknown whether HIV-1 would act in the same way as a cellular cargo for bidirectional transport.

My research strongly suggests that the HIV-1 capsid is an important binding partner for BICD2 for transport. As it traverses the cytoplasm, the HIV-1 capsid undergoes a disassembly process called uncoating, in which CA protein is shed. Current models suggest that an uncoating event occurs rapidly after virion entry into cells (~30 minutes), and subsequent loss of CA later before nuclear entry [34]. Some CA is still associated with the PIC upon nuclear entry [35, 187, 188]. Whether the remaining CA is enough for BICD2 to bind is not established. BICD2 may remain associated with the HIV PIC to transport all the way to the nucleus, but if it isn't able to bind, another mechanism may need to take over. I demonstrated that BICD2 binds to the HIV-1 capsid, but BICD2 may also bind other viral proteins that remain associated with the PIC. Binding between BICD2 and integrase or Vpr needs to be assessed, as these components remain associated with the PIC as well.

Alternatively, another set of adaptor-viral protein interactions could occur for late transport. These may not include either BICD2 or the HIV-1 capsid. For instance, an interaction between the dynein light chain and integrase has been reported to be important for HIV-1 infection, reverse transcription, and delays uncoating [77]. The interaction has not been assessed for its role in transport, but may represent a mechanism for binding after CA is lost. Understanding the interactions occurring in transport after uncoating will enrich my knowledge of the HIV-1 lifecycle and may reveal new targets for therapeutic design.

In summary, my work has revealed a new mechanism for HIV-1 transport. The dynein-dynactin-BICD2 complex is important for transport to the nucleus, and infection. BICD2 interacts with the HIV-1 capsid, suggesting this interaction is important to link the virion to the complex for transport. While I have some understanding of the HIV-1 transport process, much is still to be learned. Cellular transport is a complicated process, and understanding motor activation and bidirectional transport for cellular cargo will aid in understanding of HIV-1 transport, and whether HIV-1 "follows the rules" set forth by cellular cargo.

CHAPTER V

MATERIALS AND METHODS

Plasmids. HIV-GFP is an Env-defective HIV-1 proviral construct encoding the green fluorescent protein (GFP) in place of *nef* [32]. Plasmid NL43-GFP was constructed by replacing the SalI-BamHI region of HIV-GFP with that from pNL4-3, restoring the Env open reading frame. The VSV-G expression plasmid pHCMV-G was provided by Dr. Jane Burns (University of California, San Diego) [189]. The plasmids GFP-Vpr and S15-mCherry were obtained through the NIH AIDS Reagent Program, Division of AIDS, NIAID, NIH from Dr. Thomas Hope [185]. The plasmid psPAX2 was obtained through the NIH AIDS Reagent Program from Dr. Didier Trono. The plasmid pVPack-GP was obtained from Agilent Technologies. The SIV plasmid SIV 239IG, encoding GFP, was provided by Paul Bieniasz [190]. The MLV transfer vector construct pBABE-EGFP was constructed by inserting a BamHI-EcoRI fragment from pHR'-CMV-GFP [191] into pBABEpuro [192].

A cDNA encoding human BICD2 (Dharmacon) was cloned into EGFP-C1 (Clontech) via Gibson assembly at sites EcoR1 and Kpn1 to make EGFP-C1-BICD2. This plasmid was a gift from Dr. Ryoma Ohi. For construction of CMX-HA, an oligonucleotide duplex encoding the influenza virus hemagglutinin (HA) epitope tag sequence YPYDVPDYA was inserted into the CMX-PL1 plasmid at the KpnI and NheI sites. BICD2, BICD2-NT, BICD2-CT, and BICD2-CC2 sequences, encoding amino acids 1-824, 1-580, 485-824, and 340-539 respectively, were PCR-amplified from EGFP-C1-BICD2 and inserted into the CMX-HA plasmid at the EcoRI and

KpnI sites in frame with the hemagglutinin epitope tag sequence. GST-BICD2 fusion proteins were constructed as follows: GST-BICD2 encoding full length BICD2 (1-824); GST-NT (1-580); GST-CT (485-824); GST-CC1 (1-271); GST-CC1.5 (1-468); GST-CC2 (336-595). GST-BICD2 fusion proteins were PCR amplified from BICD2-CMX-PL1 and inserted into pGEX-6X at the BamHI and EcoRI sites. Oligonucleotide sequences used for cloning are listed in Appendix Table 1.

The recombinant mutant CA 14C/45C was made by introduction of cysteine mutations into pET21a(+) HIV-1 CA at positions 14 and 45 [193]. The HIV-1 CA-NC expression plasmid WISP-98-68 [6] was a kind gift from Wes Sundquist.

Cells and viruses. TZM-bl cells (1), Jurkat cells (2), and GHOST CXCR4+ CCR5+ cells (3) were obtained through the NIH AIDS Reagent Program, Division of AIDS, NIAID, NIH, from Dr. John C Kappes, Dr. Xiaoyun Wu, and Tranzyme Inc (1) [194-198]; Dr. Arthur Weiss (2) [199]; and Dr. Vineet N. KewalRamani and Dr. Dan R. Littman respectively (3) [200]. A431-CD4 cells were generated from A431 cells (ATCC) by retroviral transduction with pBABE-CD4 and selection in puromycin. Primary human fibroblasts were purchased from Advanced BioMatrix, Inc. 293T cells were purchased from ATCC. 293T, A431-CD4, GHOST CXCR4+ CCR5+, primary human fibroblasts and TZM-bl cells were cultured in Dulbecco's modified Eagle's medium (DMEM) supplemented with 10% fetal bovine serum (FBS), 100 IU/ml penicillin and 100 µg/ml streptomycin. Jurkat cells were cultured in Roswell Park Memorial Institute (RPMI) medium supplemented with 10% fetal bovine serum (FBS), 100 IU/ml penicillin and 100 µg/ml streptomycin. Viruses for fixed cell imaging studies were produced by

cotransfection of HIV-GFP (8 µg) with pHCMV-G (2 µg), GFP-Vpr (2 µg), and S15-mCherry (1 µg). Viruses for use in live cell imaging studies were produced by cotransfection of psPAX2 with pHCMV-G, GFP-Vpr, and S15-mCherry. HIV-1 stocks were clarified through 0.45 μm pore-sized filters, assayed for p24 antigen using an enzyme-linked immunosorbent assay (ELISA) and stored at -80°C until use. Murine leukemia reporter virus (MLV-GFP) was produced by cotransfection of pVPack-GP (Agilent Technologies) with pBABE-EGFP and pHCMV-G. SIV-GFP was produced by cotransfection with SIV 239IG and pHCMV-G.

Recombinant proteins. GST-BICD2 fusion proteins, recombinant HIV-1 CA protein encoding substitutions of Cys for positions 14 and 45 (14C/45C), and recombinant HIV-1 CA-NC were expressed in *E. coli* using induction by isopropyl β-D-1 thiogalactopyranoside (IPTG 1 mM, GoldBiotechnology). Cells were lysated by sonication, using the Sonic Dismembrator Ultrasonic Processor, and lysates cleared by centrifugation for 1 hr at 15,000 rpm at 4°C. GST-BICD2 constructs were purified by batch method on glutathione agarose beads as recommended by the bead manufacturer (Pierce). CA and CA-NC proteins were purified by anion exchange chromatography as previously described [6, 193].

siRNA transfection and knockdown efficiency screening. All siRNAs were purchased from Dharmacon (ON-TARGETplus siRNAs). Pools of four individual siRNA duplexes (SMARTpool) were used for initial screening of targets, and specific targets were verified using the four individual siRNA duplexes from the pool. The siRNA sequences are listed in Appendix Table 2. TZM-bl cells were transfected with 40 nM siRNA and Dharmafect 1 transfection reagent and washed after 16 hours. Cells were cultured for either 48 h (only in initial screening)

or 72 h before virus inoculation or cell harvesting for knockdown efficiency analysis. To quantify mRNA levels, cDNA was synthesized (Applied Biosystems), and SYBR green qPCR was performed for each gene of interest and standardized against non-targeting siRNA control, with GAPDH levels quantified as an internal control. The primers used for mRNA quantification analysis are listed in Appendix Table 3. For protein expression analysis, cytoplasmic extracts were prepared by lysing cells in NP-40 buffer (150 mM NaCl, 50 mM Tris-HCl, pH 8.0, 1% NP40) containing protease inhibitor cocktail (Roche) for 30 min on ice. Samples were centrifuged at 19,000 x*g* for 5 min at 4°C to remove nuclei, and proteins in the supernatants were separated by SDS-PAGE on 4-20% gradient gels (Genscript) and analyzed by immunoblotting.

Infection assays. Cells were seeded in a 96-well plate at 10,000 cells per well. Following one day of culture, cells were inoculated with GFP-encoding virus (native Env HIV-1, 200 ng/well; VSV-G pseudotyped viruses 0.5 ng/well +8 ug/ml polybrene) and cultured for 48 h. No polybrene treatment was utilized with native enveloped HIV-1 in order to ensure that the route of viral entry was not affected. Cells were detached with trypsin-EDTA (100 μl) and fixed with an equal volume of 4% paraformaldehyde. The extent of infection was assayed by flow cytometry for GFP expression using an Accuri C6 flow cytometer. At least 7,000 cells were analyzed for each sample. For infections including the dynein inhibitor ciliobrevin D, cells were pretreated with indicated amounts of ciliobrevin D (Sigma) for 1 hour, then inoculated. Cells were treated as before for flow cytometry analysis. For luciferase analysis, cells were washed once in PBS and lysed in 30µl TBS (50mM Tris-HCl [pH 7.8], 130mM NaCl, 10mM KCl, 5mM $MgCl_2$), containing 0.5% Triton X-100. Luminescence was determined using an Lmax luminometer

(Molecular Devices) for 5 seconds after injection of 200ul Solution 1 (75mM Tris-HCl [pH 8], 8.3mM MgOAc, 4mM ATP) and 80ul Solution 2 (1mM D-Luciferin (GoldBio)). Infectivity values were determined as the ratio of Arbitrary Light Units (ALU) per ng p24 at doses of virus corresponding to the linear range of luciferase signals from each assay.

PCR quantitation of nuclear entry and reverse transcription in target cells. TZM-bl cells were transfected with siRNA for 72 hours then inoculated with 40 ng of DNase I-treated HIV-1 pseudotyped with VSV-G. Cells were harvested 8 h after infection for second strand-transfer analysis, or 24 hours after infection for 2-LTR circle analysis. For harvesting, cells were washed with 1X PBS then treated with qPCR lysis buffer (50 mM KCl, 1.5 mM $MgCl_2$, 1.5 mM Tris-HCl pH 8.0, 0.45% NP40, and 0.45% Tween-20) containing proteinase K (1 mg/ml) for 1 h at 57°C. Samples were then incubated at 95°C for 15 min to inactivate proteinase K, and stored at -80°C. HIV-1 DNA in the samples was quantified by real-time PCR with SYBR green detection on a Stratagene MX3000p instrument. GAPDH DNA levels quantified by real-time PCR were used to normalize the total DNA in sample values. To control for possible contaminating plasmid DNA in the virus inocula, the reverse transcriptase inhibitor Efavirenz (1 μM) was added to some cultures at the time of infection.

Trafficking Analysis, fixed-cell imaging and live-cell imaging. TZM-bl cells were transfected for with 40 nM siRNA and cultured for 72 h prior to virus inoculation. One day before infection, cells were detached with trypsin, reseeded onto coverslips (fixed cell) or MatTek dishes (live cell) and allowed to adhere overnight. For fixed cell analysis, the cells were spinoculated with HIV-GFP(VSV-G) dual-labeled with GFP-Vpr and S15-mcherry at 800 x*g* for 30 minutes at

15°C to allow virus adhesion but not entry. After spinoculation, media on the cells was replaced, and the cultures were incubated for an additional 1 h at 37°C. Cells were washed and fixed with methanol at -20°C for 10 min and stained with 500 nM 4',6-diamidino-2-phenylindole (DAPI) to visualize nuclei. Stained cells were mounted in Gelvatol [13.3 mg/ml polyvinyl alcohol, 0.67 M Tris-HCl pH 8.6, 0.33 mg/ml glycerol, 2.5% 1,4-diazabicyclo[2.2.2]octane (DABCO)]. Images were acquired with a DeltaVision Elite image restoration system (GE Healthcare) equipped with a 60X 1.4 numerical aperture lens (Olympus) and a Cool SnapHQ2 charge-coupled device camera (Photometrics). Z-sections spaced 200 nm apart were acquired and deconvolved with SoftWorx (GE Healthcare). Maximum intensity z-projections were generated with Fiji [201], and distance of particles from the nucleus was measured. Particles exhibiting detectable mCherry fluorescence were omitted from analysis.

Two independent experiments were performed, each with >20 cells/condition analyzed, and >400 particles analyzed per condition. For live cell analysis, cells were spinoculated with psPax2 VSVG dual-labeled with GFP-Vpr and S15-mcherry for 30 min and then cultured at 37°C for 20 min before imaging. Live cell imaging was performed in the presence of CO_2 at 37°C in FluoroBrite DMEM medium (ThermoFisher) supplemented with 10% FBS and 7 mM Hepes-KOH, pH 7.7, using the DeltaVision Elite system. Images were captured every 0.5 s for a period of 2.5 min. Images to test for mCherry particle signal were taken immediately before the 2.5 min time frame. Particles displaying mCherry signal were considered to be unfused and were excluded from track analysis. Additionally, any particles that were not present at the start of imaging were excluded because their fusion status could not be determined. Images were taken of various individual cells over the course of one hour. Tracking was analyzed by TrackMate [202] in Fiji, and tracks were classified as retrograde or anterograde trajectories. The

distances of these trajectories and the number of trajectories were used for analysis. Two independent experiments were performed, each with >20 cells/condition analyzed, and >300 tracks analyzed for each condition. I observed efficient virion labeling efficiency, with 95-99% of particles containing both labels, and an average of 98%. At the 1 h timepoint, a fusion rate (loss of S15-mCherry signal) of 44-68% was observed, with no significant fusion differences occurring between the nontargeting and knockdown conditions.

***In vitro* binding assay.** To prepare protein extracts, 293T cells were detached with trypsin-EDTA, resuspended in complete medium, washed in PBS, and resuspended in 5x volume hypotonic buffer (10 mM Tris-HCl pH 7.5, 5 mM $MgCl_2$, 10 mM NaCl), dounce homogenized with 25 strokes with the tight pestle, and precleared by centrifugation for 15 minutes at 4°C in a microfuge (18,800 x*g*). Extracts were stored at -80°C until further use. HIV-1 CA (14C/45C) protein was assembled under high salt conditions (1 M NaCl, 50 mM Tris-HCl, pH 8), as previously described [203]. HIV-1 CA-NC was assembled by dilution to 0.3 mM concentration at 37°C for 1 h (500 mM NaCl, 50 mM Tris-HCl, pH 8, 60 µM TG50 (purchased from IDT). Crosslinked recombinant CA assemblies were incubated with cell extracts or purified GST proteins in CA tube binding buffer (50 mM Tris, pH 8.0, 150 mM NaCl, 5 mM $MgCl_2$, 0.5 mM EDTA) or CA-NC tube binding buffer (50 mM Tris, pH 8.0, 500 mM NaCl, 5 mM $MgCl_2$, 0.5 mM EDTA) for 1 h at room temperature. The higher salt concentration was required to prevent CA-NC tube disassembly. Reactions were then centrifuged for 5 min at 10,000 x*g*, and the pellets were rinsed once with binding buffer to remove unbound proteins. Pelleted proteins were separated by SDS-PAGE and analyzed by immunoblotting.

Immunodepletion of BICD2 from cell extracts. Protein A-Agarose (Santa Cruz Biotechnology) (40 µl packed beads) was washed twice in 3x volume binding buffer (10 mM Tris-HCl pH 7.5, 5 mM $MgCl_2$, 10 mM NaCl) and centrifuged for 5 min at 10,000 *xg*. Beads were resuspended in 1x volume of binding buffer and bound to BICD2 antibody (15 µg) for 1 hr rotating at 4°C or unbound beads as a negative control. Beads were then washed two more times in binding buffer to remove unbound antibody. Freshly prepared 293T cell extract (2.5 mg total protein) was then incubated with the BICD2 antibody-bound beads or beads alone for mock depletion overnight at 4°C with rotation. Beads were pelleted for 5 min at 10,000 *xg* and the supernatant recovered for use in binding reactions. The BICD2-depleted extracts were analyzed for BICD2 and dynein by immunoblotting.

Visualization of CA tube assembly by electron microscopy. Crosslinked recombinant CA assemblies were visualized by negative stain electron microscopy to check for tube assembly. Samples were stained with 0.7% uranyl formate and visualized on a FEI Morgagni electron microscope at 100 kV at a magnification of 22000X. Images were recorded on an ATM 1000x1000 CCD camera.

Antibodies and immunoblotting. To the binding assay pellets, an equal volume 2x Laemmli buffer was added followed by heating at 100°C for 5 min. Samples were loaded onto a 4-20% polyacrylamide gel (GenScript) for SDS-PAGE. After separation, the proteins were transferred to nitrocellulose membranes (Perkin Elmer) and probed with the following antibodies: BICD2 (Abcam 117818; 5 µg/ml), DYNC1H1 (Sigma D1667; 1:1000 dilution), DIC (Abcam 23905; 1 µg/ml), ACTR1A (Abcam 227425; 1:2000 dilution), HA (Sigma 3F10; 200 ng/ml), GST

(Abcam 3416; 1:5,000 dilution), and CA (183-H12-5C, NIH AIDS Research and Reference Reagent Program; 1:5,000 dilution). For protein expression analysis, the same antibodies as above were used, as well as dynamitin/DCTN2 (Abcam 133492; 1:2000 dilution), DCTN3 (Abcam 124674; 1:2000 dilution), and GAPDH (Thermo Fisher A21994; 5 ug/ml). Antibody complexes were detected with the appropriate IR dye-conjugated secondary antibodies (LI-COR Biosciences) and detected by scanning with a LI-COR Odyssey imaging system.

Statistical analysis. Statistical significance was assessed by Student's t test when compared individual targets to the non-targeting siRNA control. Results are represented as mean values and standard deviations. A one-way ANOVA was performed for statistical analysis of the imaging results, followed by a Dunnett's multiple comparisons test. Statistical analysis was performed with GraphPad Prism software.

APPENDIX

Table A-1 Oligonucleotides used in cloning procedures
Construct: EGFP-C1-BICD2
For 5’-GACTCAGATCTCGAGCTCAAGCTTCGAATTCGATGTCGGCGCCGTCA-3’
Rev 5’-TAGATCCGGTGGATCCCGGGCCCGCGGTACCCTAATCACAGTAAATGCTGTG-3’
Construct: CMX-HA
For 5’-GGCTACCCATACGATGTTCCAGATTACGCTTAGATCGATG-3’
Rev 5’-CTAGCATCGATCTAAGCGTAATCTGGAACATCGTATGGGTAGCCGGTAC-3’
Construct: BICD2 CMX-HA
For 5'-ATAGGATCCGGCATGTCGGC-3'
Rev 5'-ATAGGTACCATCACAGTAAATGCTGT-3'
Construct: BICD2 NT (1-580) CMX-HA
For 5'-ATAGGATCCGGCATGTCGGC-3'
Rev 5'-ATAGGTACCCCGGCCACG-3'
Construct: BICD2 CT (485-824) CMX-HA
For 5'-ATAGGATCCGGATGGTCTCCCTG-3'
Rev 5'-ATAGGTACCATCACAGTAAATGCTGT-3'
Construct: BICD2 CC2 CMX-HA
For 5'-CTAGGATCCGGCATGCTCAGTGAGCTCAACATCTCTG-3'
Rev 5'-CTAGGTACCGGCCAGCTCCTCACTGAAG-3'
Construct: GST-BICD2
For 5’-ATGGATCCTCGGCGCCGTC-3’
Rev 5’-GGGAATTCCTAATCACAGTAAATGCTG-3’
Construct: GST-BICD2 NT
For 5’-ATGGATCCTCGGCGCCGTC-3’
Rev 5’-AAGAATTCCTACCGGCCACGCGC-3’

Table A-1 cont'.d
Construct: GST-BICD2 CT
For 5'-ATGGATCCGTCTCCCTGCTAGAGAAG-3'
Rev 5'-GGGAATTCCTAATCACAGTAAATGCTG-3'
Construct: GST-BICD2 CC1
For 5'-ATGGATCCTCGGCGCCGTC-3'
Rev 5'-GGGAATTCCTAGAAGGAGTCATTGATGC-3'
Construct: GST-BICD2 CC1 + ½ CC2
For 5'-ATGGATCCTCGGCGCCGTC-3'
Rev 5'-GGGAATTCCTACTGGGCCTCACG-3'
Construct: GST-BICD2 CC2
For 5'-ATGGATCCGTCTCCGACCTACTCAGT-3'
Rev 5'-AAGAATTCCTACGGCCCGCCTCAG-3'

Table A-2 Sequences of siRNAs from Dharmacon					
Pool Catalog Number	Duplex Catalog Number	Gene Symbol	Gene Accession	GI Number	Sequence
L-006828-00	J-006828-05	DYNC1H1	NM_001376	33350931	GAUCAAACAUGACGGAAUU
L-006828-00	J-006828-06	DYNC1H1	NM_001376	33350931	CAGAACAUCUCACCGGAUA
L-006828-00	J-006828-07	DYNC1H1	NM_001376	33350931	GAAAUCAACUUGCCAGAUA
L-006828-00	J-006828-08	DYNC1H1	NM_001376	33350931	GCAAGAAUGUCGCUAAAUU
L-026503-01	J-026503-09	DYNC2H1	XM_931085	89034274	GGGUAUAGUUCUACGAAGA
L-026503-01	J-026503-10	DYNC2H1	XM_931085	89034274	GAGGCUAGUAGUCGAAUUA
L-026503-01	J-026503-11	DYNC2H1	XM_931085	89034274	UUACCAAGCAGUACGGCAA
L-026503-01	J-026503-12	DYNC2H1	XM_931085	89034274	GAAGAUGACACACGAGGUA
L-019799-00	J-019799-05	DYNC1I1	NM_004411	4758177	GGAAGGCACUGUUGAGUUA
L-019799-00	J-019799-06	DYNC1I1	NM_004411	4758177	GGAAAUUCGUGCUAACAGA
L-019799-00	J-019799-07	DYNC1I1	NM_004411	4758177	CAAGGGAAGUAGUGUCCUA
L-019799-00	J-019799-08	DYNC1I1	NM_004411	4758177	CGGGAGACGUCAAUAACUU
L-012574-00	J-012574-05	DYNC1I2	NM_001378	24307878	GUAAAGCUUUGGACAACUA
L-012574-00	J-012574-06	DYNC1I2	NM_001378	24307878	GAUGUUAUGUGGUCACCUA
L-012574-00	J-012574-07	DYNC1I2	NM_001378	24307878	GCAUUUCUGUGGAGGGUAA
L-012574-00	J-012574-08	DYNC1I2	NM_001378	24307878	GUGGUUAGUUGUUUGGAUU
L-021045-01	J-021045-09	DYNC1LI1	NM_016141	7705852	ACGAGAUAGCGUCGGGCAA
L-021045-01	J-021045-10	DYNC1LI1	NM_016141	7705852	CUAAACCACCUGUUCGAAA
L-021045-01	J-021045-11	DYNC1LI1	NM_016141	7705852	GAAGAAAUACUGCGUCACA
L-021045-01	J-021045-12	DYNC1LI1	NM_016141	7705852	CGGAAUAUGCUAAGAAAAC
L-020110-00	J-020110-05	DYNC1LI2	NM_006141	38505264	CACGAGAGCUUCUGAAUCU
L-020110-00	J-020110-06	DYNC1LI2	NM_006141	38505264	CCUCAUGACUAAACUACAA
L-020110-00	J-020110-07	DYNC1LI2	NM_006141	38505264	UGUGAAACCUCCCGUGAGA
L-020110-00	J-020110-08	DYNC1LI2	NM_006141	38505264	GAAAUGGGCUAGUGUUUUA
L-005281-00	J-005281-06	DYNLL1	NM_003746	83267869	GUUCAAAUCUGGUUAAAAG
L-005281-00	J-005281-07	DYNLL1	NM_003746	83267869	GAAGGACAUUGCGGCUCAU
L-005281-00	J-005281-08	DYNLL1	NM_003746	83267869	GUACUAGUUUGUCGUGGUU
L-005281-00	J-005281-09	DYNLL1	NM_003746	83267869	CAGCCUAAAUUCCAAAUAC

L-010586-00	J-010586-06	DYNLRB1	NM_014183	29570778	CGAAUAAGCCACUCUCUUG
L-010586-00	J-010586-07	DYNLRB1	NM_014183	29570778	CGUGAACACAGAAGGCAUU
L-010586-00	J-010586-08	DYNLRB1	NM_014183	29570778	GAUCUCACCUUCCUUCGAA
L-010586-00	J-010586-09	DYNLRB1	NM_014183	29570778	CACCAGAUAAAGACUAUUU
L-015304-00	J-015304-05	DYNLRB2	NM_130897	18702322	GCACAGUUCGUGAUAUUGA
L-015304-00	J-015304-06	DYNLRB2	NM_130897	18702322	GAAGGUAUUCCCAUCCGAA
L-015304-00	J-015304-07	DYNLRB2	NM_130897	18702322	GAAUAUCUUCUGAUCGUCA
L-015304-00	J-015304-08	DYNLRB2	NM_130897	18702322	GAACUAUGGUUGUAAAUGC
L-019964-00	J-019964-05	DYNLT1	NM_006519	5730084	GAAGUGAGCAACAUUGUAA
L-019964-00	J-019964-06	DYNLT1	NM_006519	5730084	GACCUGCAGUCCAGCCUAU
L-019964-00	J-019964-07	DYNLT1	NM_006519	5730084	CAAUUGGUGGUAACGCUUA
L-019964-00	J-019964-08	DYNLT1	NM_006519	5730084	AAAGUGAACCAGUGGACCA
L-019957-01	J-019957-09	DYNLT3	NM_006520	5730086	GAUGGAACCUGUACCGUAA
L-019957-01	J-019957-10	DYNLT3	NM_006520	5730086	AGGAAUAAGCUUAGCGUUA
L-019957-01	J-019957-11	DYNLT3	NM_006520	5730086	GGUCCAGAAGAGCGCAUAU
L-019957-01	J-019957-12	DYNLT3	NM_006520	5730086	AUACAUAUAGAGAGCGGAA
L-012874-00	J-012874-05	DCTN1	NM_023019	13259507	CUGGAGCGCUGUAUCGUAA
L-012874-00	J-012874-06	DCTN1	NM_023019	13259507	GAAGAUCGAGAGACAGUUA
L-012874-00	J-012874-07	DCTN1	NM_023019	13259507	GCUCAUGCCUCGUCUCAUU
L-012874-00	J-012874-08	DCTN1	NM_023019	13259507	CGAGCUCACUACUGACUUA
L-012218-00	J-012218-05	DCTN2	NM_006400	34335254	UUAUGAAACUAGCGACCUA
L-012218-00	J-012218-06	DCTN2	NM_006400	34335254	UCUCAGAUCGUAUUGGAAA
L-012218-00	J-012218-07	DCTN2	NM_006400	34335254	GGACAAUACCACCCUCUUG
L-012218-00	J-012218-08	DCTN2	NM_006400	34335254	GAGGACAGGAUAUGAAUCU
L-012365-00	J-012365-05	DCTN3	NM_007234	22165423	GGUGAAGAUUCUCUACAAA
L-012365-00	J-012365-06	DCTN3	NM_007234	22165423	UAGCAGAGGAGCAGUUUAU
L-012365-00	J-012365-07	DCTN3	NM_007234	22165423	GAGGAAUACAACAAGACUA
L-012365-00	J-012365-08	DCTN3	NM_007234	22165423	GGACAGUGCUCACAUCAAA
L-015395-00	J-015395-05	DCTN4	NM_016221	19923450	GAAACUGGCACGACGUAGA
L-015395-00	J-015395-06	DCTN4	NM_016221	19923450	ACAAACAUCUUCUGAUCAA
L-015395-00	J-015395-07	DCTN4	NM_016221	19923450	GAAUUUAACCCAACGUCAA
L-015395-00	J-015395-08	DCTN4	NM_016221	19923450	GAAGUGAGAAUCAUGUCAA
L-014901-01	J-014901-09	DCTN5	NM_032486	34147426	UGUAAGAGUUGGACGUCAU

L-014901-01	J-014901-10	DCTN5	NM_032486	34147426	GCACAUGAGCCUUCGCCUU
L-014901-01	J-014901-11	DCTN5	NM_032486	34147426	GUGCUGAUGUAUUCGAAGA
L-014901-01	J-014901-12	DCTN5	NM_032486	34147426	GAAAAGUCGUAGUGUCAUA
L-012302-01	J-012302-09	DCTN6	NM_006571	18426895	AGAUGUAACUAUCGGACCU
L-012302-01	J-012302-10	DCTN6	NM_006571	18426895	GCAUAGACUAAACUGAAUA
L-012302-01	J-012302-11	DCTN6	NM_006571	18426895	AAGCAUAUGUAGGCAGAAA
L-012302-01	J-012302-12	DCTN6	NM_006571	18426895	AUAAAUGCUUACCCAGAUA
L-012074-00	J-012074-05	ACTR1A	NM_005736	13325058	GUAAGGAGGGCUACGACUU
L-012074-00	J-012074-06	ACTR1A	NM_005736	13325058	GACAACGGAUCCGGUGUGA
L-012074-00	J-012074-07	ACTR1A	NM_005736	13325058	GUACUCAGCCUUUACGCUA
L-012074-00	J-012074-08	ACTR1A	NM_005736	13325058	GGAACGAGCUGCCGAAGUU
L-012212-00	J-012212-05	CAPZA1	NM_006135	5453596	CACUAACUGUUUCGAAUGA
L-012212-00	J-012212-06	CAPZA1	NM_006135	5453596	GACGUUCGGCUACUACUUA
L-012212-00	J-012212-07	CAPZA1	NM_006135	5453596	GAUGGGCAACAGACUAUUA
L-012212-00	J-012212-08	CAPZA1	NM_006135	5453596	UCUGUACUGUUUAUGCUAA
L-011990-00	J-011990-05	CAPZB	NM_004930	4826658	GGAGUGAUCCUCAUAAAGA
L-011990-00	J-011990-06	CAPZB	NM_004930	4826658	GAAGUACGCUGAACGAGAU
L-011990-00	J-011990-07	CAPZB	NM_004930	4826658	CAAAGGAUAUCGUCAAUGG
L-011990-00	J-011990-08	CAPZB	NM_004930	4826658	CACCAUGGAGUAACAAGUA
L-010330-00	J-010330-06	PAFAH1B1	NM_000430	6031206	CAAUUAAGGUGUGGGAUUA
L-010330-00	J-010330-07	PAFAH1B1	NM_000430	6031206	UGAACUAAAUCGAGCUAUA
L-010330-00	J-010330-08	PAFAH1B1	NM_000430	6031206	GGAGUGCCGUUGAUUGUGU
L-010330-00	J-010330-09	PAFAH1B1	NM_000430	6031206	UGACAAGACCCUACGCGUA
L-020625-00	J-020625-05	NDE1	NM_017668	8923109	GGACCCAGCUCAAGUUUAA
L-020625-00	J-020625-06	NDE1	NM_017668	8923109	GCGCAGACCAAAGCCAUUA
L-020625-00	J-020625-07	NDE1	NM_017668	8923109	GCUGAAGCCUGUUCUUGGU
L-020625-00	J-020625-08	NDE1	NM_017668	8923109	GCAGCACUCUGAAGGCUAC
L-018571-00	J-018571-05	NDEL1	NM_030808	71284428	GAGACUUGCAGGCUGAUAA
L-018571-00	J-018571-06	NDEL1	NM_030808	71284428	GGACCAAGCAUCACGAAAA
L-018571-00	J-018571-07	NDEL1	NM_030808	71284428	GAAGCUAGAGCAUCAAUAU
L-018571-00	J-018571-08	NDEL1	NM_030808	71284428	GCUAGGAUAUCAGCACUAA
L-019496-00	J-019496-06	BICD1	NM_001003398	51093829	GCAAAGAGCCAAUGAAUAU
L-019496-00	J-019496-07	BICD1	NM_001003398	51093829	GCAACUGUCUCGUCAAAGA

L-019496-00	J-019496-08	BICD1	NM_001003398	51093829	GGGAGCAGAUCGCCACAUU
L-019496-00	J-019496-09	BICD1	NM_001003398	51093829	GGACUUAGAGUUUGACCAU
L-014060-00	J-014060-05	BICD2	NM_015250	51479169	AGACGGAGCGCGAACAGAA
L-014060-00	J-014060-06	BICD2	NM_015250	51479169	UAAAGAAGGUGAGCGACGU
L-014060-00	J-014060-07	BICD2	NM_015250	51479169	GCAAGUACCAUGUGGCUGU
L-014060-00	J-014060-08	BICD2	NM_015250	51479169	GGAAGGUGCUAGAGCUGCA
L-006829-00	J-006829-05	KNTC1	NM_014708	41327744	GUAAAUAACUUGCGAGAGU
L-006829-00	J-006829-06	KNTC1	NM_014708	41327744	GAUAAAGCAUGGCAGAAUU
L-006829-00	J-006829-07	KNTC1	NM_014708	41327744	CUCAAGAGAUGCUGAAUUA
L-006829-00	J-006829-08	KNTC1	NM_014708	41327744	GGAGCUAGCCCUAAGAUUU
L-003948-00	J-003948-07	ZW10	NM_004724	17136150	GCAAUAUGAUUAGCAAGAA
L-003948-00	J-003948-08	ZW10	NM_004724	17136150	GAUCAGACUGGUACUAGAA
L-003948-00	J-003948-09	ZW10	NM_004724	17136150	CGUAUCAACCGGUGAAUUU
L-003948-00	J-003948-10	ZW10	NM_004724	17136150	UAAUGGAACUCGCCUAUCA
L-019377-00	J-019377-05	ZWILCH	NM_017975	33300636	GGUAAGAUGUGACAGUUCA
L-019377-00	J-019377-06	ZWILCH	NM_017975	33300636	CCAUAGACCAUCUGAAUUU
L-019377-00	J-019377-07	ZWILCH	NM_017975	33300636	UCUACAACGUGGUGAUAUA
L-019377-00	J-019377-08	ZWILCH	NM_017975	33300636	GCUCACAAUCCUAAUAUGA
L-016970-00	J-016970-05	SPDL1	NM_017785	21361652	GGGAGAAGUUUAUCGAUUA
L-016970-00	J-016970-06	SPDL1	NM_017785	21361652	GAAAGGGUCUCAAACUGAA
L-016970-00	J-016970-07	SPDL1	NM_017785	21361652	GGAUAAAUGUCGUAAUGAA
L-016970-00	J-016970-08	SPDL1	NM_017785	21361652	CAGGUUAGCUGCUGAAUCA
L-005294-00	J-005294-05	CLIP1	NM_198240	38044111	GAAGAUGCCAUGCAGAUAA
L-005294-00	J-005294-06	CLIP1	NM_198240	38044111	CAGUAUAACUAGUGCCUUA
L-005294-00	J-005294-07	CLIP1	NM_198240	38044111	GCUCAAUAAUCAGUUGUUA
L-005294-00	J-005294-08	CLIP1	NM_198240	38044111	CGACGAAACCUUCUGAUGA
L-013511-00	J-013511-05	CLIP2	NM_032421	14702161	CCAAGAAGACCAAGCGUAU
L-013511-00	J-013511-06	CLIP2	NM_032421	14702161	GUAAGUCAGGCGAGAAGAA
L-013511-00	J-013511-07	CLIP2	NM_032421	14702161	CGUAUCGGCUUCCCAUCUA
L-013511-00	J-013511-08	CLIP2	NM_032421	14702161	GCAAUUCCGGUUCUGCAAA
L-014609-02	J-014609-21	SPTBN4	NM_025213	115430238	GGACAAGGGCAAGGACGAA
L-014609-02	J-014609-22	SPTBN4	NM_025213	115430238	CGUGGAGAACUACGAGGAA
L-014609-02	J-014609-23	SPTBN4	NM_025213	115430238	GCCUGUACGUGGCGCUCAA

L-014609-02	J-014609-24	SPTBN4	NM_025213	115430238	GUGGAUGAGCUGAUCGAGU
L-018149-01	J-018149-09	SPTBN1	NM_178313	30315657	CCUGAAAGUGAGCGCAUUA
L-018149-01	J-018149-10	SPTBN1	NM_178313	30315657	CCGCAUACGAGGAGCGUGU
L-018149-01	J-018149-11	SPTBN1	NM_178313	30315657	GGACAUGUCUUACGAUGAA
L-018149-01	J-018149-12	SPTBN1	NM_178313	30315657	GUGACAAGGCCGACGAUAU
L-009933-00	J-009933-05	SPTAN1	NM_003127	4507190	CAACAGAGGUAAGGAUUUA
L-009933-00	J-009933-06	SPTAN1	NM_003127	4507190	GAGACUAUCAGUUGGAUUA
L-009933-00	J-009933-07	SPTAN1	NM_003127	4507190	CGGGAGGCCUUCUUGAAUA
L-009933-00	J-009933-08	SPTAN1	NM_003127	4507190	GCAAUUUAAUCGCAAUGUU
L-012708-00	J-012708-05	BCAS2	NM_005872	49472833	GCAGAUACCGACCUACUAA
L-012708-00	J-012708-06	BCAS2	NM_005872	49472833	GCAUCAAGCAGUUAGAAUU
L-012708-00	J-012708-07	BCAS2	NM_005872	49472833	UGGAUGCGCUGCCGUAUUU
L-012708-00	J-012708-08	BCAS2	NM_005872	49472833	GAGAUUGAACGGACUAUUG
L-009582-01	J-009582-09	SEC23A	NM_006364	38202213	GGGCUUUGGUGGUACGCUA
L-009582-01	J-009582-10	SEC23A	NM_006364	38202213	CGAGAUGGAGUCCGAUUUA
L-009582-01	J-009582-11	SEC23A	NM_006364	38202213	CCAUAUAUUUUGAGGUUGU
L-009582-01	J-009582-12	SEC23A	NM_006364	38202213	GGAGAAUGGUUCAGGUUCA
L-009592-01	J-009592-09	SEC23B	NM_032986	66932900	CGUAAAGACCUCUCGGGAA
L-009592-01	J-009592-10	SEC23B	NM_032986	66932900	GAAAGAUAAUGCACGAUUC
L-009592-01	J-009592-11	SEC23B	NM_032986	66932900	CAGGUUGAUUAUCGAGCAA
L-009592-01	J-009592-12	SEC23B	NM_032986	66932900	GGUGAAUCAACCUGCCGAA
L-024405-01	J-024405-05	SEC24A	NM_001252231	356582354	GGACGUACAUCAAUCCUUU
L-024405-01	J-024405-06	SEC24A	NM_001252231	356582354	CCAAGAAGGUAUUACAUCA
L-024405-01	J-024405-08	SEC24A	NM_001252231	356582354	GUGGUUACCUCCAGUACAA
L-024405-01	J-024405-14	SEC24A	NM_001252231	356582354	CAGUAGUUACGACGAGAUU
L-008299-02	J-008299-18	SEC24B	NM_001042734	112382213	CUUCAGAGACCUAACGCAA
L-008299-02	J-008299-19	SEC24B	NM_001042734	112382213	CCAGAUUCAUUUCGGUGUA
L-008299-02	J-008299-20	SEC24B	NM_001042734	112382213	CUUCAUUGAUCAACGUAGA
L-008299-02	J-008299-21	SEC24B	NM_001042734	112382213	GCUAUAGAGUAAACGAUGU
L-008467-02	J-008467-19	SEC24C	NM_198597	38373670	GCACAGAGAUCCCGGUACA
L-008467-02	J-008467-20	SEC24C	NM_198597	38373670	UGGCUGAUCUAUAUCGAAA
L-008467-02	J-008467-21	SEC24C	NM_198597	38373670	CCUUUCAGGUGGAGAACGA
L-008467-02	J-008467-22	SEC24C	NM_198597	38373670	CCUGGAUCAUACCGGCAAA

L-008493-01	J-008493-09	SEC24D	NM_014822	7662658	GGUAAAUCACGGCGAGAGU
L-008493-01	J-008493-10	SEC24D	NM_014822	7662658	GAUCUCAACUGAUGAACGA
L-008493-01	J-008493-11	SEC24D	NM_014822	7662658	UUGAAGGUCAUCCGGGAAA
L-008493-01	J-008493-12	SEC24D	NM_014822	7662658	CGUUAGAUGUCAAGAGUAC
L-008787-01	J-008787-09	RILP	NM_031430	93204880	GGCCUAUGGUAUCGGGGUA
L-008787-01	J-008787-10	RILP	NM_031430	93204880	UGAAGGUGGCUGUCCGGAA
L-008787-01	J-008787-11	RILP	NM_031430	93204880	UGGCCUACUUCCAGCGGGA
L-008787-01	J-008787-12	RILP	NM_031430	93204880	AAUAAAGAACUGCCCGUAA
L-010388-00	J-010388-05	RAB7A	NM_004637	40807361	CUAGAUAGCUGGAGAGAUG
L-010388-00	J-010388-06	RAB7A	NM_004637	40807361	AAACGGAGGUGGAGCUGUA
L-010388-00	J-010388-07	RAB7A	NM_004637	40807361	GAUGGUGGAUGACAGGCUA
L-010388-00	J-010388-08	RAB7A	NM_004637	40807361	GGGAAGACAUCACUCAUGA
L-018225-00	J-018225-05	RAB7B	NM_177403	38490536	GUAGGGCUCUGUCGAGGUA
L-018225-00	J-018225-06	RAB7B	NM_177403	38490536	GAAACUCAUUAUCGUCGGA
L-018225-00	J-018225-07	RAB7B	NM_177403	38490536	UCAAUGUGGUGCAAGCGUU
L-018225-00	J-018225-08	RAB7B	NM_177403	38490536	GGAAGUAGCUCAAGGCUGG
L-003596-00	J-003596-06	MAPK8IP3	NM_033392	41350322	GCAUGGCUGUUGUGUACGA
L-003596-00	J-003596-07	MAPK8IP3	NM_033392	41350322	CAAGAACUAUGCCGAUCAG
L-003596-00	J-003596-08	MAPK8IP3	NM_033392	41350322	GCAGAGCGCAGUCACAUCA
L-003596-00	J-003596-09	MAPK8IP3	NM_033392	41350322	CGAGUGGUCUGAUGUUCAA
L-015777-01	J-015777-09	CCDC155	NM_144688	40255068	ACAUCACAUCUGCGGGAAA
L-015777-01	J-015777-10	CCDC155	NM_144688	40255068	AGAUCUUGGCUCUGCGUAA
L-015777-01	J-015777-11	CCDC155	NM_144688	40255068	CCACUGUUGCGCAGGCUUA
L-015777-01	J-015777-12	CCDC155	NM_144688	40255068	CGAGCGGGAUGGAGUGAAA
L-025277-00	J-025277-05	SUN1	NM_025154	51100963	GGUAACUGCUGGGCAUUUA
L-025277-00	J-025277-06	SUN1	NM_025154	51100963	GGUACCAGUUUGUUACUUU
L-025277-00	J-025277-07	SUN1	NM_025154	51100963	GCGCUCAGUUCCAGCUAUU
L-025277-00	J-025277-08	SUN1	NM_025154	51100963	GAAAAGACCCGACGACACA
L-021079-02	J-021079-17	RAB11FIP3	NM_014700	41281455	CGGACGAGUUCGAUGACUU
L-021079-02	J-021079-18	RAB11FIP3	NM_014700	41281455	GAUUAAAGCUGUUACUGCA
L-021079-02	J-021079-19	RAB11FIP3	NM_014700	41281455	GCUUUAAUUCCCCGAGAAA
L-021079-02	J-021079-20	RAB11FIP3	NM_014700	41281455	AGGCCAACAUUGAGCGUCU
L-016845-01	J-016845-09	HOOK1	NM_015888	34147678	CUAAUUGAGCAGCGUGAUA

L-016845-01	J-016845-10	HOOK1	NM_015888	34147678	GCAGCUUGGUUUAACGAAU
L-016845-01	J-016845-11	HOOK1	NM_015888	34147678	GAAUGAACGUAUUGAGGAA
L-016845-01	J-016845-12	HOOK1	NM_015888	34147678	GCACGUACACAAUUAGAAA
L-020408-02	J-020408-18	HOOK2	NM_001100176	154354986	GGGCCAUGGAGGAGCGAUA
L-020408-02	J-020408-19	HOOK2	NM_001100176	154354986	AGAAGAAGGACGCGGACUU
L-020408-02	J-020408-20	HOOK2	NM_001100176	154354986	UCACCUGGUUACAGACGUU
L-020408-02	J-020408-21	HOOK2	NM_001100176	154354986	GCUCCAGGGCAUCUCGGAA
L-013558-01	J-013558-09	HOOK3	NM_032410	33356164	CGUGGAAGAUUUAACGAAU
L-013558-01	J-013558-10	HOOK3	NM_032410	33356164	CCAAAGAUGAUUAUCGAAU
L-013558-01	J-013558-11	HOOK3	NM_032410	33356164	CCAAGAAGGUUCGGACAAU
L-013558-01	J-013558-12	HOOK3	NM_032410	33356164	GAUAAUUGGAGGCUAAAGA
L-013482-00	J-013482-05	MAP1A	NM_002373	45580726	CCACUGAGCAUGUCUCUUA
L-013482-00	J-013482-06	MAP1A	NM_002373	45580726	GGAGGAGACAGCAAACGUA
L-013482-00	J-013482-07	MAP1A	NM_002373	45580726	GAUAAGCCAUUCCCUCUAG
L-013482-00	J-013482-08	MAP1A	NM_002373	45580726	GUAAGACCCUCUAUAAAGC
L-016881-00	J-016881-05	MAP1S	NM_018174	50428934	CGAAAGAGGCAUCCGGUCU
L-016881-00	J-016881-06	MAP1S	NM_018174	50428934	CCACCGUGCUCUUCGAGAA
L-016881-00	J-016881-07	MAP1S	NM_018174	50428934	ACGCAAGACUGAGAAAGAA
L-016881-00	J-016881-08	MAP1S	NM_018174	50428934	CCUGCAAGGUGGAGUUCUA
L-010348-00	J-010348-07	MAP1B	NM_032010	14165455	AGAAGUAGAUCUCCCGAUU
L-010348-00	J-010348-08	MAP1B	NM_032010	14165455	CCAGAGAUAUGUCCUUAUA
L-010348-00	J-010348-09	MAP1B	NM_032010	14165455	GUACAAAGACCAAGUCAUC
L-010348-00	J-010348-10	MAP1B	NM_032010	14165455	GCUGAGAGGUCCCUUAUGU
L-020186-01	J-020186-09	TBCB	NM_001281	50428924	GGGAAACGCUACUUCGAAU
L-020186-01	J-020186-10	TBCB	NM_001281	50428924	CUACGGGUUGGACGAGAUA
L-020186-01	J-020186-11	TBCB	NM_001281	50428924	UGUAUGGAGUUGACGACAA
L-020186-01	J-020186-12	TBCB	NM_001281	50428924	CUGGAUUGGUGUCCGCUAU
L-004702-00	J-004702-07	KPNA2	NM_002266	62388891	GCAUGUGGCUACUUACGUA
L-004702-00	J-004702-08	KPNA2	NM_002266	62388891	GAAUUGGCAUGGUGGUGAA
L-004702-00	J-004702-09	KPNA2	NM_002266	62388891	GCAUAAAUAGCAGCAAUGU
L-004702-00	J-004702-10	KPNA2	NM_002266	62388891	GAAAUGAGGCGUCGCAGAA
L-009837-01	J-009837-09	TTL	NM_153712	42734436	AGACAUGGGCACCGGAGUA
L-009837-01	J-009837-10	TTL	NM_153712	42734436	AAAGAAAGGCAACUCGCAA

L-009837-01	J-009837-11	TTL	NM_153712	42734436	GAGAAAAUUCAGUGACGUA
L-009837-01	J-009837-12	TTL	NM_153712	42734436	UGUAAACAGACACGAAAUU
L-014059-00	J-014059-05	AGTPBP1	NM_015239	7662451	UAUCAUAGAUCGUGUGGUA
L-014059-00	J-014059-06	AGTPBP1	NM_015239	7662451	GCUUAUCACUAUCCAUAUA
L-014059-00	J-014059-07	AGTPBP1	NM_015239	7662451	AUACAAGGGUUUACAGAUU
L-014059-00	J-014059-08	AGTPBP1	NM_015239	7662451	UGAAAGGAACGUUGGAAUA
L-017591-01	J-017591-09	WIPF2	NM_133264	75812910	CAUCAAAAUAUCACGAGUA
L-017591-01	J-017591-10	WIPF2	NM_133264	75812910	CAACAUUAAUGAUCGGAGU
L-017591-01	J-017591-11	WIPF2	NM_133264	75812910	CAUCAAAACCACACGCAAA
L-017591-01	J-017591-12	WIPF2	NM_133264	75812910	AAGGAUAACUUUAACCGAA
L-011557-00	J-011557-05	WASF1	NM_001024936	68161503	AAACAAGACCUCAGACAUA
L-011557-00	J-011557-06	WASF1	NM_001024936	68161503	CAACUAAGUAGCCUAAGUA
L-011557-00	J-011557-07	WASF1	NM_001024936	68161503	UAGAUUGGUUGGAGUAAGA
L-011557-00	J-011557-08	WASF1	NM_001024936	68161503	CCAUCAACCCUACCUGUAA
L-013010-00	J-013010-05	FEZ1	NM_005103	17105402	GAACCUAGCUCCCGUGAAG
L-013010-00	J-013010-06	FEZ1	NM_005103	17105402	GAGUCUGGAUGAAGAGUUU
L-013010-00	J-013010-07	FEZ1	NM_005103	17105402	CCGAAAUAAUCAGCUUCAA
L-013010-00	J-013010-08	FEZ1	NM_005103	17105402	UUUCGGAACUACAACGCCA
L-011580-00	J-011580-05	ARF1	NM_001658	66879658	UGACAGAGAGCGUGUGAAC
L-011580-00	J-011580-06	ARF1	NM_001658	66879658	CGGCCGAGAUCACAGACAA
L-011580-00	J-011580-07	ARF1	NM_001658	66879658	ACGAUCCUCUACAAGCUUA
L-011580-00	J-011580-08	ARF1	NM_001658	66879658	GAACCAGAAGUGAACGCGA
L-004008-00	J-004008-05	ARF6	NM_001663	6996000	CGGCAUUACUACACUGGGA
L-004008-00	J-004008-06	ARF6	NM_001663	6996000	UCACAUGGUUAACCUCUAA
L-004008-00	J-004008-07	ARF6	NM_001663	6996000	GAGCUGCACCGCAUUAUCA
L-004008-00	J-004008-08	ARF6	NM_001663	6996000	GAUGAGGGACGCCAUAAUC
L-016355-00	J-016355-05	RUFY1	NM_025158	22095370	GAACUUAACCGGCACUUGA
L-016355-00	J-016355-06	RUFY1	NM_025158	22095370	CAUCAGAUAUAGCGACUAG
L-016355-00	J-016355-07	RUFY1	NM_025158	22095370	GAAAGAUGACGAAGCGACA
L-016355-00	J-016355-08	RUFY1	NM_025158	22095370	AUAAACAUCUCUUAAGCGA
L-016834-00	J-016834-05	SAP30BP	NM_013260	47834346	GCAAGUGGGAUUCGGCUAU
L-016834-00	J-016834-06	SAP30BP	NM_013260	47834346	GAGAAAGGCGGAUUGGUAU
L-016834-00	J-016834-07	SAP30BP	NM_013260	47834346	CCAGAAGCUUUAUGAACGA

L-016834-00	J-016834-08	SAP30BP	NM_013260	47834346	CCAACUACCCAAAGGAUAU
L-015681-00	J-015681-05	SPG20	NM_015087	40806197	UAACAAAGGUCUGAAUACA
L-015681-00	J-015681-06	SPG20	NM_015087	40806197	GGAUGUACGUCAUAAAGGA
L-015681-00	J-015681-07	SPG20	NM_015087	40806197	CUAAAUGCAUCGUUAACAA
L-015681-00	J-015681-08	SPG20	NM_015087	40806197	UGAAUUAGGUCAGAAGGAA
L-003499-00	J-003499-05	HDAC6	NM_006044	13128863	GGGAGGUUCUUGUGAGAUC
L-003499-00	J-003499-06	HDAC6	NM_006044	13128863	GGAGGGUCCUUAUCGUAGA
L-003499-00	J-003499-07	HDAC6	NM_006044	13128863	GCAGUUAAAUGAAUUCCAU
L-003499-00	J-003499-08	HDAC6	NM_006044	13128863	GUUCACAGCCUAGAAUAUA
L-017668-00	J-017668-05	KAT7	NM_007067	34222309	GAACCGAAGAUUCCGAUUU
L-017668-00	J-017668-06	KAT7	NM_007067	34222309	GAGGGAAGCAACAUGAUUA
L-017668-00	J-017668-07	KAT7	NM_007067	34222309	UAGGACACCUUACAGGAAA
L-017668-00	J-017668-08	KAT7	NM_007067	34222309	GGCAAGAUGCUUAUUGAUU
L-012172-00	J-012172-05	PCNT	NM_006031	81295808	GGACGAAGCUUGCUCACUU
L-012172-00	J-012172-06	PCNT	NM_006031	81295808	GCAUGAAACUCGUCUGAAG
L-012172-00	J-012172-07	PCNT	NM_006031	81295808	CAGCACAGGUUGUCAGGAA
L-012172-00	J-012172-08	PCNT	NM_006031	81295808	CGAAACGGCUCCACAGAGU
L-020556-00	J-020556-05	LAMTOR2	NM_014017	7661727	CCAAGUGGCGGCAUCUUAA
L-020556-00	J-020556-06	LAMTOR2	NM_014017	7661727	GAUCACUGCUGGCCUACUC
L-020556-00	J-020556-07	LAMTOR2	NM_014017	7661727	UCAAAUUCAUCCUCAUGGA
L-020556-00	J-020556-08	LAMTOR2	NM_014017	7661727	CCAAGGAGACCGUGGGCUU
L-006824-00	J-006824-05	MAPRE1	NM_012325	6912493	GGAAAGCUACGGAACAUUG
L-006824-00	J-006824-06	MAPRE1	NM_012325	6912493	AAACGACCCUGUAUUGCAG
L-006824-00	J-006824-07	MAPRE1	NM_012325	6912493	UGACAAAGAUCGAACAGUU
L-006824-00	J-006824-08	MAPRE1	NM_012325	6912493	AGAUGAAGGCUUUGUGAUA
L-012501-00	J-012501-05	MAPRE2	NM_014268	10346134	GAACAGGUACAUUCAUUAA
L-012501-00	J-012501-06	MAPRE2	NM_014268	10346134	GAAUGGCGGUCAAUGUGUA
L-012501-00	J-012501-07	MAPRE2	NM_014268	10346134	GAACGUUGAUAAGGUAAUU
L-012501-00	J-012501-08	MAPRE2	NM_014268	10346134	GGAGUAUGAUCCUGUAGAG
L-006831-00	J-006831-05	CLASP1	NM_015282	31563536	GGACAGCUCUGGAUAACAA
L-006831-00	J-006831-06	CLASP1	NM_015282	31563536	GCACUGGCGUUAAGAGUUU
L-006831-00	J-006831-07	CLASP1	NM_015282	31563536	GCCAAGAACUGAUAGACUA
L-006831-00	J-006831-08	CLASP1	NM_015282	31563536	GGCCACAUCUGGUGUUGUA

L-023462-00	J-023462-06	CLASP2	NM_015097	57863300	GCACUUAAACUUUCAGCUA
L-023462-00	J-023462-07	CLASP2	NM_015097	57863300	CAAAUGGUCUACAGCAAAU
L-023462-00	J-023462-08	CLASP2	NM_015097	57863300	CAAUUAAUCUGGCUGCAAU
L-023462-00	J-023462-09	CLASP2	NM_015097	57863300	UCAGAACGCUCCUAUAGUU
L-009637-01	J-009637-09	BLOC1S6	NM_012388	38505202	CAAAAGAGGCAGCGUGAUA
L-009637-01	J-009637-10	BLOC1S6	NM_012388	38505202	CAAAGGUAGUACAGCGUUU
L-009637-01	J-009637-11	BLOC1S6	NM_012388	38505202	CAAACAAACAAACAACGUA
L-009637-01	J-009637-12	BLOC1S6	NM_012388	38505202	GAACCAAGUUGUAUUGUUA
L-016485-01	J-016485-09	CSPP1	NM_024790	50355983	UGAGAAAUGAGGAACGAAU
L-016485-01	J-016485-10	CSPP1	NM_024790	50355983	UGAAGAGCAUAUUCGGUUA
L-016485-01	J-016485-11	CSPP1	NM_024790	50355983	GAAUACGGUUGGACAGAAU
L-016485-01	J-016485-12	CSPP1	NM_024790	50355983	GCGUACAGCCUGCAGCUUA
L-015884-01	J-015884-09	MID1IP1	NM_021242	39725681	UCUCGAAACUCACGCGCAA
L-015884-01	J-015884-10	MID1IP1	NM_021242	39725681	CAGCACUGUCUGUCGGUAA
L-015884-01	J-015884-11	MID1IP1	NM_021242	39725681	UGUGUGAAGUAUUUCGAAU
L-015884-01	J-015884-12	MID1IP1	NM_021242	39725681	GGAGAUCGGCUUCGGCAAU
L-011724-01	J-011724-13	MAP4	NM_030885	197276597	GGAGUAGAAGGGAGCGAUA
L-011724-01	J-011724-14	MAP4	NM_030885	197276597	GGAGAGAUAAAGCGGGACU
L-011724-01	J-011724-15	MAP4	NM_030885	197276597	GAUGAUGUUGUGGGAGAAA
L-011724-01	J-011724-16	MAP4	NM_030885	197276597	GAGUCAAAGAAGAAACCGU
L-026895-00	J-026895-05	FGD6	NM_018351	55742696	GAAGGGACCGGUUUUAUAA
L-026895-00	J-026895-06	FGD6	NM_018351	55742696	GAAUUCCGAGUCUAAAGUA
L-026895-00	J-026895-07	FGD6	NM_018351	55742696	CUAAGCAGCUCAAAUUAAC
L-026895-00	J-026895-08	FGD6	NM_018351	55742696	GCUCGUCUGUUACGCCAAA
L-024646-02	J-024646-09	TTLL8	XM_003403494	397139792	UGCUGAACCACUACGCAAA
L-024646-02	J-024646-12	TTLL8	XM_003403494	397139792	AGGAGUACCUGCAGCGCCA
L-024646-02	J-024646-19	TTLL8	XM_003403494	397139792	GAGCAUGAGGACAUCGACA
L-024646-02	J-024646-20	TTLL8	XM_003403494	397139792	GAGAGUUACUUGCGGUUCU
L-005234-00	J-005234-06	CD4	NM_000616	21314613	GAACUGACCUGUACAGCUU
L-005234-00	J-005234-07	CD4	NM_000616	21314613	GAGCGGAUGUCUCAGAUCA
L-005234-00	J-005234-08	CD4	NM_000616	21314613	UAACUAAAGGUCCAUCCAA
L-005234-00	J-005234-09	CD4	NM_000616	21314613	GCAAAGGUCUCGAAGCGGG
D-001810-	D-001810-	ON-TARGETplus Non-targeting		0	UGGUUUACAUGUCGACUAA

10	01	Control		
D-001810-10	D-001810-02	ON-TARGETplus Non-targeting Control	0	UGGUUUACAUGUUGUGUGA
D-001810-10	D-001810-03	ON-TARGETplus Non-targeting Control	0	UGGUUUACAUGUUUUCUGA
D-001810-10	D-001810-04	ON-TARGETplus Non-targeting Control	0	UGGUUUACAUGUUUUCCUA

Table A-3 Sequences of primers used for quantification of mRNA levels by qPCR	
Name	Sequence 5'->3'
DYNC1H1-F	TCGGTAACCCCCTTCTGGTC
DYNC1H1-R	GGTGGGAACTCGACAGTTGG
DYNC2H1-F	ACCTGTTTGGAAGAATGGACC
DYNC2H1-R	GCACACTCGACTCCATGATTTC
DYNC1I1-F	AGCGCAAAAAGCAGCGCTTAG
DYNC1I1-R	AGCGGCTGCACTAGAGGC
DYNC1I2-F	TGGAACGTAAGAAGCAGCGA
DYNC1I2-R	GGGGATTCTGGAGTTAGCCC
DYNC1LI1-F	TGGGTGCGGATACACTTACAC
DYNC1LI1-R	GTGCTGCACCATACTGTAAAC
DYNC1LI2-F	TTCTGAGCGAAGTGTCCACC
DYNC1LI2-R	CGCGTGTGATCATCTCGGT
DYNLL1-F	CCGCGCCTCAGTTTCTCTCT
DYNLL1-R	CCTTTCGGTCGCACATGGTT
DYNLRB1-F	TACCGGATCGGTCGGAAATG
DYNLRB1-R	TGGGAATGCCTTCTGTGTTCA
DYNLRB2-F	TTGGGCGAACCTCAGGCAG
DYNLRB2-R	TCACGAACTGTGCTTTTGGC
DYNLT1-F	CTGCGGAGGAGACTGCTTT
DYNLT1-R	TGCATAATTACACAGGTCACGA
DYNLT3-F	GCCACTGCGACGAGGTTG
DYNLT3-R	TCCACTATGCTTGCAGTCCAC
DCTN1-F	ATCTTTGTGCGCCAGTCCC
DCTN1-R	TGTCGGTGCCTTCTTAGGCTTC
DCTN2-F	CACGAGCAAGCCATGCAGTTT
DCTN2-R	TCCCAGCTTCTTCATCCGTTC
DCTN3-F	TATCCTTTCCCAGGTTGCACTC
DCTN3-R	ATTTCCACACACTGGTCCTGCT
DCTN4-F	GTGGGCATGGCAGACAAATC
DCTN4-R	AGTATGTTGCGAAAAAGCCAGA
DCTN5-F	ATCGAGACGGCATCTGGGAA
DCTN5-R	TGGGCTCAGGAAAACAGAAATG

DCTN6-F	AGTGATTGGCGAAGGGAACC
DCTN6-R	ATGGCTTGGGAATAACAGCC
ACTR1A-F	TACGATGTGATCGCCAACCAG
ACTR1A-R	TCGGCCCACATAGTTTGGAAAG
CAPZA1-F	AACTTCTGGAATGGTCGTTGG
CAPZA1-R	CCTTGGCAGTTTGGGCTTCA
CAPZB-F	CGACCTGGTCCCCAGTCTAT
CAPZB-R	ATCCTCCAAGGGAGGGTCAT
PAFAH1B1-F	GCAAGCTTCTGGCTTCCTGT
PAFAH1B1-R	CACAGTAGCCAGTTTGCACTT
NDE1-F	GGGAGACCTACTGCGGAAAG
NDE1-R	TCGTGTCCAACCCCTTATCAC
NDEL1-F	TGCAAAGGACCAAGCATCAC
NDEL1-R	CCGTTTACTGCCCCATGAAC
BICD1-F	ACCGTGGCTCCACCAGATTG
BICD1-R	TGAAGACTAGGGGTGAGGAGG
BICD2-F	GCAGGACTACTCGGAACTGG
BICD2-R	CTGGCTGTTGAGGTACTCGG
KNTC1-F	GCAGACCATCGAATCCTGCT
KNTC1-R	CGTTTTTCGTCCTGCGATGG
ZW10-F	ACCAGTAGTGATCAATGTGCTG
ZW10-R	GGGCAAGACGCAATCTGAAC
ZWILCH-F	GCAGTTCAGTTTGGCGGTTC
ZWILCH-R	ACATCAGCCTCATAGAGAAATGGG
SPDL1-F	TGCAGAGGTGGAAGATCGAA
SPDL1-R	CTCCAACATGGCAAGCAACC
CLIP1-F	CAGAGTATTGGTTGGTGGCA
CLIP1-R	TTGTGGACAGGAGCGAACAA
CLIP2-F	GAGAATTAGCGGACAACAGGCTGA
CLIP2-R	GGACCCGAGTGCAACAGG
SPTBN4-F	AACTACGAGGAAAGCATCGC
SPTBN4-R	AGTACTGCTGTTCCAGAGCCA
SPTBN1-F	TCTCCACGGATGGCAGAAAC
SPTBN1-R	CTGGGTTCTGGCTGGTAAGG

SPTAN1-F	CCCACCAACATCCAGCTTTC
SPTAN1-R	TTGCCCATGTCGATAACCCC
BCAS2-F	GCCCCGGATTATTCTGCCTT
BCAS2-R	GGCTGGAAGCTCATATCGTTT
SEC23A-F	ATGTGCTTAGGTGGCTGGAC
SEC23A-R	TGAAACATAAACTGTGGATAAAGGG
SEC23B-F	TGCAGCAGGCCAACTTGTAA
SEC23B-R	TGAGCACCTCGCTGTATCAC
SEC24A-F	CTCACGCCCCTGACATCATC
SEC24A-R	GGTGTTGCCAATAAGCCACC
SEC24B-F	AGCCCAGATTCATTTCGGTGT
SEC24B-R	ATACGTTCGACAGGATCGGC
SEC24C-F	CCTGGGAGCCTTGACGTTAG
SEC24C-R	GATCTCACCTTATCAGACAGTGAT
SEC24D-F	AGGGTTTGACGTGGCAGTTC
SEC24D-R	AAAAGAAGTCTGTTCCCGCTCC
RILP-F	GCGGAATGAACTCAAAGCCAA
RILP-R	CAGCCTCATCCTCACTGCTCTC
RAB7A-F	GGCCGCGTTTGAAGGATGAC
RAB7A-R	CACCATCACCTCCTTGGTCAG
RAB7B-F	CCATGGTGTTGTTGGGGAAC
RAB7B-R	TGCTCTGGTACCTCGACAGAG
MAPK8IP3-F	CCTCATCCACTGCTACGACG
MAPK8IP3-R	TGAATTTCTCCTCCGCCTGCC
CCDC155-F	TTCGTGGATGTCCGTTGTGT
CCDC155-R	CGGAGGTACATTTCCGCAGT
SUN1-F	GGCCCGTGTCGAGAGTTTATT
SUN1-R	GCCTTCCCTGGAGCAACC
RAB11FIP3-F	TCCGAGCCGTGTTCGATG
RAB11FIP3-R	GCCATCAGGATCTCCGTTTCT
HOOK1-F	GGAGCAACAGCTTAAAAGAGCC
HOOK1-R	AGAGCCATCCAACTGGTCAAG
HOOK2-F	GTGCTGAACCAGATAGACCCC
HOOK2-R	CTTCTGACACAGGATGCGCC

HOOK3-F	AGTTAAGAAAGGCCAACGCA
HOOK3-R	TTTCTGTTCTCAGCCTGTCCTT
MAP1A-F	AGTTAAGAAAGGCCAACGCA
MAP1A-R	TTTCTGTTCTCAGCCTGTCCTT
MAP1S-F	GACCTGGCGTTTCATTGCAT
MAP1S-R	AGACCGGATGCCTGTGTTGG
MAP1B-F	GTTCTACTTGCTGGTGGTCGT
MAP1B-R	GGATCTTTTGTCCTGGGACTTCA
TBCB-F	CATCGCTGAGTTCAAGTGTAAA
TBCB-R	TCATACTCACCAAGGCGGG
KPNA2-F	GGTGGACCCTTTGAACGCAG
KPNA2-R	GACGCCTCATTTCTGTACTGTCT
TTL-F	GGAGAGGGCAACGTTTGGAT
TTL-R	CAAGACCCAGCTTCGGATGT
AGTPBP1-F	CCTGAGCCGCCTTACCAATA
AGTPBP1-R	TCCTGTAGAACCTTTGGCTGTC
WIPF2-F	TCACCACTGTCCGGTCTTTC
WIPF2-R	CGGGCAGCTCGGTTTGTTT
WASF1-F	CGATGTTTGTGAACAGCCTCC
WASF1-R	ATTTTTCTGCTTCTGCTTCCTCT
FEZ1-F	CCTCTCCTCCCTCAGTGGAA
FEZ1-R	TAGGTAGGGCAGAGCACTTT
ARF1-F	GTTTGCTGTGAAGACGGTGTC
ARF1-R	AGAGGATCGTGGTCTTCCCT
ARF6-F	GCGGCATTACTACACTGGGA
ARF6-R	CCTGGATCTCGTGGGGTTTC
RUFY1-F	ACTGAAAAAGGAGTTGCGGGA
RUFY1-R	CCTACAGTGTGTCGCTTCGT
SAP30BP-F	TGAGGAGAAAGGCGGATTGG
SAP30BP-R	TGTGCCGAGCTTCTCCTTTG
SPG20-F	GCAGCAAGTAGTGTTCAAGGATT
SPG20-R	GCCAACATTGACCGCAGAAT
HDAC6-F	CTGGTGCTTCCCATTGCCTA
HDAC6-R	AGCCACCCTCTAGGATAAGGA

KAT7-F	TGCCGCGAAGGAAGAGGAAT
KAT7-R	GCAGATTTCGAACAGGACTGGA
PCNT-F	TCACAAAGGAGTGTGAACAAGA
PCNT-R	CAATGCCGTCTCCTTCTCCTT
LAMTOR2-F	GCACCCTGCTGCTGAATAACG
LAMTOR2-R	GCCACTCGGGTGATGGCTAC
MAPRE1-F	TTTGAACGAGACGAAGACGGAA
MAPRE1-R	GCAGCCCCTGAGCACAACT
MAPRE2-F	ACGGGACCATCATTCCTTTCC
MAPRE2-R	AATAGGCCGCTCCTGAACAA
CLASP1-F	GCTCTCAGGCGCTCTTACTC
CLASP1-R	TCGCGGGACACAATATCACA
CLASP2-F	CGAGCAACTACCGGGTATCA
CLASP2-R	TCTCGAACCTTGTCTTTGGCA
BLOC1S6-F	AAGGCGGTTGATGGTGAAGC
BLOC1S6-R	CTTGGTTCTGTGTGAGTTCCTG
CSPP1-F	AGTCAACAGACCAGGGGTTC
CSPP1-R	TCAACCTTTCCTGAGTAAGATAACG
MID1IP1-F	CAACATGGACCAGACGGTGA
MID1IP1-R	GCTGTACATGTCCCGAGAGG
MAP4-F	ACCGTGCTCAGAAACTAGCC
MAP4-R	TGGAGACCCTGTAGTATCGCT
FGD6-F	ATTTGAGATGAGCCCTCGCTG
FGD6-R	ATGGTGTCATTGGCGTGGTT
TTLL8-F	GATCCAAACCAGCTAAATGCG
TTLL8-R	TTCAATGTTCGGCGGGAGA
CD4-F	CAAGAAAGACGCAAGCCCAG
CD4-R	GACTCCCCGGTTCATTGTGG
GAPDH-F	GACAGTCAGCCGCATCTT
GAPDH-R	TGGAACATGTAAACCATGTAGTTG

Host Proteins Involved in Microtubule-Dependent HIV-1 Intracellular Transport and Uncoating

Stephanie K. Carnes and Christopher Aiken*

Department of Pathology, Microbiology, and Immunology, Vanderbilt University Medical Center, Nashville, Tennessee, USA

*Author to whom correspondence should be addressed; E-mail: chris.aiken@vanderbilt.edu; Tel.: (615) 343-7037; A-5301 Medical Center North, 1161 21st Ave S. Nashville, TN 37232

Keywords: HIV-1, microtubule, transport, dynein, kinesin, motor proteins, infection, uncoating, reverse transcription

Abstract

Microtubules and microtubule-associated proteins are critical for cargo transport throughout the cell. Many viruses are able to usurp these transport systems for their own replication and spread. HIV-1 utilizes these proteins for many of its early events post-entry, including transport, uncoating and reverse transcription. The molecular motor proteins dynein and kinesin-1 are the primary drivers of cargo transport, and HIV-1 utilizes these proteins for infection. In this review, I highlight recent developments in the understanding of how HIV-1 hijacks motor transport, the key cellular and viral proteins involved, and the ways that transport influences other steps in the HIV-1 lifecycle. Studying these processes and interactions is critical for the development of antivirals targeting HIV-1 transport.

Introduction

The cytoplasm of cells is an aqueous solution that is crowded by organelles, proteins, and RNA that restrict passive diffusion of cargo to its required destinations within the cell. Crowding with macromolecules makes it necessary for cargo to use active transport along microtubules (MTs) by molecular motor proteins, specifically dynein and kinesins [204-206]. Viruses, including HIV-1, are adept at hijacking MTs for their intracellular transport. HIV-1 depends on a series of events to productively infect cells. The microtubule network and its associated proteins are involved in several of the early steps in HIV-1 infection, including entry [76], reverse transcription [77-79], uncoating [78, 80-82], and transport to the nucleus [51, 60, 80, 82-85]. HIV-1 egress and assembly also utilize the microtubule network to efficiently assemble particles for budding and spread (reviewed in [86]). It was established over a decade ago that the microtubule network is involved in HIV-1 infection, but only recently has research begun to define the transport machinery and mechanisms involved in the early stage of infection, which will be the focus of this review.

The Microtubule Network

The microtubule (MT) network is the dynamic and complex arrangement of microtubules within a cell. MTs are part of the cell cytoskeleton, which gives the cell structure, shape, and in some cell types, polarity. MTs are made up of repeating alpha and beta tubulin heterodimers, which nucleate from gamma tubulin at centrosomes. Since MTs emanate from centrosomes near the nucleus, this area is often called the MT Organizing Center (MTOC). Due to the repeating heterodimer structure of microtubules, they are polarized, with the negative end located at the MTOC, and the positive end extending outward [38]. In a nonpolarized interphase cell, this MT polarity results in the positive end of MTs extending toward the cell periphery. The polarity of these tracks is important for cargo transport and the directionality of microtubule-associated proteins (MAPs), as discussed below.

Although most MTs nucleate from centrosomes, MTs can emanate from kinetochores, the Golgi apparatus, the nuclear envelope, and other MTs, increasing the complexity of the overall network [39].

Adding to the complexity, MTs exhibit a phenomenon called dynamic instability, in which they undergo a series of growth and shrinkage events at their plus ends. Dynamic instability is influenced by microtubule-associated proteins (MAPs) and is marked by post-translational modifications [40, 41]. The adaptable structure of the microtubule network allows it to form the mitotic spindle, which is crucial for the search, capture, and separation of chromosomes during mitosis. The fine-tuned regulation of MT stability also influences cargo transport during interphase, as MT stabilization or depolymerization by drugs can both alter transport by molecular motor proteins [42, 43].

Microtubule Motor Proteins

Intracellular cargo transport requires the actions of a subset of MAPs that exhibit motor function. Two types of motor complexes, dynein and kinesins, hydrolyze ATP to move along microtubules and transport cellular cargo, including vesicles, organelles, RNA, etc. In general, kinesins walk toward the positive end of microtubules (anterograde movement) to transport cargo, and dynein walks toward the negative end of microtubules (retrograde movement) [44, 45]. In non-dividing cells, cargo gets transported toward the nucleus predominantly by dynein and away from the nucleus by kinesins. Nonetheless, owing to the dynamics and branching of the microtubule network, both types of motors can be involved in the transport of a specific cargo.

Dynein, a large protein complex, transports vesicles and endosomes within the cytoplasm, and it helps position organelles and the mitotic spindle during cell division [reviewed in [44, 46-48]]. Dynein is composed up of several proteins with distinct functions. The dynein complex is composed of two copies of a heavy chain containing the ATPase activity required for movement, two intermediate chains that stabilize the structure of the complex, and two light intermediate chains that link cargo to the complex. The complex also contains multiple copies of various light chains that link dynein to other proteins and to cargo.

Dynein interacts with dynactin, a multi-subunit complex that links dynein to some cargo and increases dynein's processivity while walking along microtubules [104, 109, 110]. The dynactin complex

consists of at least five polypeptides: (1) an Arp1 backbone [111, 112]; (2) a p150 side-arm that aids in microtubule processivity [104, 107]; (3) a shoulder complex that attaches the side-arm to the backbone and binds additional interacting proteins [115]; (4) a pointed end complex that binds the nuclear envelope prior to mitosis [116]; and (5) a barbed end complex that aids in structure stabilization [111]. Together, the five components interact to form the dynactin complex. The interactions between dynactin and dynein result in increased speed and processivity of cargo transport [111, 118].

In contrast to the single dynein complex, there are 15 different kinesin families, termed kinesin 1 to kinesin 14B, based on phylogenetic analyses. Kinesins are variable in form and function, but all contain two heavy chains and two light chains which form two globular head motor domains and a coiled-coil tail allowing heavy chain dimerization. The kinesin families can be grouped based on the position of their motor domain in the molecule, with N-kinesins having a motor domain in the amino-terminal region, M-kinesins in the middle, and C-kinesins in the carboxy-terminal region. Most N- and C-kinesins bind vesicles, organelles, and other microtubules and function in microtubule plus end and minus end-directed transport, and M-kinesins function to depolymerize microtubules, which is critical for mitotic spindle arrangement [45]. For the purposes of this review, I will primarily focus on kinesin-1, a plus-end directed microtubule motor implicated in HIV-1 transport.

Molecular motors must transport a variety of protein cargos to various destinations within the cell, raising the question of how specificity is achieved. Dynein and kinesins interact with numerous cargo-specific adaptor proteins, which connect the molecular motors to the various cargoes [49-51]. While some adaptors are in protein families, (e.g. Hook family, Bicaudal D proteins, etc.) there is no common sequence across all adaptors. Interestingly, several adaptors have a similar structural coiled-coil region which has been hypothesized to bind to the dynactin complex, and may represent a conserved binding mechanism across adaptors. Adaptors can also activate the motors to move along microtubules: recent studies have confirmed this function for BICD2, Hook3, Spindly, and Rab11-FIP3 [52]. Many adaptors can perform cellular functions other than cargo transport, including nuclear and spindle positioning during mitosis. Kinesin and dynein motors can simultaneously bind to a single

microtubule, and there is evidence for simultaneous binding of motors to a single cargo molecule, suggesting that the net transport of a particular cargo relies on coordination of its movement by opposing motors. Thus, regulation of transport appears to depend on regulation of motor activity by adaptors [53-55].

HIV and Microtubule Stabilization

In early studies, treatment of cells with nocodazole and other MT depolymerizing agents did not substantially affect their susceptibility to infection, suggesting that HIV-1 infection does not depend on the MT network [207]. However, HIV-1 pre-integration complexes, which deliver the reverse-transcribed viral DNA for integration into the host genome, were shown to be associated with the MT network. This association suggested that HIV-1 utilizes MTs for transport [83]. Recent studies have reconciled these seemingly contradictory findings by revealing that HIV-1 transport depends on a subset of MTs that are resistant to nocodazole [84, 208].

Microtubule stabilization can occur through the action of a subset of MAPs termed "MT plus-end tracking proteins (+TIPs). They are called MT +TIPs because they accumulate at the plus end of MTs, and move with the plus end even during MT shrinkage events. Interestingly, +TIPs can function to increase or decrease MT stabilization. For +TIPs involved in stabilization, most act to reduce MT shrinkage events or assist in the addition of tubulin to the MT, either through direct binding to the MT or through the recruitment of other proteins [209]. Post-translational modifications of tubulin, including detyrosination or acetylation, mark long-lived MTs and are recognized by specific kinesins for transport routes. Some post-translational modifications can also influence MT stability by recruiting MAPs with stabilizing or destabilizing functions [210].

HIV-1 particles can induce MT stabilization: entry of HIV-1 increases the formation of acetylated and detyrosinated MTs, both markers of stabilized MTs [84]. The mechanism of stabilization is thought to occur through the actions of EB1, a +TIP, and its binding partner Kif4, as depletion or inhibition of either protein prevented the virus-induced stabilization of MTs and

suppressed infection. Kif4 binds the HIV-1 matrix protein, potentially recruiting EB1 to the incoming virion (Figure A-1). Whether the matrix protein is involved in the downstream signaling for MT stabilization, or if it acts only to tether Kif4 to the HIV-1 capsid is not well understood. Downstream of this interaction, the EB1-Kif4 complex stabilizes MTs by recruiting other +TIP proteins, including the diaphanous-related formins 1 and 2 (Dia1 and Dia2), which also promote HIV-1-induced MT stabilization and virus intracellular transport [80]. Whether Dia1 and Dia2 are the only +TIPs activated by EB1, or if others are involved in the MT stabilization process, has yet to be determined.

In addition to EB1-induced MT stabilization, the MAP1 family proteins MAP1A and MAP1S were also reported to stabilize MTs upon HIV-1 infection, and their depletion reduced infection [85]. MAP1 proteins stabilize MTs by promoting growth at the MT + ends [211]. It is unknown whether the activity of MAP1 proteins is a direct result of EB1-induced activation or whether MAP1 proteins are activated by a separate signaling pathway. Interestingly, MAP1 depletion also reduced the association of HIV cores with both dynamic and stable MT subsets. MAP1 interacts with HIV-1 cores *in vitro* and in cells via binding of the HIV-1 capsid to MAP1 light chain LC2. Together, these findings suggest that MAP1 proteins may facilitate HIV-1 infection by tethering the viral core to MTs before active transport begins (Figure A-1).

Bidirectional Transport of HIV-1 by Dynein and Kinesin-1

For an incoming HIV-1 particle to utilize the microtubule network to reach the nucleus, the motor proteins dynein and kinesin are key. An early study suggested that dynein is responsible for the transport, as microinjection of antibodies against the dynein intermediate chain abolished HIV-1 pre-integration complex localization to MTOCs [83]. More recently, siRNA depletion of the dynein heavy chain, or dynein inhibition by ciliobrevin D treatment, was shown to reduce viral DNA accumulation in the nucleus and inhibit HIV-1 infection [51, 60, 78]. The reduction in infection appeared to result, at least in part, from impaired intracytoplasmic trafficking [60, 78, 83]. Live cell imaging analysis of cytoplasmic HIV-1 particles suggested that dynein depletion decreased the overall movement of the virus and specifically

decreased its movement in the retrograde direction [60] (Figure A-2). Hence, the net effect of dynein

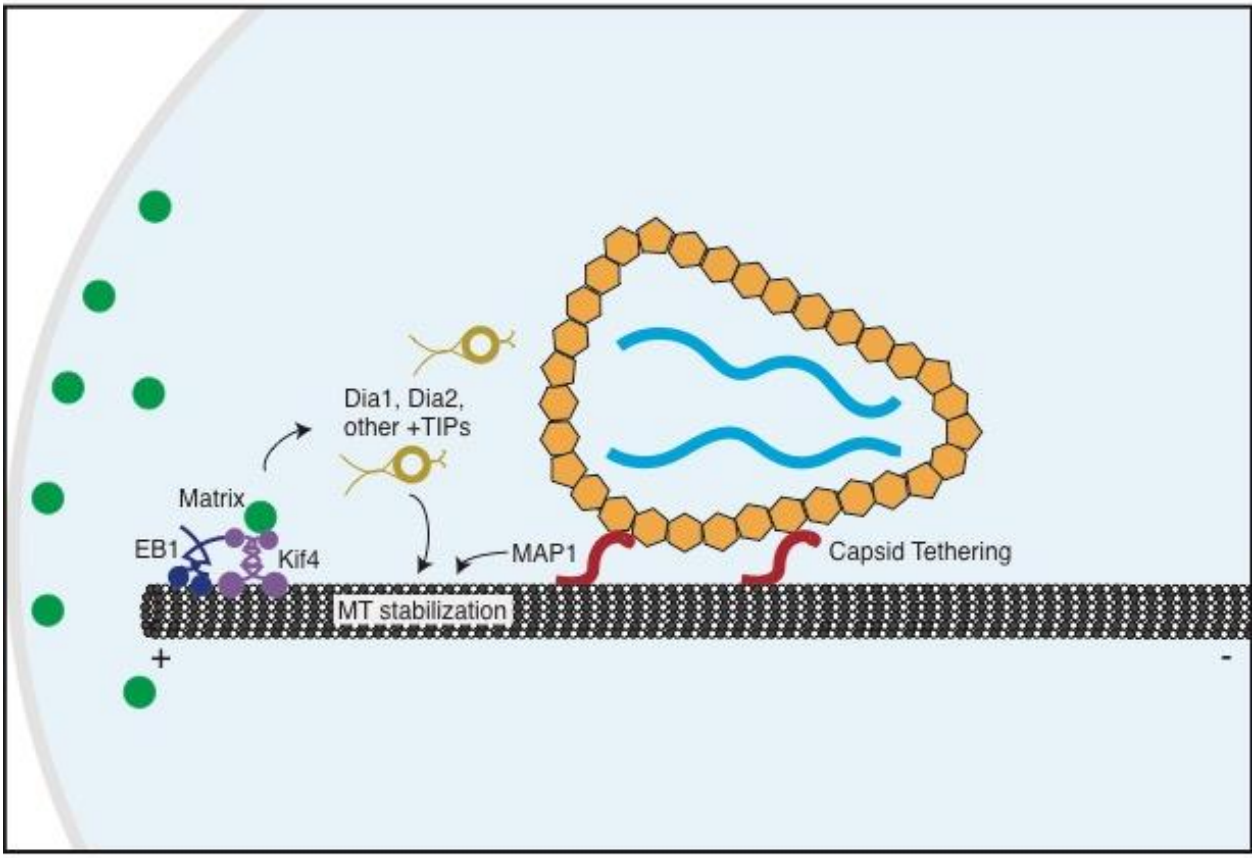

Figure A-1. HIV and Microtubule Stabilization. Upon cell entry, HIV-1 induces microtubule stabilization. The HIV-1 matrix protein binds the Kif4-EB1 complex, resulting in the recruitment of microtubule-stabilizing proteins, including Dia1 and Dia2. The MAP1 family of proteins also stabilize microtubules and may act to tether the HIV-1 capsid to microtubules before transport.

depletion was an increase in the net distance of HIV-1 particles from the nucleus.

Each subset of dynein components (light chains, intermediate chains, etc) can have overlapping functions, allowing them to be interchangeable and leading to variability in the protein composition of each dynein complex, depending on the cargo being transported. The specificity for cargo suggests that HIV-1 may utilize a subset of dynein proteins for its transport and infection. Employing a targeted siRNA screening-based approach, I showed that the dynein heavy chain is important for HIV-1 infection and transport. The experiments did not reveal other components of the core dynein complex to be necessary for HIV-1 infection, but this may be due to the redundant functions of the proteins or to insufficient siRNA depletion. By contrast to dynein, the experiments identified multiple components of the dynactin complex as important for HIV-1 infection, including the Arp1 backbone and the shoulder complex (containing both DCTN2 and DCTN3 proteins) [60]. Additionally, using *in vitro* capsid-binding assays with cell extracts, I observed that the dynein heavy chain and the dynactin complex interacted with capsid-like tubular assemblies *in vitro*. These observations were noteworthy because the dynactin shoulder complex is critical for linking dynein adaptors to the dynein complex, suggestive of a role for a dynein adaptor in HIV-1 transport and infection.

Dynein adaptors are important for cargo specificity and to activate motor protein movement along microtubules. The dynein adaptor, bicaudal D 2 (BICD2), was recently demonstrated to promote HIV-1 transport [60, 82]. BICD2 is one of two homologues of bicaudal D and is important for organelle and mRNA transport [127]. BICD1 and BICD2 have similar functions in the cell, but BICD2 is expressed at higher levels. In cultured mammalian cells, BICD2 facilitates dynein-mediated cargo transport from the ER to the Golgi and within the Golgi by moving RAB6-positive endosomes. BICD2 is also important for proper cell division: prior to mitotic entry, BICD2 interacts with RANBP2 at nuclear pore complexes and recruits dynein and dynactin to ensure proper positioning of the nucleus [reviewed in [12, 49]].

BICD2 was initially found to play a role in HIV-1 infection in a genome-wide siRNA screen of host factors [89]. Recently, I and others (Dharan et al.,[82]) confirmed the initial infection results and further explored the mechanism of BICD2-mediated HIV-1 transport [60, 82]. Depletion of cellular

BICD2 via siRNA or CRISPR disruption of the gene resulted in an impairment to HIV-1 transport and a build-up of particles near the cell periphery akin to the effect of dynein depletion. Experiments using live cell imaging of intracellular HIV-1 particles suggested that the peripheral accumulation of the virus resulted from decreased particle movement in the retrograde direction. Dharan et al. also reported a decrease in HIV-1 particle speed and run length in BICD2 knockout cells [82]. In cells depleted of BICD2 by siRNA, I observed that the number of particles moving at any given time was decreased but motile particles acted normally in terms of speed and run length [60]. Regardless of the specific trafficking defect, the combined observations establish that BICD2 promotes HIV-1 movement to the nucleus (Figure A-2).

BICD2 was observed to associate with HIV-1, both *in vivo* in a proximity ligation assay, and *in vitro* to capsid tubular assemblies [60, 82]; this association is in line with its proposed function as an adaptor for HIV-1. Specific BICD2 domains were also tested for binding to HIV-1 capsid tubes. In both types of analyses, I observed that the canonical cargo binding domain of BICD2 (CC3) bound the capsid tubes. Interestingly, I observed that the BICD2 domain that links BICD2 to dynein (CC1) also bound the capsid, suggesting there may be an additional domain that HIV-1 employs to recruit BICD2 for transport. In order to determine if BICD2 links the HIV-1 capsid to the dynein-dynactin complex, I immunodepleted BICD2 from cell extracts and tested them for binding of dynein to HIV-1 capsid-like tubes *in vitro*. BICD2 depletion resulted in reduced binding of dynein to the tubes, suggesting that BICD2 promotes interation of the dynein complex to the HIV-1 capsid *in vitro.* Together, my findings and those of Dharan *et al.* indicate that BICD2 functions as an adaptor for dynein-dependent HIV-1 transport.

HIV-1 infection appears to involve bidirectional transport. In addition to HIV-1 requiring the retrograde action of dynein, anterograde movement by kinesin-1 also contributes to HIV-1 infection and transport to the nucleus (Figure A-2). Specifically, the kinesin-1 heavy chain Kif5B was shown to be a critical component of kinesin for HIV-1 transport. Kinesin-1 has been proposed to affect dynein cargo transport by redistributing dynein to MT + ends. The dependence of HIV-1 transport and infection on

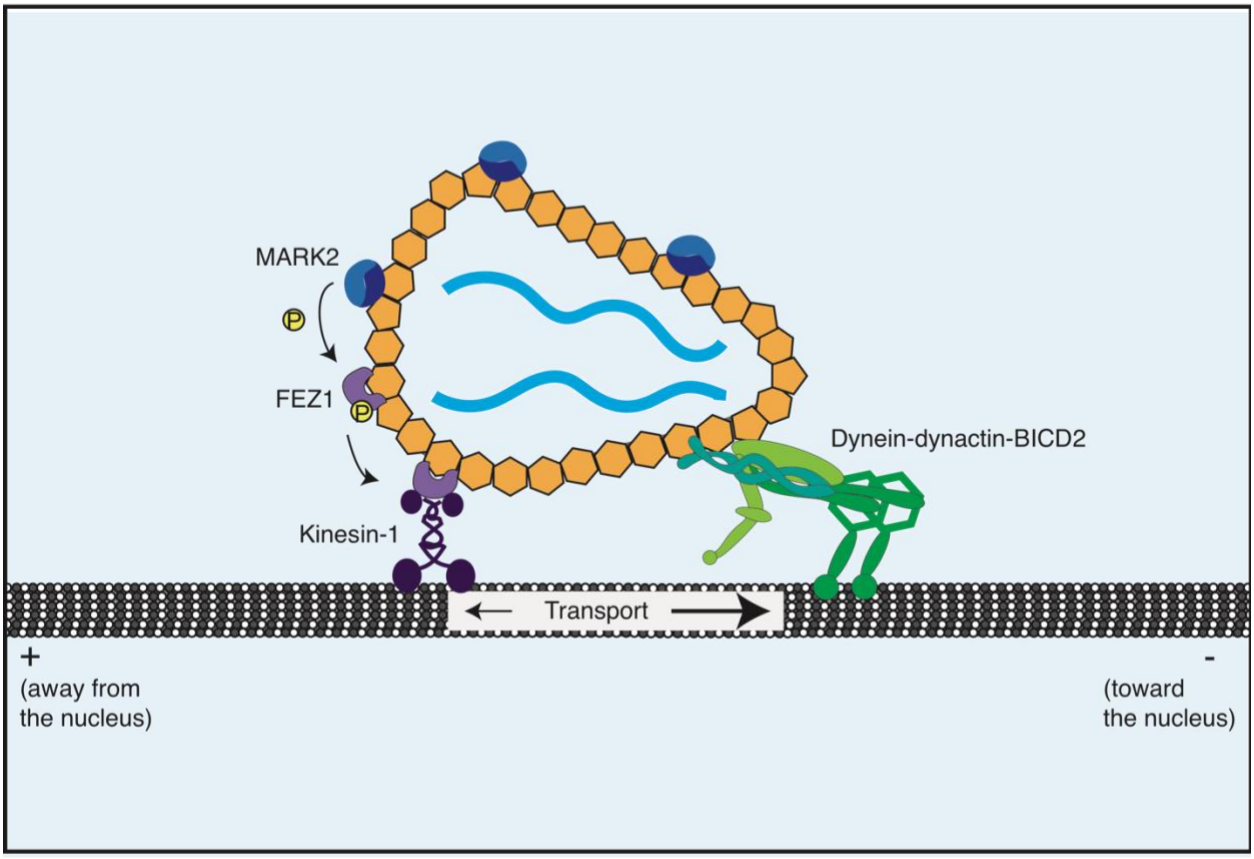

Figure A-2. Bidirectional Transport of HIV-1 by Dynein and Kinesin-1. The dynein-dynactin-BICD2 complex transports the HIV-1 core toward the nucleus. Paradoxically, kinesin-1 also plays a role in this transport, although it moves towards the positive end of microtubules. The host cell protein kinase MARK2 activates the kinesin adaptor FEZ1 by phosphorylation, enabling it to form a bridge between kinesin-1 and the HIV-1 capsid.

kinesin-1 was not attributed to an effect on dynein, as kinesin-1 depletion did not affect dynein levels or intracellular distribution [51, 160]. Thus, it appears that kinesin-1 acts directly to transport the virus. This finding may seem counterintuitive, as kinesin-1 would be expected to move HIV-1 away from the nucleus, but this view is oversimplistic. The MT network is complex, and while the majority of microtubules radiate from the MTOC near the nucleus, others can nucleate from other MTs and the golgi apparatus, thereby changing the direction of the polarity of MTs in the cell. Thus, anterograde movement by kinesin is potentially necessary for HIV-1 to make the turns required for proper routing through the cytoplasm. The mechanisms by which kinesin-1 and dynein activities are coordinated to transport cargo are an ongoing area of research [53, 54].

Similar to dynein, kinesins can utilize adaptor molecules for transporting cargo. The results of depletion experiments suggest that kinesin-1 facilitates HIV-1 transport through the kinesin adaptor protein Fasiculation and Elongation Factor zeta 1 (FEZ1), which was also shown to be important for early HIV-1 infection [51]. FEZ1 was initially observed to influence HIV-1 infection in a study focused on the resistance of a chemically mutagenized cell line to infection by the murine leukemia virus [159], in which overexpression of FEZ1 inhibited the accumulation of 2-LTR circles (a marker of nuclear entry). The effect appears particularly strong in neuronal cells, in which FEZ1 is expressed in high levels. Overexpression of FEZ1 and the depletion of it from cells both reduce HIV-1 infection, suggesting that the interactions of FEZ1 with kinesin must be properly balanced. This necessary balance emphasizes the regulatory role that bidirectional movement may play in HIV-1 infection. These effects may also be due to differences in cell types, possibly owing to differences in FEZ1 levels or to neuron-specific transport machinery components.

Consistent with its established function as an adaptor for kinesin-1, FEZ1 associates with kinesin-1 via KIF5B and binds recombinant capsid-like assemblies *in vitro*, suggesting that it links the HIV-1 core to kinesin-1 [51]. FEZ1 activation and binding to kinesin-1 is regulated by the cellular protein kinase MT affinity-regulating kinase 2 (MARK2) which phosphorylates FEZ1. Interestingly, HIV-1 cores have been reported to bind MARK2, and upon HIV-1 cellular entry, FEZ1 phosphorylation by

MARK2 is specifically localized to FEZ1 near HIV-1 cores. In this way, MARK2 acts to activate FEZ1 for its role as an adaptor between kinesin-1 and HIV-1 cores [160] (Figure A-2). Depletion of FEZ1 resulted in inhibition of HIV-1 infection and a reduction of net particle movement toward the nucleus, although virus particles still exhibited bidirectional motility, suggesting there may be more to the mechanism [51]. Together, the observed effect of FEZ1 on HIV-1 transport and the linkage of kinesin-1 to the HIV-1 capsid suggests that HIV-1 exploits FEZ1 as a kinesin-1 adaptor for transport and infection.

Effects of MT-Dependent Transport on HIV-1 Uncoating

In addition to their transport function, MAPs may also play a role in HIV-1 uncoating. Uncoating is the disassembly of the HIV-1 capsid that occurs during the post-entry phase of infection. Although uncoating is an active area of study, it appears to be necessary for the genetic material to enter the cell nucleus, as an intact HIV-1 core is too large (~40 x 100 nm) to traverse the nuclear pore. Recent studies have suggested that uncoating in the cytoplasm is a two-step process, with a fast, initial uncoating event within 30 min after fusion, with partial retention of CA protein through nuclear import [34]. The rate of uncoating has been studied by various approaches. Uncoating can be analyzed *in vitro* by quantifying the release of soluble capsid protein from purified HIV-1 cores [212]. Additionally, in microscopy based *in situ* systems, the loss in mean fluorescent intensity of the viral particle is determined over time, with innovations on the approach being developed [34, 35, 187, 188, 213]. Another cell-based system, the fate-of-capsid assay, allows infection to proceed for several hours, after which cells are lysed and uncoating assayed by quantifying the levels of pelletable and soluble capsid protein [214].

Finally, the cyclosporine A (CsA) washout assay exploits the ability of the capsid-targeting host factor TRIMCyp to inhibit HIV-1 infection. TRIMCyp binds to the intact HIV-1 capsid and inhibits infection, making its ability to restrict infection a good readout of an intact capsid. The drug cyclosporine A (CsA) inhibits the binding of TRIMCyp to the HIV-1 capsid, rendering it unable to restrict infection. In the assay, TRIMCyp-expressing cells are inoculated with HIV-1 in the presence of CsA, and CsA is washed out at various times post-infection. The rate at which HIV-1 escapes restriction by TRIMCyp is

interpreted as a measure of the rate of uncoating [215].

Although the intrinsic stability of the viral capsid can be influenced by mutations and by pharmacological inhibitors, the MT network and motor proteins may also play a role in uncoating. Treatment of cells with nocodazole resulted in delayed HIV-1 uncoating as determined by an *in situ* fluorescence microscopy assay, the fate-of-capsid assay, and the CsA-washout assay [81]. These results are interesting because they suggest that uncoating requires both unstable and stable MTs, instead of only the stable, nocodazole-resistant subset that appears to be important for transport and infection [84]. The microtubule-associated proteins Dia1 and Dia2 appear to promote uncoating, as deduced using an *in situ* microscopy based assay and the fate-of-capsid assay [80] (Figure A-3). The effect of the Dia proteins on uncoating was genetically separable from their MT-stabilizing activity: genetic analysis mapped the two functions to distinct domains in the proteins, revealing a mutation that inactivated MT stabilization but not the uncoating activity. Although the mechanism is still unclear, the effect on Dia proteins on uncoating may be direct, as they have been reported to bind to capsid-like assemblies *in vitro* [80].

The dynein complex also appears to be important for HIV-1 uncoating. Depletion of the dynein heavy chain by siRNA, pharmacological inactivation of dynein, and loss-of-function perturbations by overexpression of the dynactin component dynamitin (DCTN2) all delayed HIV-1 uncoating [78, 81]. These analyses were performed using an *in situ* fluorescence-based system, the CsA washout assay, and the fate-of-capsid assay, respectively. Additionally, depletion of the dynein adaptor BICD2 reduced the rate of uncoating in an *in situ* fluorescence-based system, suggesting BICD2 has a role in promoting uncoating [82] (Figure A-3). In vitro, BICD2 can bind the HIV-1 capsid and link the capsid to dynein [60], but whether these interactions are important for uncoating is not known.

Interestingly, one of the dynein light chains, DYNL1, appears to act oppositely to the rest of the dynein complex. Depletion of DYNL1 increased the levels of pelletable CA, as determined by the fate-of-capsid assay [77]. This suggests that DYNL1 delays uncoating (Figure A-3). The mechanism for this delay is not well understood, but an interaction between DYNL1 and HIV-1 integrase was critical for the effect. DYNL1 was not observed to bind the capsid directly, suggesting that the effect on uncoating may

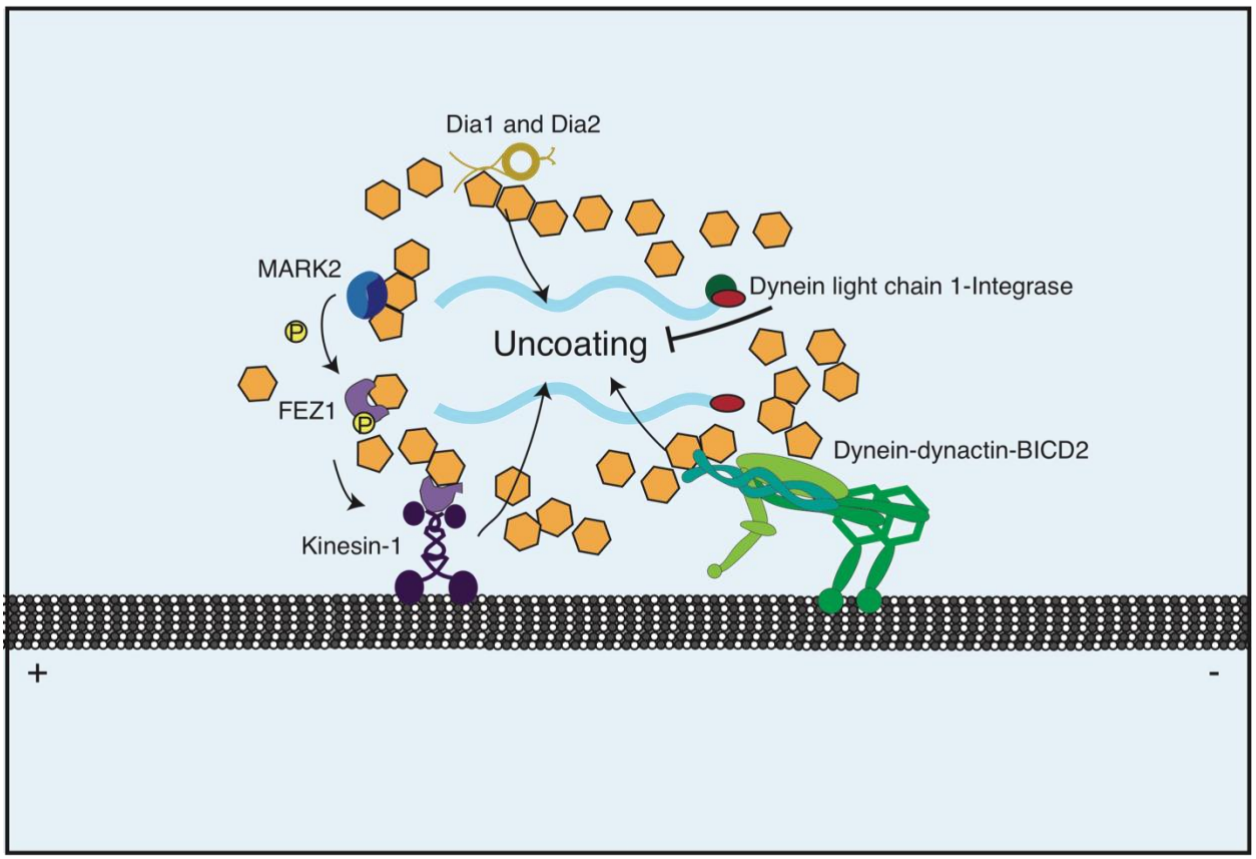

Figure A-3. Effects of MT-Dependent Transport on HIV-1 Uncoating. The breakdown of the HIV-1 capsid, termed uncoating, is influenced by the dynein-dynactin-BICD2 complex and kinesin-1-FEZ1 in a poorly understood mechanism. Additionally, Dia1 and Dia2 promote uncoating by a mechanism distinct from their role as microtubule stabilizers. By constrast, the dynein light chain delays uncoating, acting oppositely from the rest of the dynein complex.

be indirect. Whether its ability to delay uncoating is important for regulating the initiation or location of HIV-1 uncoating in cells has yet to be determined.

Similar to the dynein complex, kinesin-1 depletion by siRNA also delayed HIV-1 uncoating (Figure A-3). The effect of kinesin-1 on uncoating relies on the same machinery and processes as it does for transport: specifically, MARK2 activation of FEZ1 on cores, which activates binding of FEZ1 to the kinesin heavy chain KIF5B. Depletion of FEZ1, and the perturbation of binding to kinesin-1, both slowed HIV-1 uncoating as determined by the fate-of-capsid assay [160].

Overall, the importance of dynein and kinesin in HIV-1 uncoating is currently murky. The role that dynein and kinesin play in bidirectional transport suggests that these proteins transport the HIV-1 core to a location in the cytoplasm conducive to uncoating. New studies indicate that uncoating is a two-stage process involving an early loss of CA protein followed by a further dissociation of CA just prior to nuclear entry [34, 35]. Whether uncoating is only temporally controlled or there is also spatial control depends on transport, remains to be determined.

Because BICD2 and FEZ1 both bind to the viral capsid, it is plausible that these proteins affect uncoating by directly influencing the stability of the capsid. On the other hand, the roles in transport and capsid binding of these motors suggest a possible secondary model: simultaneous pulling by motors in opposite directions may rupture the capsid by brute force. However, it is unclear whether the forces exerted by motor proteins are sufficient to fracture the capsid [216-218]. Adenovirus uncoating is known to be influenced by the forces applied by kinesin-1. After adenovirus binds to the nuclear pore through Nup214, kinesin-1 is recruited and also binds to the capsid. As it moves back toward the plus end of MTs, the "tug of war" between kinesin-1 and Nup214 for the capsid results in its partial rupture [219]. This suggests that a similar mechanism for HIV-1 could be at play. Since the primary HIV-1 uncoating event occurs early in the cytoplasm, this may suggest that dynein and kinesin are the opposing forces in this "tug of war" type model.

Although initial models of cargo transport suggested that the number of each opposing motors determined the directionality of transport, newer reports suggest that there may be more regulation to the

transport. Specifically, cross-talk between the opposing motors and the activation or inactivation of motors depending on the directionality is now thought to occur [55]. Concerted transport would argue against a mechanism where dynein and kinesin physically pull the capsid apart. However, whether a foreign cargo like the viral core would activate these regulatory mechanisms is unknown. Further understanding of the regulatory mechanisms of bidirectional transport will aid in an understanding of HIV-1 uncoating.

Reverse Transcription and Microtubule-Associated Proteins (MAPs)

Reverse transcription is the process by which retroviruses convert their RNA genome into a double-strand DNA provirus. Although MTs and motor proteins appear to participate in HIV-1 uncoating, the link between these components and reverse transcription is less clear. MT depletion by nocodazole treatment did not alter reverse transcription [81], although one study reported that depletion of MAP4, which stabilizes MTs, suppressed reverse transcription and infection [79] (Figure A-4). Together, these findings suggest that the stable subset of MTs is important for reverse transcription, potentially suggesting a role for active transport along these tracks for components necessary for reverse transcription. A role for EB1 in HIV-1 reverse transcription has not been reported at this time. Alternatively, MAP4 may play a separate role beyond MT stabilization in promoting reverse transcription.

By contrast to uncoating, the role that motor proteins and active transport play in HIV-1 reverse transcription is unclear. A role for kinesin-1 in HIV-1 reverse transcription has not been reported, making this an attractive area for research. The role of dynein in reverse transcription has been examined but a clear picture has not yet emerged. One study reported that depletion of the dynein heavy chain resulted in a slight delay in reverse transcription with the levels of viral DNA accumulation recovering 24 hours after virus inoculation [78]. I also found no significant difference in reverse transcription in dynein knockdown cells by 8 hours post infection [60]. Similarly, depletion of BICD2 or dynactin components that are important for HIV-1 infection did not affect reverse transcription [60, 82]. These observations

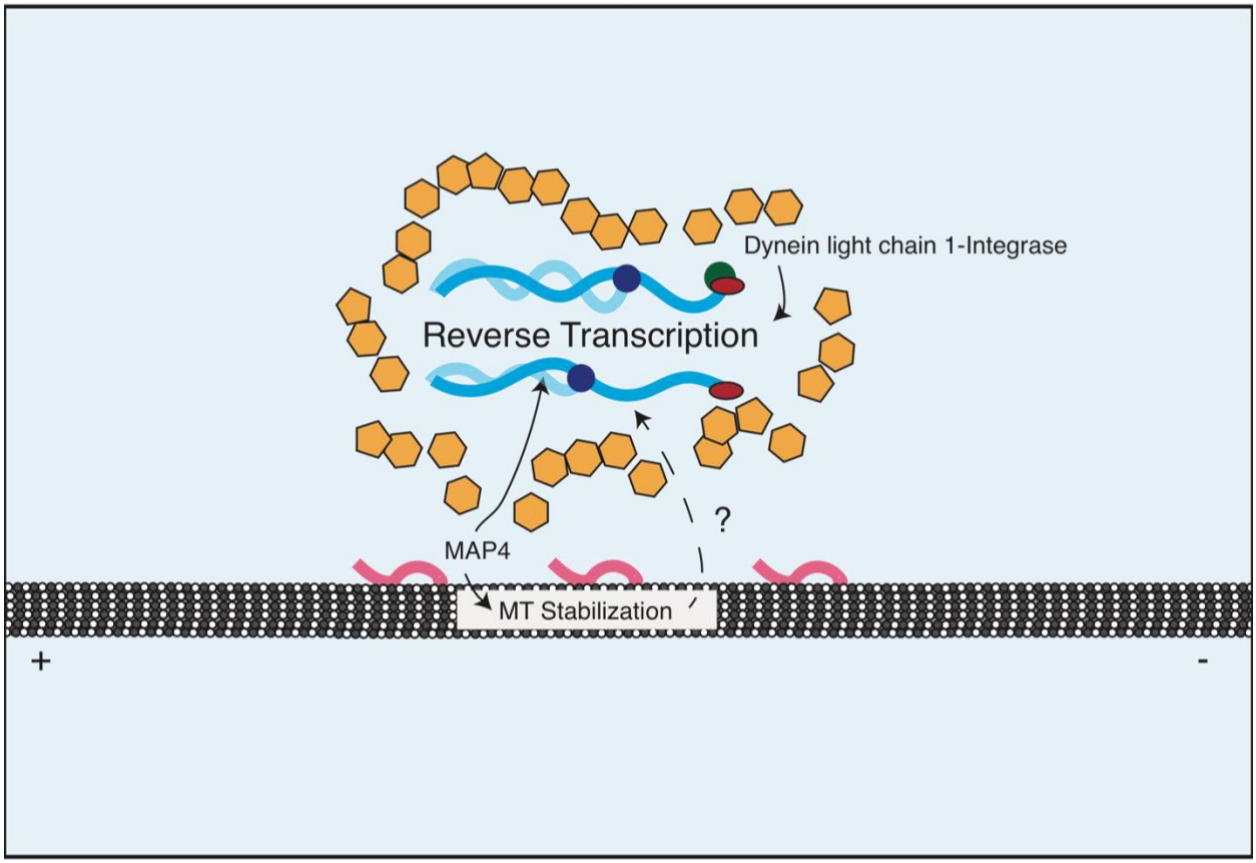

Figure A-4. Hypothetical Role of MAPs in HIV-1 Reverse Transcription. The roles of MAPs in HIV-1 reverse transcription are not well understood. The dynein-dynactin-BICD2 complex does not seem to play a role in this process, but the dynein light chain itself promotes reverse transcription through binding to the viral integrase protein. The microtubule-stabilizing protein MAP4 also promotes reverse transcription, but it is unclear whether this is a direct effect or is a consequence of its microtubule-stabilizing activity.

suggest that active transport mediated by dynein is not necessary for HIV-1 reverse transcription.

Interestingly, knockdown of the cytoplasmic dynein light chain, DYNL1 did inhibit HIV-1 reverse transcription (Figure A-4). DYNL1 was found to interact with integrase at positions Q53 and Q252, and mutations to alanines at these residues abolished integrase binding to DYNL1. This integrase mutant was also defective in reverse transcription, suggesting that the role of DYNL1 in reverse transcription requires binding to integrase. DYNL1 depletion also resulted in increased HIV-1 uncoating measured in the fate-of-capsid assay [77]. Therefore, the attenuated reverse transcription observed may be a consequence of premature uncoating, as observed for capsid-destabilizing mutations in the CA protein. The axonemal dynein light chain, DNAL1, which is expressed in lymphoblastoid cells, also promotes HIV-1 reverse transcription and infection, further supporting a role of dynein light chains in reverse transcription [79]. The apparent lack of an effect on reverse transcription from depletion studies of the dynein motor domain and dynactin [60, 78], suggests that the light chain's effect on reverse trancription is independent of the active dynein complex.

Future Perspectives

Recent advances in the understanding of HIV-1 and the MT network have revealed mechanisms by which HIV-1 usurps cellular processes to promote its replication, both through direct and indirect means. The findings suggest an overall model for transport and uncoating as depicted in Figure A-5. Upon entry, HIV-1 utilizes stabilized tracks to be transported by MT motor protein complexes dynein-dynactin-BICD2 and kinesin-FEZ1 [51, 60, 78, 82, 83]. Interestingly, HIV-1 induced MT stabilization is promoted by MA. An understanding of the mechanism of MA activation of MT stabilization may render MA a promising therapeutic target to thwart HIV-1 transport and infection. Additionally, since kinesin-1 transport is primarily toward the cell periphery, understanding the requirement for kinesin-1 in HIV-1 transport is an intriguing future direction. The role of kinesin-1 in transport will likely be unveiled as the understanding of bidirectional motility of cellular cargoes and the interplay between dynein and kinesin

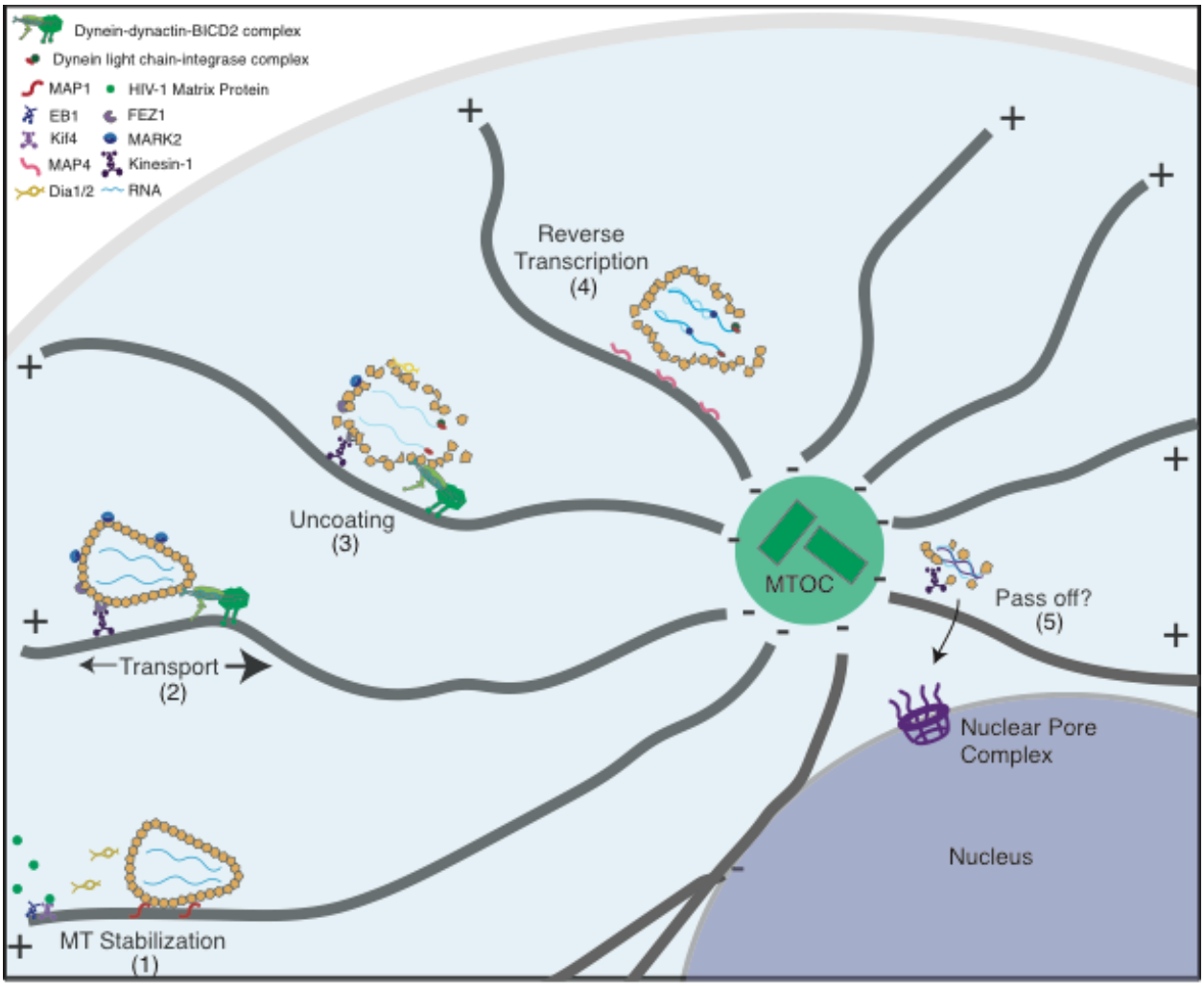

Figure A-5. MAPs Influence Many HIV-1 Early Events. The microtubule network and its associated proteins influence many aspects of HIV-1 infection. These include: 1. microtubule stabilization, 2. transport, 3. uncoating and 4. reverse transcription. Mechanisms by which HIV-1 exploits MAPs for many of its functions represent attractive areas for future research.

are further understood.

Studies have also uncovered surprising interactions between the mechanism of HIV-1 transport and other steps in the viral lifecycle, namely uncoating and reverse transcription (Figure A-5). The roles that motor complexes play in uncoating have yet to be fully elucidated, but may represent a model in which the oppositional forces from their "walking" in differing directions aids in physically breaking apart the capsid. This tug-of-war model is reminiscent of the mechanism of adenovirus uncoating by kinesin pulling the capsid apart after binding at the nuclear pore complex [219]. The role of transport in uncoating may also result from indirect effects on the viral capsid, such as positioning it at a particular location in the cell or transporting other cellular proteins and components needed for uncoating. Interestingly, the dynein light chains DYNL1 (cytoplasmic) and DNAL1 (axonemal) promote reverse transcription as well as uncoating and infection [77, 79] but may be working outside the dynein complex. The mechanism of the light chain's action in HIV-1 reverse transcription is unclear, and whether it is functioning through a direct effect on the core, or is having a secondary effect on other cellular components required for reverse transcription is unknown.

A stage of the viral lifecycle that is poorly understood is the end of transport along MTs and the "pass-off" of HIV pre-integration complex (PIC) from the MT network to the nucleus (Figure A-5). Whether the interactions between the motor complexes and the HIV-1 capsid are maintained throughout the transport process, or these connections are lost as the core begins to uncoat, are not well understood. It is known that some CA protein remains associated with the PIC throughout this process, but whether this amount is enough to sustain transport has not been shown. As discussed above, other viral proteins, including integrase, have been shown to interact with dynein complex components, and these interactions may provide a secondary mode of contact for transport of the PIC. It has not been determined whether integrase is important for transport, and especially transport after uncoating begins.

While microtubules can originate from the nuclear envelope, the majority begin at the MTOC. This leads to the question then, of how the viral PIC is transferred from the ends of MTs (at the MTOC) to the nucleus for entry (Figure A-5). Cargo movement along MTs is not a simple direct process:

transport can start and stop along the MT many times before cargo is delivered to its destination. It is possible that the PIC naturally detaches from the MT in one of these pauses, and is close enough to the nucleus to finish its transfer by diffusion alone. Another possible mechanism involves transport by kinesin-1. With the MTOC being the nucleation site for many MTs pointed in different directions, the polarity of some of these can be directed toward the nucleus. This may represent an opportunity for transport by kinesin-1 with MT positive-end walking in the direction of the nucleus. Studies have yet to reveal the way in which this transfer between MTs would occur, and the necessary signaling to switch transport.

With kinesin transport toward the nucleus, the virus still must be transferred to the nuclear envelope. It is possible that additional MAPs assist in this transfer. For instance, BICD2 anchors MTs at the nucleus during some phases of the cell cycle. Such moonlighting functions of motor-associated proteins are common and may suggest other ways in which the MT network and proteins can be exploited by HIV-1. This aspect of the viral lifecycle represents an opportunity for research and further exploration. With the current resolution and time-scale of live-cell microscopy, studies would likely be able to image this type of event. Capturing enough events at the moment of virion transfer to draw convincing conclusions might be challenging: at any given time, the majority of HIV-1 particles are nonmotile, with trafficking events occurring in short bursts. Advances in imaging techniques seem likely to overcome this limitation. While many details of the transport process remain to be worked out, it is clear that HIV-1 exploits the MT transport machinery to accomplish the early steps in infection.

The important roles that dynein, kinesins, and the MT network play in cell division and homeostasis suggest these specific components will be challenging targets for antiviral therapy. Targeting specific interactions of the adaptors BICD2 and FEZ1 may be easier, as these components, while still important, are not universally required for transport. Specifically, understanding the interactions occurring between these adaptors and the HIV-1 capsid may prove useful for the design of small molecules that selectively target the viral capsid and disrupt the interactions. Targeting the capsid to prevent BICD2 and FEZ1 binding would lessen the potential for off-target effects on cellular transport.

The potential for therapeutic targeting would be greatly enhanced with a further understanding of the mechanisms of HIV-1 transport, including initiation, active movement before and after uncoating, and the pass-off from the MT network to the nucleus. The importance of transport on other viral steps in the lifecycle, including uncoating and reverse transcription, also represents a promising area of future research.

Inhibitors of the HIV-1 capsid, a target of opportunity

Stephanie K. Carnes[a], Jonathan H. Sheehan[b], and Christopher Aiken[a]*

[a]Department of Pathology, Microbiology, and Immunology, Vanderbilt University Medical Center, and [b]Department of Biochemistry and Center for Structural Biology, Vanderbilt University, Nashville, Tennessee, USA

*Author to whom correspondence should be addressed; E-mail: chris.aiken@vanderbilt.edu; Tel.: (615) 343-7037; A-5301 Medical Center North, 1161 21st Ave S. Nashville, TN 37232

Keywords: capsid, HIV, inhibitor, maturation, uncoating

Purpose of review

To summarize recent advances in the discovery of chemical inhibitors targeting the HIV capsid and research on their mechanisms of action.

Recent findings

HIV infection is critically dependent on functions of the viral capsid. Numerous studies have reported the identification of a variety of compounds that bind to the capsid protein; some of these inhibit reverse transcription and nuclear entry, steps required for infection. Other capsid-targeting compounds appear to act by perturbing capsid assembly, resulting in noninfectious progeny virions. Inhibitors may bind to several different positions on the capsid protein, including sites in both protein domains. However, the antiviral activity of many reported capsid-targeting inhibitors has not been definitively linked to capsid binding. Until recently, the low-to-moderate potency of reported capsid-targeting inhibitors has precluded their further clinical development. In 2017, GS-CA1, a highly potent capsid inhibitor, was described that holds promise for clinical development.

Summary

Small molecules that bind to the viral capsid protein can be potent inhibitors of HIV infection. Capsid-targeting drugs are predicted to exhibit high barriers to viral resistance, and ongoing work in this area is contributing to an understanding of the molecular biology of HIV uncoating and maturation.

Introduction

Infection by HIVs remains a global public health threat. Although advances in antiretroviral therapy have been instrumental in reducing the spread and severity of HIV/AIDs, there remains no effective vaccine. Moreover, treatment is not curative; consequently, patients must be treated for their entire lives. Poor adherence to therapy leads to viral resistance to existing drugs, resulting in a continuing need for new therapeutics, preferably against new drug targets. In this review, I highlight recent research efforts aimed at identifying inhibitors that directly target the HIV-1 capsid and determining their antiviral mechanisms. Although there are currently no capsid-targeting compounds approved for clinical use, a potent capsid-targeting inhibitor recently reported holds promise for therapeutic development.

The HIV-1 capsid is a conical protein shell composed of a repeating hexameric lattice of the viral CA protein. Within the capsid are housed the viral RNA genome and associated proteins, including the enzymes reverse transcriptase and integrase. The capsid and its contents are collectively referred to as the viral core. The capsid is composed of an assembly of CA protein subunits, each consisting of two domains (N-terminal and C-terminal domains, or NTD and CTD respectively) connected by a flexible linker (Figure A-6)[1, 9, 13]. The capsid is organized into hexameric and pentameric rings of CA, and the overall lattice is stabilized by several types of CA-CA interactions (Figure A-7)[2]. The hexamers contain a central ring formed by CA-NTD interactions as well as an external ring formed by CA-CTD/CA-NTD interactions. Hexamers are connected by CTD-CTD interactions at two- and three-fold symmetry axes in the lattice [reviewed in [25]]. Of the 1200 or so CA subunits in the capsid, the majority are hexamers, but the capsid also contains 12 CA pentamers that result in closure of the lattice according to the principles of fullerene geometry. The presence of CA pentamers in the capsid of native HIV-1 particles has recently been confirmed by cryo-EM [2]. The placement of the pentamers determines the shape of the capsid, which is generally conical but can also be tubular or spherical.

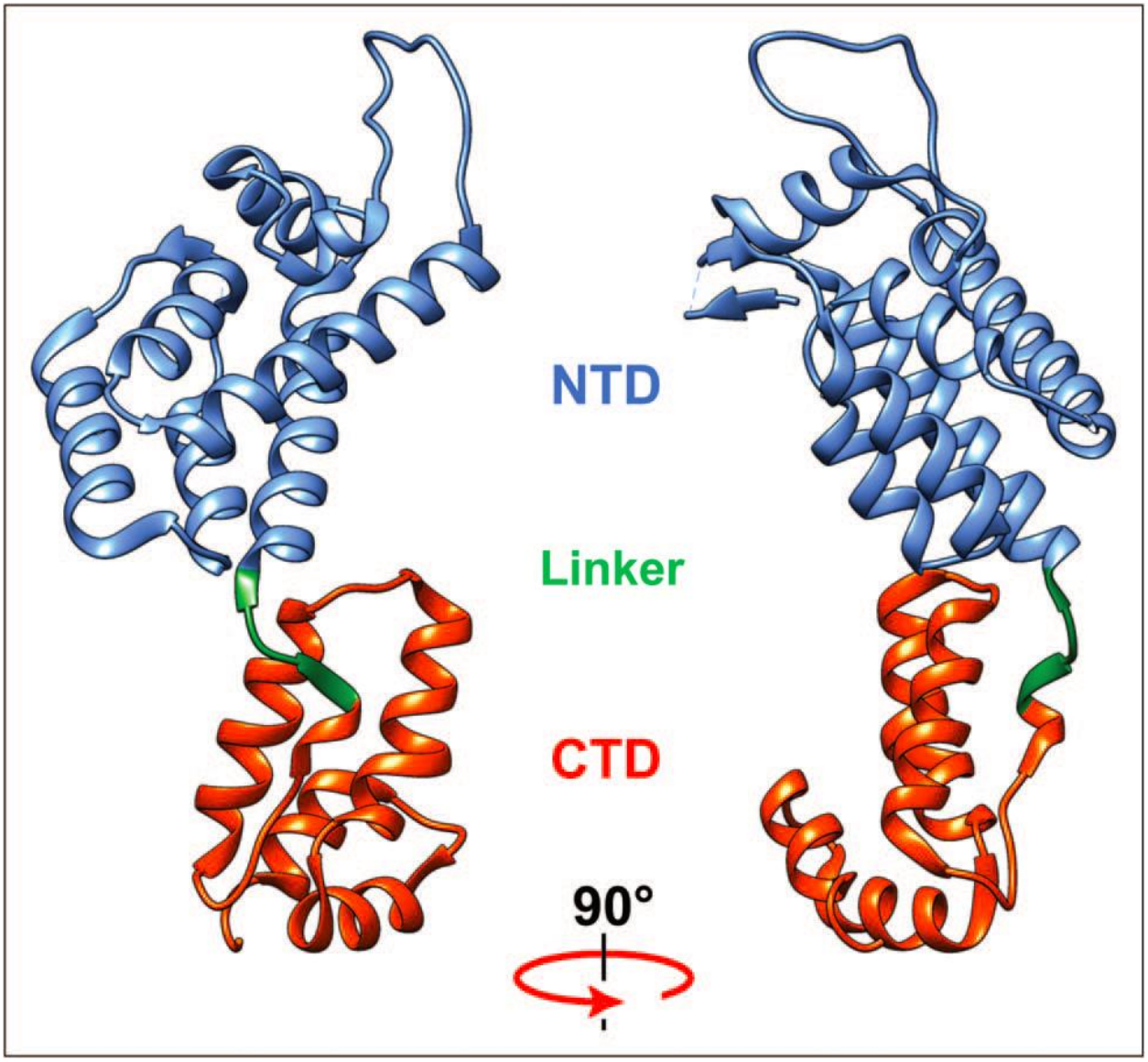

Figure A-6. Structure of the HIV-1 CA protein. CA is shown as the conformation present within the X-ray crystal structure of the CA hexamer (4xfx.pdb)[1]. Shown are the N-terminal domain (NTD), the flexible linker and the C-terminal domain (CTD). The structure was rendered with UCSF Chimera [9]as provided by SBGRID[13]. CA, capsid protein.

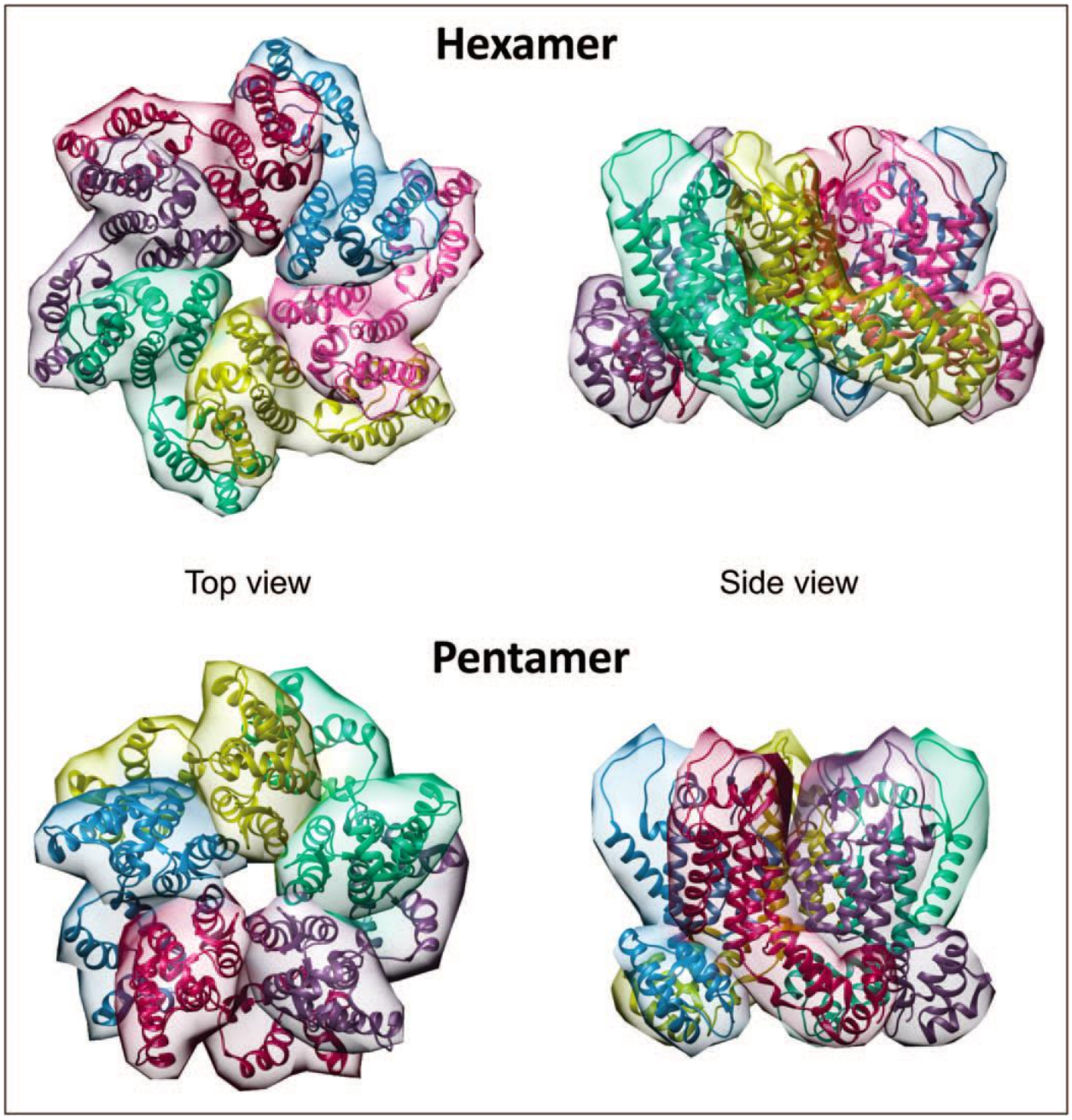

Figure A-7. Structures of the HIV-1 CA hexamer and pentamer. The hexamer represents the X-ray crystal structure of the wild-type CA hexamer (4xfx.pdb coordinates), and the pentamer was rendered from the electron tomographic structure of the native viral capsid (5mcy.pdb) [2]. The structures were rendered with Chimera's Multiscale Models tool. CA, capsid protein.

The HIV capsid is a metastable structure: mutations that either stabilize or destabilize it generally result in low viral infectivity. Following penetration into target cells, HIV must undergo reverse transcription (copying the viral RNA into DNA), intracytoplasmic transport, nuclear entry, and integration. All of these functions appear to depend on the viral capsid. During these early post-entry steps in infection, the capsid undergoes a stepwise disassembly process known as uncoating [34, 188, 212, 213, 220-224]. Perturbations in HIV capsid stability can result in premature uncoating; this frequently results in attenuated reverse transcription and a failure to establish productive infection. During its journey to the nucleus, the HIV capsid interacts with several host proteins that determine both the efficiency of nuclear entry and the distribution of integration sites in the host genome. Most of these interactions promote infection, but the noteworthy capsid-binding host proteins TRIM5□ and MxB inhibit HIV infection, further demonstrating the critical role of the of the viral capsid during infection. Small molecule inhibitors that bind to the capsid can perturb the stability balance of the capsid and compete for host factor binding, thereby interfering with infection.

In the late phase of the HIV-1 life cycle, the capsid must assemble and mature into its final conical structure [225]. CA is formed by proteolytic cleavage of the viral Gag structural polyprotein during virus maturation. The CA region of Gag is critical for both HIV particle assembly and maturation (core formation); therefore, CA-targeting small molecule inhibitors may act at early as well as late stages of replication. The many critical functions of CA make it highly attractive as a pharmacologic target. HIV is highly sensitive to mutations in CA, thus explaining its high sequence conservation relative to other HIV proteins. [13, 226, 227]. For these reasons, I expect that HIV resistance to CA-targeting drugs will require mutations that compromise the fitness of the virus, thus resulting in a high barrier to resistance and excellent therapeutic durability.

Old and New CA-targeting Inhibitors

CAP-1: The first report of a CA-targeting HIV inhibitors appeared in 2003, when Summers and coworkers identified N-(3-chloro-4-methylphenyl)-N'-{2-[({5-[dimethylamino)-methyl]-2-furyl}-

methyl)-sulfanyl]ethyl}urea) (CAP-1) via a computational search for small molecules that bound to the CA-NTD. CAP-1 reduced HIV-1 replication by 95% at a concentration of 100 µM. The compound binds to CA at the base of the NTD, near the linker region (Figure A-8). NMR spectroscopy and X-ray crystallography studies have shown that CAP-1 binding alters the conformation of the NTD; Phe32 is displaced from a buried position, opening a deep hydrophobic cavity where CAP-1 resides [3]. The compound inhibits the ability of CA to self-assemble *in vitro*, and results in virus particles of altered size and core morphology. CAP-1 does not inhibit infection at an early step, and does not appear to affect assembled capsid complexes in vitro [228]. Rather, it acts late during particle maturation, resulting in a defective core and thus noninfectious particles [229]. HIV resistance to CAP-1 have not been reported, leaving open the formal possibility of a functional target other than CA. Identification of more potent inhibitors targeting the CAP-1 binding site on CA would be helpful for further mechanistic studies.

PF74: PF-3450074 (PF74), first reported in 2010, exhibits broad spectrum inhibition of HIV isolates, with submicromolar potentcy (EC_{50} = 8-640 nM) [230-232]. High concentrations of PF74 interfere with early and late events in the virus lifecycle by destabilizing the HIV-1 capsid, resulting in premature uncoating and loss of reverse transcription and infection in early stages, and later, disrupting particle formation [232-234]. Interestingly, PF74 also stabilizes preassembled CA-NC tubes and stimulates the rate of capsid self-assembly *in vitro* [228, 235]. This may be due to the dual effects exhibited by PF74; at concentrations lower than 2 µM, the compound competes for host protein binding to the capsid, but at 10 µM it induces premature uncoating, resulting in impaired reverse transcription [236-238]. PF74 occupies a pocket in CA at the NTD-CTD intersubunit interface, at which the host proteins CPSF6 and Nup153 also bind (Figure A-8) [239, 240]. CPSF6 and Nup153 are two of many host proteins that enhance HIV infection by facilitating nuclear entry and/or integration [reviewed in [241]]. PF74's antiviral activity is also influenced by another CA-binding host factor, cyclophilin A. Cyclophilin A binds the HIV-1 capsid and promotes HIV infection, but its precise mechanism is not well understood. Inhibition of CypA binding to capsid in target cells reduces the antiviral activity of PF74, likely by modulating capsid

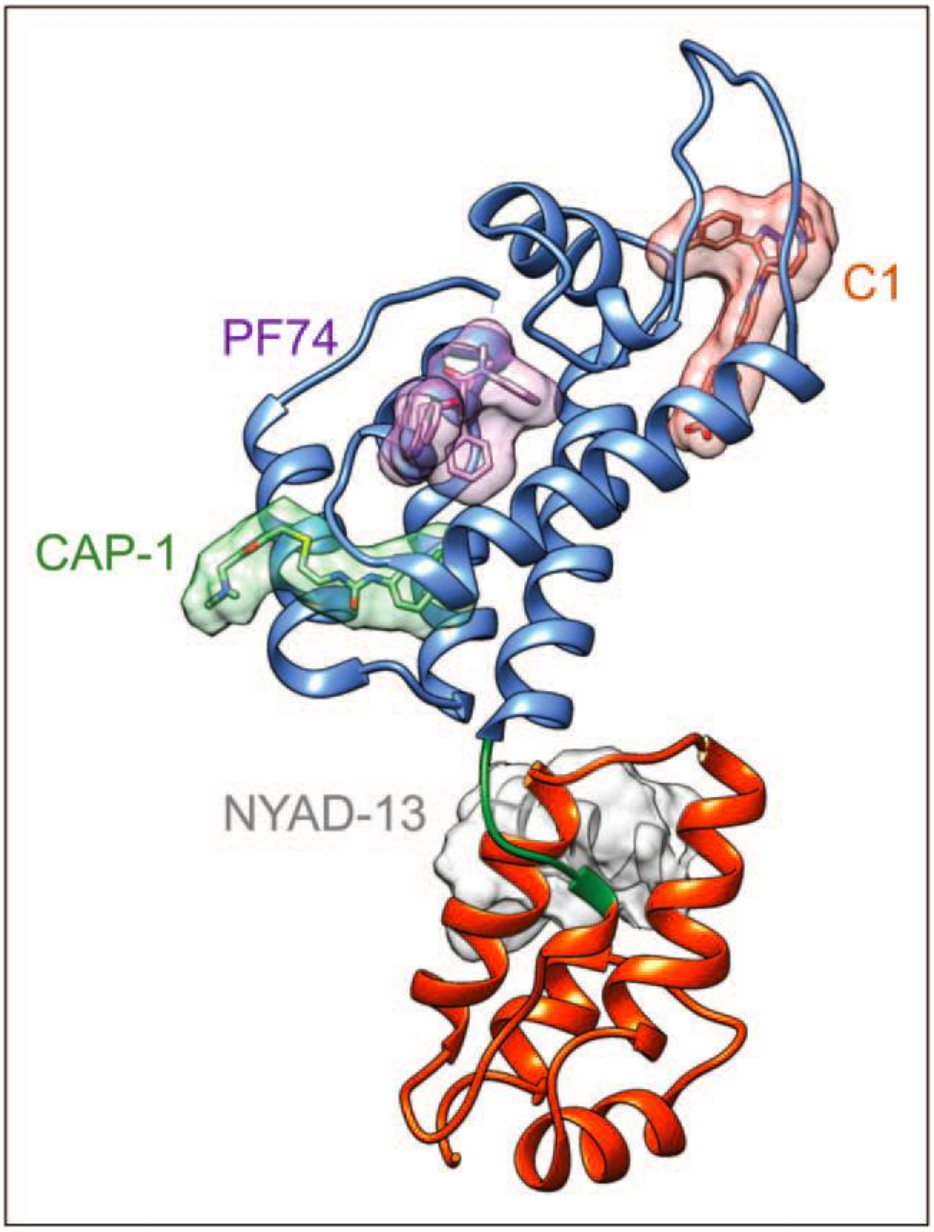

Figure A-8. HIV-1 CA binding sites for three antiviral compounds and one peptide. C1, PF74, and CAP-1 occupy distinct sites on the NTD; the stapled peptide ligand NYAD-13, an analogue of CAI, binds to the CTD dimer interface. This figure illustrates several known binding sites for CA-targeting HIV inhibitors and is a composite generated using the CA monomer from 4xfz.pdb [1]with the ligand coordinates aligned from 2jpr.pdb [3], 4e91.pdb[6], and 216e.pdb [11]. CA, capsid protein.

structure and/or other host protein interactions with the capsid [236]. The weight of evidence suggests that a major antiviral mechanism of PF74 is to perturb the binding of host factors to the incoming HIV capsid.

HIV resistance to PF74 is complex, requiring multiple of substitutions at or near the binding pocket, which lies at the NTD-CTD intersubunit interface (Figure A-8) [240]. High level resistance requires at least three amino acid changes in this region of CA [242]. Intriguingly, a substitution outside the PF74 binding site (E45A) that does not inhibit binding to PF74 also conferred resistance. The E45A mutant alters dependence of HIV-1 on specific host proteins involved in nuclear entry, including Nup153 and TNPO3 [233]. Another PF74-resistant mutant (4Mut), encoding four amino acid substitutions in CA, showed moderately reduced binding to PF74, and its replication was actually dependent on the inhibitor. The 4Mut virus encodes two amino acid substitutions each in CA-NTD and the CA-CTD within the PF74-binding pocket. Like the 5Mut virus, the dependence of 4Mut on Nup153, Nup358, and TNPO3 was also reduced, further supporting the view that PF74 acts by perturbing host factor binding and/or dependence [243].

BI Compounds: BI-1 and BI-2 are pyrrolopyrazolones that were discovered from a screen for HIV-1 replication inhibitors that stabilize capsid complexes [244]. Although they both block replication in single and multiple round infections, BI-2 is more potent (EC_{50} values are 8.2 µM and 1.8 µM, respectively). As observed for PF74, BI-2 appears to destabilize the HIV-1 core, yet it promotes the self-assembly of capsid-like complexes of recombinant CA-NC protein *in vitro* [228, 234, 244]. BI-2 does not result in impaired HIV reverse transcription in target cells, but it inhibits HIV nuclear entry. BI-2 binds to the same site in the NTD as PF74; the compound is smaller, and does not make contacts with the CTD of the adjacent CA subunit [240]. Like PF74, BI-2 can influence the binding of CPSF6 and Nup153 to the viral capsid [234, 240]. Substitutions in the binding pocket (A105 and T107) conferred resistance to both BI-1 and BI-2 [244], confirming CA as the antiviral target. Overall, BI-2 appears to inhibit HIV infection by a mechanism similar to that exhibited at low concentrations of PF74.

Peptide Inhibitors: CAI (CA inhibitor), first reported in 2005, is a CA-binding 12-mer peptide that was discovered in a phage display library screen [245]. CAI inhibits assembly of HIV-1 CA as well as a longer Gag fragment *in vitro;* it inhibits capsid self-assembly by interacting with a conserved hydrophobic groove at the CA dimerization interface (Figure A-8), altering the structure of CA in this region. CTD substitutions in this region reduce the affinity for CAI and impair the maturation of particles, resulting in reduced HIV infectivity. Like many peptides, CAI cannot penetrate cell membranes [228, 245, 246], thus precluding its use as an antiviral. To improve its cell penetration, hydrocarbon stapling was utilized to convert CAI into a cell-penetrating peptide (named NYAD-1). NYAD-1 disrupts the assembly of immature and mature-like virus particles in *in vitro* assembly assays; it also reduces particle formation and inhibits HIV-1 maturation in cell culture. Remarkably, NYAD-1 can also target the incoming HIV capsid and inhibits infection at an early postentry stage. NYAD-1 shows broad-spectrum HIV-1 infection inhibition at low micromolar potency (IC_{50} 4-15 μM), making it attractive for therapeutic development [247].

CAC-1 is another peptide that was binds to and promotes dissociation of the CTD dimer [248, 249]. In addition, CAC-1 inhibits particle production. Initial solubility and aggregation limitations prompted the design of the related peptides CAC1-M and CAC1-C with improved solubility but lower CA-binding affinities than CAC-1. These peptides exhibit limited antiviral activity but worked additively with other CA binding peptides to reduce infection by 80%-90%. Hydrocarbon stapling was employed to improve their cellular uptake, resulting in NYAD-201 and NYAD-202, which inhibit CTD dimerization and particle production, and exhibit antiviral activity at a post-entry stage [248, 250].

C-A1: The gyrase B inhibitor coumermycin A1 (C-A1) was observed to inhibit HIV-1 infection in a focused screen of known inhibitors targeting ATP-dependent DNA motors. CA-1 appears to have dual antiviral effects: it inhibits viral gene expression by targeting Hsp90, but it also

inhibits HIV integration. C-A1 had no effect on nuclear entry or reverse transcription, indicating that it acts between nuclear entry and integration. C-A1 binds the capsid directly, resistance to the compound is conferred by a point mutation at CA position 105, suggesting that C-A1-mediated inhibition may be partially due to a capsid-based mechanism. The capsid mutant N74D is also resistant to C-A1; this mutant exhibits altered dependence on specific host factors involved in nuclear entry, suggesting a functional connection between C-A1 and HIV interactions with the nuclear pore complex. Interestingly, C-A1 also promotes the binding of CPSF6 to the capsid; CPSF6, normally a nuclear protein, blocks HIV-1 infection when it is mislocalized to the cytoplasm and may hyperstabilize the HIV-1 core, thus perturbing normal HIV uncoating. In the nucleus, however, CPSF6 aids in HIV-1 integration. These findings suggest a potential model in which C-A1 prevents capsid dissociation/PIC dissociation from CPSF6 in the nucleus, therefore blocking movement and integration. This coorelates with the finding that N74D, which is independent of capsid for nuclear entry, is resistant to C-A1 [251, 252].

CK026, I-XW-053, and compound 34: The compound CK206 emerged from a virtual (i.e. *in silico*) screen of 3 million small molecules aimed at designing inhibitors of the CA-NTD/CA-NTD interface. It was found to inhibit HIV replication in single and multiple round replication of many cell types, but had no effect on PBMCs. To ameliorate this, I-XW-053 was designed based on CK026, which broadly inhibited HIV infection in PBMCs. I-XW-053 was found to interact with CA at a novel site on the NTD-NTD interface and decrease late reverse transcription products [253]. There is no impact on stability of HIV-1 CA-NC complexes in vitro, but these studies have not been performed in cells. Two CA mutants, Ile37Ala and Arg173Ala were determined to reduce binding of I-XW-053 to the capsid, and also showed a dramatic decrease in HIV-1 infection. Compound 34 was optimized from I-XW-053 to improve

antiviral potency by 11 fold (EC_{50} = 14.2 +/- 1.7 µM). It binds the same region in the CA-NTD/CA-NTD that I-XW-053 does [254].

C1: Boehringer-Ingelheim compound 1 (C1) was initially discovered as a novel inhibitor of CA assembly *in vitro* [255]. C1 binds to a unique site of the CA-NTD, near the base of the CypA-binding loop (Figure A-8). It inhibits HIV-1 replication by acting at a late step to disrupt proper assembly of the mature viral capsid, without altering Gag processing. C1 is inactive at the time of virus infection of target cells, indicating that the compound does not affect HIV-1 early events. C1 exhibits moderate antiviral activity (IC_{50} =57 µM); HIV-1 resistance can result from a single amino acid substitution within the compound binding site [6, 256], thus confirming that CA is the *bona fide* antiviral target of the compound. Though the antiviral mechanism is not fully understood, C1 may act by perturbing the kinetics of CA assembly in the maturing particle, or may promote an off-target CA assembly pathway. Further exploration of this CA target should prove informative.

Ebselen- The small molecule ebselen was recently discovered by a novel screening approach employing a time-resolved fluorescence resonance energy transfer assay to identify inhibitors of CA dimerization [257]. This assay was used to screen a library of 1280 *in vivo* active drugs. Ebselen is an efficient inhibitor of CA dimerization *in vitro* and, and was shown to inhibit HIV infection in a dose-dependent manner with moderate potency (EC_{50} = 3.37 µM). Ebselen inhibited HIV reverse transcription in target cells; it also resulted in impaired uncoating based on the fate-of-capsid assay, but these results could be due to aggregation of the CTD in the presence of ebselen, which was seen with NMR. Particle assembly and maturation were not affected, indicating that ebselen acts during early stages of infection. Whether CA is the bona fide antiviral target of ebselen remains to be determined.

Antibodies- Recently, monoclonal antibody research to inhibit viral infection within cells has flourished. Plagued by the same issue of poor cellular penetration that some peptide inhibitors face, monoclonal

antibodies are now being conjugated to cell-penetrating peptides to generate cell-internalizing antibodies. A recent antibody against CA was discovered to reduce HIV-1 replication up to 73% and 49% in T lymphocytes and PBMCs, respectively, at a concentration of 10 ug/ml. Pretreatment of cells with the antibody was more efficient at reducing HIV replication than adding antibody after viral incubation had begun, suggesting the antibody may be working at an early stage in infection. Together, these findings support that this approach has valuable promise for future therapeutic development [258].

GS-CA1- A new CA-targeting HIV inhibitor from Gilead Sciences, Inc. was recently described at scientific meetings and corporate press releases. The compound, currently named GS-CA1, exhibits highly antiviral potency in human peripheral blood mononuclear cells (EC_{50} = 140 pM) with broad spectrum inhibition across all HIV clades. GS-CA1 binds to the same broadly conserved site occupied by with PF74, lying at the NTD-CTD intersubunit interface within CA hexamers. Like PF74, GS-CA1 exhibits a dual antiviral mechanism: it acts late to reduce HIV-1 particle infectivity (presumably via perturbation of maturation); it also targets the incoming mature viral capsid to inhibit infection. GS-CA1 also binds to the same location on CA as CPSF6 and NUP153. Overall, the current unpublished descriptions of the compound's mechanism indicates that it acts like PF74, but with much greater potency. *In vitro* resistance selection experiments identified 5 amino acid substitutions in the GS-CA1 binding pocket that independently conferred resistance. However, a recent study found that none of those mutations were actively circulating or found among 132 sample patients. Studies in rats indicate that a single subcutaneous injection maintains plasma concentrations of GS-CA1 well above the plasma-binding—adjusted effective concentration required to inhibit HIV replication by 95% ($paEC_{95}$) for greater than 10 weeks, suggesting the efficacy of long-acting treatment. Gilead Sciences has announced plans to begin Investigational New Drug-enabling toxicology studies and Phase 1 clinical trials in 2018, with the goal of developing a long-acting injectable formulation [259, 260].

Perspective

Efforts to identify capsid-targeting HIV inhibitors date back 15 years, with a variety of approaches and types of molecules being described. In the past few years, this area has gained momentum, though with setbacks resulting from two major pharmaceutical companies (Pfizer and Boehringer-Ingelheim) discontinuing their HIV antivirals research efforts. Renewed optimism in this area has been stimulated by structural and mechanistic information from basic research, and there is hope that a clinically useful HIV capsid inhibitor will be licensed for therapy within the next several years.

REFERENCES

1. Gres AT, Kirby KA, Kewalramani VN, Tanner JJ, Pornillos O, Sarafianos SG. STRUCTURAL VIROLOGY. X-ray crystal structures of native HIV-1 capsid protein reveal conformational variability. *Science* 349(6243), 99-103 (2015).
2. Mattei S, Glass B, Hagen WJ, Krausslich HG, Briggs JA. The structure and flexibility of conical HIV-1 capsids determined within intact virions. *Science* 354(6318), 1434-1437 (2016).
3. Kelly BN, Kyere S, Kinde I *et al*. Structure of the antiviral assembly inhibitor CAP-1 complex with the HIV-1 CA protein. *J Mol Biol* 373(2), 355-366 (2007).
4. Campbell EM, Hope TJ. HIV-1 capsid: the multifaceted key player in HIV-1 infection. *Nat Rev Microbiol* 13(8), 471-483 (2015).
5. Pornillos O, Ganser-Pornillos BK, Yeager M. Atomic-level modelling of the HIV capsid. *Nature* 469(7330), 424-427 (2011).
6. Lemke CT, Titolo S, Von Schwedler U *et al*. Distinct effects of two HIV-1 capsid assembly inhibitor families that bind the same site within the N-terminal domain of the viral CA protein. *J Virol* 86(12), 6643-6655 (2012).
7. Katze CSaMG. Mathematical Models of viral latency. *Current Opinion in Virology* 3 402-407 (2013).
8. Schliwa M, Woehlke G. Molecular motors. *Nature* 422(6933), 759-765 (2003).
9. Pettersen EF, Goddard TD, Huang CC *et al*. UCSF Chimera--a visualization system for exploratory research and analysis. *J Comput Chem* 25(13), 1605-1612 (2004).
10. Grotjahn DA, Chowdhury S, Xu Y, Mckenney RJ, Schroer TA, Lander GC. Cryo-electron tomography reveals that dynactin recruits a team of dyneins for processive motility. *Nat Struct Mol Biol* 25(3), 203-207 (2018).
11. Bhattacharya S, Zhang H, Debnath AK, Cowburn D. Solution structure of a hydrocarbon stapled peptide inhibitor in complex with monomeric C-terminal domain of HIV-1 capsid. *J Biol Chem* 283(24), 16274-16278 (2008).
12. Hoogenraad CC, Akhmanova A. Bicaudal D Family of Motor Adaptors: Linking Dynein Motility to Cargo Binding. *Trends Cell Biol* 26(5), 327-340 (2016).
13. Morin A, Eisenbraun B, Key J *et al*. Collaboration gets the most out of software. *Elife* 2 e01456 (2013).
14. Gallo RC, Montagnier L. The discovery of HIV as the cause of AIDS. *N Engl J Med* 349(24), 2283-2285 (2003).
15. Barre-Sinoussi F, Chermann JC, Rey F *et al*. Isolation of a T-lymphotropic retrovirus from a patient at risk for acquired immune deficiency syndrome (AIDS). *Science* 220(4599), 868-871 (1983).
16. Barre-Sinoussi F, Mathur-Wagh U, Rey F *et al*. Isolation of lymphadenopathy-associated virus (LAV) and detection of LAV antibodies from US patients with AIDS. *JAMA* 253(12), 1737-1739 (1985).
17. Vilmer E, Barre-Sinoussi F, Rouzioux C *et al*. Isolation of new lymphotropic retrovirus from two siblings with haemophilia B, one with AIDS. *Lancet* 1(8380), 753-757 (1984).
18. Services USDOHH. Global HIV/AIDS Overview. (2018).
19. Lackner AA, Lederman MM, Rodriguez B. HIV pathogenesis: the host. *Cold Spring Harb Perspect Med* 2(9), a007005 (2012).
20. Services USDOHaH. What are HIV and AIDS? (2018).

21. Briggs JA, Simon MN, Gross I *et al*. The stoichiometry of Gag protein in HIV-1. *Nat Struct Mol Biol* 11(7), 672-675 (2004).
22. Ganser BK, Li S, Klishko VY, Finch JT, Sundquist WI. Assembly and analysis of conical models for the HIV-1 core. *Science* 283(5398), 80-83 (1999).
23. Li S, Hill CP, Sundquist WI, Finch JT. Image reconstructions of helical assemblies of the HIV-1 CA protein. *Nature* 407(6802), 409-413 (2000).
24. Ganser-Pornillos BK, Cheng A, Yeager M. Structure of full-length HIV-1 CA: a model for the mature capsid lattice. *Cell* 131(1), 70-79 (2007).
25. Byeon IJ, Meng X, Jung J *et al*. Structural convergence between Cryo-EM and NMR reveals intersubunit interactions critical for HIV-1 capsid function. *Cell* 139(4), 780-790 (2009).
26. Zhao G, Perilla JR, Yufenyuy EL *et al*. Mature HIV-1 capsid structure by cryo-electron microscopy and all-atom molecular dynamics. *Nature* 497(7451), 643-646 (2013).
27. Accola MA, Ohagen A, Gottlinger HG. Isolation of human immunodeficiency virus type 1 cores: retention of Vpr in the absence of p6(gag). *J Virol* 74(13), 6198-6202 (2000).
28. Kotov A, Zhou J, Flicker P, Aiken C. Association of Nef with the human immunodeficiency virus type 1 core. *J Virol* 73(10), 8824-8830 (1999).
29. Mariani R, Chen D, Schrofelbauer B *et al*. Species-specific exclusion of APOBEC3G from HIV-1 virions by Vif. *Cell* 114(1), 21-31 (2003).
30. Wilen CB, Tilton JC, Doms RW. HIV: cell binding and entry. *Cold Spring Harb Perspect Med* 2(8), (2012).
31. Endres MJ, Clapham PR, Marsh M *et al*. CD4-independent infection by HIV-2 is mediated by fusin/CXCR4. *Cell* 87(4), 745-756 (1996).
32. He J, Chen Y, Farzan M *et al*. CCR3 and CCR5 are co-receptors for HIV-1 infection of microglia. *Nature* 385(6617), 645-649 (1997).
33. Hu WS, Hughes SH. HIV-1 reverse transcription. *Cold Spring Harb Perspect Med* 2(10), (2012).
34. Mamede JI, Cianci GC, Anderson MR, Hope TJ. Early cytoplasmic uncoating is associated with infectivity of HIV-1. *Proc Natl Acad Sci U S A* 114(34), E7169-E7178 (2017).
35. Francis AC, Melikyan GB. Single HIV-1 Imaging Reveals Progression of Infection through CA-Dependent Steps of Docking at the Nuclear Pore, Uncoating, and Nuclear Transport. *Cell Host Microbe* 23(4), 536-548 e536 (2018).
36. Craigie R, Bushman FD. HIV DNA integration. *Cold Spring Harb Perspect Med* 2(7), a006890 (2012).
37. Sundquist WI, Krausslich HG. HIV-1 assembly, budding, and maturation. *Cold Spring Harb Perspect Med* 2(7), a006924 (2012).
38. Kollman JM, Merdes A, Mourey L, Agard DA. Microtubule nucleation by gamma-tubulin complexes. *Nat Rev Mol Cell Biol* 12(11), 709-721 (2011).
39. Petry S, Vale RD. Microtubule nucleation at the centrosome and beyond. *Nat Cell Biol* 17(9), 1089-1093 (2015).
40. Akhmanova A, Steinmetz MO. Control of microtubule organization and dynamics: two ends in the limelight. *Nat Rev Mol Cell Biol* 16(12), 711-726 (2015).
41. Janke C, Bulinski JC. Post-translational regulation of the microtubule cytoskeleton: mechanisms and functions. *Nat Rev Mol Cell Biol* 12(12), 773-786 (2011).
42. Xiao PJ, Samulski RJ. Cytoplasmic trafficking, endosomal escape, and perinuclear

accumulation of adeno-associated virus type 2 particles are facilitated by microtubule network. *J Virol* 86(19), 10462-10473 (2012).
43. Giannakakou P, Nakano M, Nicolaou KC *et al*. Enhanced microtubule-dependent trafficking and p53 nuclear accumulation by suppression of microtubule dynamics. *Proc Natl Acad Sci U S A* 99(16), 10855-10860 (2002).
44. Hook P, Vallee RB. The dynein family at a glance. *J Cell Sci* 119(Pt 21), 4369-4371 (2006).
45. Hirokawa N, Noda Y, Tanaka Y, Niwa S. Kinesin superfamily motor proteins and intracellular transport. *Nat Rev Mol Cell Biol* 10(10), 682-696 (2009).
46. Kato Y, Miyakawa T, Tanokura M. Overview of the mechanism of cytoskeletal motors based on structure. *Biophys Rev* doi:10.1007/s12551-017-0368-1 (2017).
47. Liu JJ. Regulation of dynein-dynactin-driven vesicular transport. *Traffic* 18(6), 336-347 (2017).
48. Schmidt H, Carter AP. Review: Structure and mechanism of the dynein motor ATPase. *Biopolymers* 105(8), 557-567 (2016).
49. Kardon JR, Vale RD. Regulators of the cytoplasmic dynein motor. *Nat Rev Mol Cell Biol* 10(12), 854-865 (2009).
50. Mckenney RJ, Huynh W, Tanenbaum ME, Bhabha G, Vale RD. Activation of cytoplasmic dynein motility by dynactin-cargo adapter complexes. *Science* 345(6194), 337-341 (2014).
51. Malikov V, Da Silva ES, Jovasevic V *et al*. HIV-1 capsids bind and exploit the kinesin-1 adaptor FEZ1 for inward movement to the nucleus. *Nat Commun* 6 6660 (2015).
52. Cianfrocco MA, Desantis ME, Leschziner AE, Reck-Peterson SL. Mechanism and regulation of cytoplasmic dynein. *Annu Rev Cell Dev Biol* 31 83-108 (2015).
53. Hancock WO. Bidirectional cargo transport: moving beyond tug of war. *Nat Rev Mol Cell Biol* 15(9), 615-628 (2014).
54. Rezaul K, Gupta D, Semenova I *et al*. Engineered Tug-of-War Between Kinesin and Dynein Controls Direction of Microtubule Based Transport In Vivo. *Traffic* 17(5), 475-486 (2016).
55. Blehm BH, Selvin PR. Single-molecule fluorescence and in vivo optical traps: how multiple dyneins and kinesins interact. *Chem Rev* 114(6), 3335-3352 (2014).
56. Dohner K, Sodeik B. The role of the cytoskeleton during viral infection. *Curr Top Microbiol Immunol* 285 67-108 (2005).
57. Dodding MP, Way M. Coupling viruses to dynein and kinesin-1. *EMBO J* 30(17), 3527-3539 (2011).
58. Dohner K, Wolfstein A, Prank U *et al*. Function of dynein and dynactin in herpes simplex virus capsid transport. *Mol Biol Cell* 13(8), 2795-2809 (2002).
59. Douglas MW, Diefenbach RJ, Homa FL *et al*. Herpes simplex virus type 1 capsid protein VP26 interacts with dynein light chains RP3 and Tctex1 and plays a role in retrograde cellular transport. *J Biol Chem* 279(27), 28522-28530 (2004).
60. Carnes SK, Zhou J, Aiken C. HIV-1 Engages a Dynein-Dynactin-BICD2 Complex for Infection and Transport to the Nucleus. *J Virol* doi:10.1128/JVI.00358-18 (2018).
61. Cao J, Lin C, Wang H *et al*. Circovirus transport proceeds via direct interaction of the cytoplasmic dynein IC1 subunit with the viral capsid protein. *J Virol* 89(5), 2777-2791 (2015).
62. Bremner KH, Scherer J, Yi J, Vershinin M, Gross SP, Vallee RB. Adenovirus transport

via direct interaction of cytoplasmic dynein with the viral capsid hexon subunit. *Cell Host Microbe* 6(6), 523-535 (2009).
63. Kelkar S, De BP, Gao G, Wilson JM, Crystal RG, Leopold PL. A common mechanism for cytoplasmic dynein-dependent microtubule binding shared among adeno-associated virus and adenovirus serotypes. *J Virol* 80(15), 7781-7785 (2006).
64. Kelkar SA, Pfister KK, Crystal RG, Leopold PL. Cytoplasmic dynein mediates adenovirus binding to microtubules. *J Virol* 78(18), 10122-10132 (2004).
65. Cortese M, Goellner S, Acosta EG *et al*. Ultrastructural Characterization of Zika Virus Replication Factories. *Cell Rep* 18(9), 2113-2123 (2017).
66. Banerjee I, Miyake Y, Nobs SP *et al*. Influenza A virus uses the aggresome processing machinery for host cell entry. *Science* 346(6208), 473-477 (2014).
67. Ye GJ, Vaughan KT, Vallee RB, Roizman B. The herpes simplex virus 1 U(L)34 protein interacts with a cytoplasmic dynein intermediate chain and targets nuclear membrane. *J Virol* 74(3), 1355-1363 (2000).
68. Wolfstein A, Nagel CH, Radtke K, Dohner K, Allan VJ, Sodeik B. The inner tegument promotes herpes simplex virus capsid motility along microtubules in vitro. *Traffic* 7(2), 227-237 (2006).
69. Radtke K, Kieneke D, Wolfstein A *et al*. Plus- and minus-end directed microtubule motors bind simultaneously to herpes simplex virus capsids using different inner tegument structures. *PLoS Pathog* 6(7), e1000991 (2010).
70. Valle-Tenney R, Opazo T, Cancino J, Goff SP, Arriagada G. Dynein Regulators Are Important for Ecotropic Murine Leukemia Virus Infection. *J Virol* 90(15), 6896-6905 (2016).
71. Naghavi MH, Walsh D. Microtubule Regulation and Function during Virus Infection. *J Virol* 91(16), (2017).
72. Roberts KL, Smith GL. Vaccinia virus morphogenesis and dissemination. *Trends Microbiol* 16(10), 472-479 (2008).
73. Ward BM. The taking of the cytoskeleton one two three: how viruses utilize the cytoskeleton during egress. *Virology* 411(2), 244-250 (2011).
74. Ward BM. Visualization and characterization of the intracellular movement of vaccinia virus intracellular mature virions. *J Virol* 79(8), 4755-4763 (2005).
75. Smith GA, Gross SP, Enquist LW. Herpesviruses use bidirectional fast-axonal transport to spread in sensory neurons. *Proc Natl Acad Sci U S A* 98(6), 3466-3470 (2001).
76. Haedicke J, De Los Santos K, Goff SP, Naghavi MH. The Ezrin-radixin-moesin family member ezrin regulates stable microtubule formation and retroviral infection. *J Virol* 82(9), 4665-4670 (2008).
77. Jayappa KD, Ao Z, Wang X *et al*. Human immunodeficiency virus type 1 employs the cellular dynein light chain 1 protein for reverse transcription through interaction with its integrase protein. *J Virol* 89(7), 3497-3511 (2015).
78. Pawlica P, Berthoux L. Cytoplasmic dynein promotes HIV-1 uncoating. *Viruses* 6(11), 4195-4211 (2014).
79. Gallo DE, Hope TJ. Knockdown of MAP4 and DNAL1 produces a post-fusion and pre-nuclear translocation impairment in HIV-1 replication. *Virology* 422(1), 13-21 (2012).
80. Delaney MK, Malikov V, Chai Q, Zhao G, Naghavi MH. Distinct functions of diaphanous-related formins regulate HIV-1 uncoating and transport. *Proc Natl Acad Sci U S A* 114(33), E6932-E6941 (2017).

81. Lukic Z, Dharan A, Fricke T, Diaz-Griffero F, Campbell EM. HIV-1 uncoating is facilitated by dynein and kinesin 1. *J Virol* 88(23), 13613-13625 (2014).
82. Dharan A, Opp S, Abdel-Rahim O *et al*. Bicaudal D2 facilitates the cytoplasmic trafficking and nuclear import of HIV-1 genomes during infection. *Proc Natl Acad Sci U S A* 114(50), E10707-E10716 (2017).
83. Mcdonald D, Vodicka MA, Lucero G *et al*. Visualization of the intracellular behavior of HIV in living cells. *J Cell Biol* 159(3), 441-452 (2002).
84. Sabo Y, Walsh D, Barry DS *et al*. HIV-1 induces the formation of stable microtubules to enhance early infection. *Cell Host Microbe* 14(5), 535-546 (2013).
85. Fernandez J, Portilho DM, Danckaert A *et al*. Microtubule-associated proteins 1 (MAP1) promote human immunodeficiency virus type I (HIV-1) intracytoplasmic routing to the nucleus. *J Biol Chem* 290(8), 4631-4646 (2015).
86. Afonso PV, Zamborlini A, Saib A, Mahieux R. Centrosome and retroviruses: the dangerous liaisons. *Retrovirology* 4 27 (2007).
87. Brass AL, Dykxhoorn DM, Benita Y *et al*. Identification of host proteins required for HIV infection through a functional genomic screen. *Science* 319(5865), 921-926 (2008).
88. Konig R, Zhou Y, Elleder D *et al*. Global analysis of host-pathogen interactions that regulate early-stage HIV-1 replication. *Cell* 135(1), 49-60 (2008).
89. Zhou H, Xu M, Huang Q *et al*. Genome-scale RNAi screen for host factors required for HIV replication. *Cell Host Microbe* 4(5), 495-504 (2008).
90. Dharan A, Talley S, Tripathi A *et al*. KIF5B and Nup358 Cooperatively Mediate the Nuclear Import of HIV-1 during Infection. *PLoS Pathog* 12(6), e1005700 (2016).
91. Gaudin R, De Alencar BC, Arhel N, Benaroch P. HIV trafficking in host cells: motors wanted! *Trends Cell Biol* 23(12), 652-662 (2013).
92. Desfarges S, Salin B, Calmels C, Andreola ML, Parissi V, Fournier M. HIV-1 integrase trafficking in S. cerevisiae: a useful model to dissect the microtubule network involvement of viral protein nuclear import. *Yeast* 26(1), 39-54 (2009).
93. Neuwald AF, Aravind L, Spouge JL, Koonin EV. AAA+: A class of chaperone-like ATPases associated with the assembly, operation, and disassembly of protein complexes. *Genome Res* 9(1), 27-43 (1999).
94. Vallee RB, Williams JC, Varma D, Barnhart LE. Dynein: An ancient motor protein involved in multiple modes of transport. *J Neurobiol* 58(2), 189-200 (2004).
95. Pawlica P, Berthoux L. Cytoplasmic dynein promotes HIV-1 uncoating. *Viruses* 6(11), 4195-4211 (2014).
96. Crackower MA, Sinasac DS, Xia J *et al*. Cloning and characterization of two cytoplasmic dynein intermediate chain genes in mouse and human. *Genomics* 55(3), 257-267 (1999).
97. Granger E, Mcnee G, Allan V, Woodman P. The role of the cytoskeleton and molecular motors in endosomal dynamics. *Semin Cell Dev Biol* 31 20-29 (2014).
98. Tan SC, Scherer J, Vallee RB. Recruitment of dynein to late endosomes and lysosomes through light intermediate chains. *Mol Biol Cell* 22(4), 467-477 (2011).
99. Jones LA, Villemant C, Starborg T *et al*. Dynein light intermediate chains maintain spindle bipolarity by functioning in centriole cohesion. *J Cell Biol* 207(4), 499-516 (2014).
100. Mische S, He Y, Ma L, Li M, Serr M, Hays TS. Dynein light intermediate chain: an essential subunit that contributes to spindle checkpoint inactivation. *Mol Biol Cell* 19(11), 4918-4929 (2008).

101. Jager S, Cimermancic P, Gulbahce N *et al*. Global landscape of HIV-human protein complexes. *Nature* 481(7381), 365-370 (2011).
102. Nyarko A, Hall J, Hall A, Hare M, Kremerskothen J, Barbar E. Conformational dynamics promote binding diversity of dynein light chain LC8. *Biophys Chem* 159(1), 41-47 (2011).
103. Dunsch AK, Hammond D, Lloyd J, Schermelleh L, Gruneberg U, Barr FA. Dynein light chain 1 and a spindle-associated adaptor promote dynein asymmetry and spindle orientation. *J Cell Biol* 198(6), 1039-1054 (2012).
104. Ayloo S, Lazarus JE, Dodda A, Tokito M, Ostap EM, Holzbaur EL. Dynactin functions as both a dynamic tether and brake during dynein-driven motility. *Nat Commun* 5 4807 (2014).
105. Lehmann M, Milev MP, Abrahamyan L, Yao XJ, Pante N, Mouland AJ. Intracellular transport of human immunodeficiency virus type 1 genomic RNA and viral production are dependent on dynein motor function and late endosome positioning. *J Biol Chem* 284(21), 14572-14585 (2009).
106. King SJ, Schroer TA. Dynactin increases the processivity of the cytoplasmic dynein motor. *Nat Cell Biol* 2(1), 20-24 (2000).
107. Culver-Hanlon TL, Lex SA, Stephens AD, Quintyne NJ, King SJ. A microtubule-binding domain in dynactin increases dynein processivity by skating along microtubules. *Nat Cell Biol* 8(3), 264-270 (2006).
108. Ross JL, Wallace K, Shuman H, Goldman YE, Holzbaur EL. Processive bidirectional motion of dynein-dynactin complexes in vitro. *Nat Cell Biol* 8(6), 562-570 (2006).
109. Tripathy SK, Weil SJ, Chen C, Anand P, Vallee RB, Gross SP. Autoregulatory mechanism for dynactin control of processive and diffusive dynein transport. *Nat Cell Biol* 16(12), 1192-1201 (2014).
110. Kobayashi T, Miyashita T, Murayama T, Toyoshima YY. Dynactin has two antagonistic regulatory domains and exerts opposing effects on dynein motility. *PLoS One* 12(8), e0183672 (2017).
111. Urnavicius L, Zhang K, Diamant AG *et al*. The structure of the dynactin complex and its interaction with dynein. *Science* 347(6229), 1441-1446 (2015).
112. Cheong FK, Feng L, Sarkeshik A, Yates JR, 3rd, Schroer TA. Dynactin integrity depends upon direct binding of dynamitin to Arp1. *Mol Biol Cell* 25(14), 2171-2180 (2014).
113. Melkonian KA, Maier KC, Godfrey JE, Rodgers M, Schroer TA. Mechanism of dynamitin-mediated disruption of dynactin. *J Biol Chem* 282(27), 19355-19364 (2007).
114. Goodson HV, Skube SB, Stalder R *et al*. CLIP-170 interacts with dynactin complex and the APC-binding protein EB1 by different mechanisms. *Cell Motil Cytoskeleton* 55(3), 156-173 (2003).
115. Jacquot G, Maidou-Peindara P, Benichou S. Molecular and functional basis for the scaffolding role of the p50/dynamitin subunit of the microtubule-associated dynactin complex. *J Biol Chem* 285(30), 23019-23031 (2010).
116. Yeh TY, Quintyne NJ, Scipioni BR, Eckley DM, Schroer TA. Dynactin's pointed-end complex is a cargo-targeting module. *Mol Biol Cell* 23(19), 3827-3837 (2012).
117. Schroeder CM, Vale RD. Assembly and activation of dynein-dynactin by the cargo adaptor protein Hook3. *J Cell Biol* 214(3), 309-318 (2016).
118. Schlager MA, Hoang HT, Urnavicius L, Bullock SL, Carter AP. In vitro reconstitution of a highly processive recombinant human dynein complex. *EMBO J* 33(17), 1855-1868

(2014).
119. Splinter D, Razafsky DS, Schlager MA *et al*. BICD2, dynactin, and LIS1 cooperate in regulating dynein recruitment to cellular structures. *Mol Biol Cell* 23(21), 4226-4241 (2012).
120. Yamada M, Toba S, Yoshida Y *et al*. LIS1 and NDEL1 coordinate the plus-end-directed transport of cytoplasmic dynein. *EMBO J* 27(19), 2471-2483 (2008).
121. Lam C, Vergnolle MA, Thorpe L, Woodman PG, Allan VJ. Functional interplay between LIS1, NDE1 and NDEL1 in dynein-dependent organelle positioning. *J Cell Sci* 123(Pt 2), 202-212 (2010).
122. Hoogenraad CC, Akhmanova A, Howell SA *et al*. Mammalian Golgi-associated Bicaudal-D2 functions in the dynein-dynactin pathway by interacting with these complexes. *EMBO J* 20(15), 4041-4054 (2001).
123. Gassmann R, Essex A, Hu JS *et al*. A new mechanism controlling kinetochore-microtubule interactions revealed by comparison of two dynein-targeting components: SPDL-1 and the Rod/Zwilch/Zw10 complex. *Genes Dev* 22(17), 2385-2399 (2008).
124. Williams BC, Li Z, Liu S *et al*. Zwilch, a new component of the ZW10/ROD complex required for kinetochore functions. *Mol Biol Cell* 14(4), 1379-1391 (2003).
125. Zhang J, Qiu R, Arst HN, Jr., Penalva MA, Xiang X. HookA is a novel dynein-early endosome linker critical for cargo movement in vivo. *J Cell Biol* 204(6), 1009-1026 (2014).
126. Epie N, Ammosova T, Sapir T *et al*. HIV-1 Tat interacts with LIS1 protein. *Retrovirology* 2 6 (2005).
127. Hoogenraad CC, Wulf P, Schiefermeier N *et al*. Bicaudal D induces selective dynein-mediated microtubule minus end-directed transport. *EMBO J* 22(22), 6004-6015 (2003).
128. Stein MP, Dong J, Wandinger-Ness A. Rab proteins and endocytic trafficking: potential targets for therapeutic intervention. *Adv Drug Deliv Rev* 55(11), 1421-1437 (2003).
129. Galvez T, Gilleron J, Zerial M, O'sullivan GA. SnapShot: Mammalian Rab proteins in endocytic trafficking. *Cell* 151(1), 234-234 e232 (2012).
130. Amin MA, Kobayashi K, Tanaka K. CLIP-170 tethers kinetochores to microtubule plus ends against poleward force by dynein for stable kinetochore-microtubule attachment. *FEBS Lett* 589(19 Pt B), 2739-2746 (2015).
131. Folker ES, Baker BM, Goodson HV. Interactions between CLIP-170, tubulin, and microtubules: implications for the mechanism of Clip-170 plus-end tracking behavior. *Mol Biol Cell* 16(11), 5373-5384 (2005).
132. Tanenbaum ME, Galjart N, Van Vugt MA, Medema RH. CLIP-170 facilitates the formation of kinetochore-microtubule attachments. *EMBO J* 25(1), 45-57 (2006).
133. Tse WT, Tang J, Jin O *et al*. A new spectrin, beta IV, has a major truncated isoform that associates with promyelocytic leukemia protein nuclear bodies and the nuclear matrix. *J Biol Chem* 276(26), 23974-23985 (2001).
134. Berghs S, Aggujaro D, Dirkx R, Jr. *et al*. betaIV spectrin, a new spectrin localized at axon initial segments and nodes of ranvier in the central and peripheral nervous system. *J Cell Biol* 151(5), 985-1002 (2000).
135. Shoeman RL, Hartig R, Hauses C, Traub P. Organization of focal adhesion plaques is disrupted by action of the HIV-1 protease. *Cell Biol Int* 26(6), 529-539 (2002).
136. Lammers LG, Markus SM. The dynein cortical anchor Num1 activates dynein motility by relieving Pac1/LIS1-mediated inhibition. *J Cell Biol* 211(2), 309-322 (2015).

137. Bi X, Corpina RA, Goldberg J. Structure of the Sec23/24-Sar1 pre-budding complex of the COPII vesicle coat. *Nature* 419(6904), 271-277 (2002).
138. Fromme JC, Orci L, Schekman R. Coordination of COPII vesicle trafficking by Sec23. *Trends Cell Biol* 18(7), 330-336 (2008).
139. Caillet M, Janvier K, Pelchen-Matthews A *et al*. Rab7A is required for efficient production of infectious HIV-1. *PLoS Pathog* 7(11), e1002347 (2011).
140. Drerup CM, Nechiporuk AV. JNK-interacting protein 3 mediates the retrograde transport of activated c-Jun N-terminal kinase and lysosomes. *PLoS Genet* 9(2), e1003303 (2013).
141. Gaudet P, Livstone MS, Lewis SE, Thomas PD. Phylogenetic-based propagation of functional annotations within the Gene Ontology consortium. *Brief Bioinform* 12(5), 449-462 (2011).
142. Stewart-Hutchinson PJ, Hale CM, Wirtz D, Hodzic D. Structural requirements for the assembly of LINC complexes and their function in cellular mechanical stiffness. *Exp Cell Res* 314(8), 1892-1905 (2008).
143. Morimoto A, Shibuya H, Zhu X *et al*. A conserved KASH domain protein associates with telomeres, SUN1, and dynactin during mammalian meiosis. *J Cell Biol* 198(2), 165-172 (2012).
144. Luo X, Yang W, Gao G. SUN1 Regulates HIV-1 Nuclear Import in a Manner Dependent on the Interaction between the Viral Capsid and Cellular Cyclophilin A. *J Virol* 92(13), (2018).
145. Horgan CP, Oleksy A, Zhdanov AV *et al*. Rab11-FIP3 is critical for the structural integrity of the endosomal recycling compartment. *Traffic* 8(4), 414-430 (2007).
146. Del Rio-Iniguez I, Vazquez-Chavez E, Cuche C, Di Bartolo V, Bouchet J, Alcover A. HIV-1 Nef Hijacks Lck and Rac1 Endosomal Traffic To Dually Modulate Signaling-Mediated and Actin Cytoskeleton-Mediated T Cell Functions. *J Immunol* 201(9), 2624-2640 (2018).
147. Xiang X, Qiu R, Yao X, Arst HN, Jr., Penalva MA, Zhang J. Cytoplasmic dynein and early endosome transport. *Cell Mol Life Sci* 72(17), 3267-3280 (2015).
148. Minton K. Molecular motors: Hook-ing up early endosomes. *Nat Rev Mol Cell Biol* 15(5), 297 (2014).
149. Lajoie-Mazenc I, Tovar D, Penary M *et al*. MAP1A light chain-2 interacts with GTP-RhoB to control epidermal growth factor (EGF)-dependent EGF receptor signaling. *J Biol Chem* 283(7), 4155-4164 (2008).
150. Serna M, Carranza G, Martin-Benito J *et al*. The structure of the complex between alpha-tubulin, TBCE and TBCB reveals a tubulin dimer dissociation mechanism. *J Cell Sci* 128(9), 1824-1834 (2015).
151. Cattaruzzi G, Altamura S, Tessari MA *et al*. The second AT-hook of the architectural transcription factor HMGA2 is determinant for nuclear localization and function. *Nucleic Acids Res* 35(6), 1751-1760 (2007).
152. Naji S, Ambrus G, Cimermancic P *et al*. Host cell interactome of HIV-1 Rev includes RNA helicases involved in multiple facets of virus production. *Mol Cell Proteomics* 11(4), M111 015313 (2012).
153. Gautier VW, Gu L, O'donoghue N, Pennington S, Sheehy N, Hall WW. In vitro nuclear interactome of the HIV-1 Tat protein. *Retrovirology* 6 47 (2009).
154. Miyatake H, Sanjoh A, Murakami T *et al*. Molecular Mechanism of HIV-1 Vpr for Binding to Importin-alpha. *J Mol Biol* 428(13), 2744-2757 (2016).

155. Barisic M, Silva E Sousa R, Tripathy SK *et al*. Mitosis. Microtubule detyrosination guides chromosomes during mitosis. *Science* 348(6236), 799-803 (2015).
156. Rodriguez De La Vega Otazo M, Lorenzo J, Tort O, Aviles FX, Bautista JM. Functional segregation and emerging role of cilia-related cytosolic carboxypeptidases (CCPs). *FASEB J* 27(2), 424-431 (2013).
157. Aspenstrom P. The mammalian verprolin homologue WIRE participates in receptor-mediated endocytosis and regulation of the actin filament system by distinct mechanisms. *Exp Cell Res* 298(2), 485-498 (2004).
158. Alborghetti MR, Furlan Ada S, Da Silva JC *et al*. Structural analysis of intermolecular interactions in the kinesin adaptor complex fasciculation and elongation protein zeta 1/ short coiled-coil protein (FEZ1/SCOCO). *PLoS One* 8(10), e76602 (2013).
159. Haedicke J, Brown C, Naghavi MH. The brain-specific factor FEZ1 is a determinant of neuronal susceptibility to HIV-1 infection. *Proc Natl Acad Sci U S A* 106(33), 14040-14045 (2009).
160. Malikov V, Naghavi MH. Localized Phosphorylation of a Kinesin-1 Adaptor by a Capsid-Associated Kinase Regulates HIV-1 Motility and Uncoating. *Cell Rep* 20(12), 2792-2799 (2017).
161. Radhakrishna H, Al-Awar O, Khachikian Z, Donaldson JG. ARF6 requirement for Rac ruffling suggests a role for membrane trafficking in cortical actin rearrangements. *J Cell Sci* 112 (Pt 6) 855-866 (1999).
162. Kameoka M, Kitagawa Y, Utachee P *et al*. Identification of the suppressive factors for human immunodeficiency virus type-1 replication using the siRNA mini-library directed against host cellular genes. *Biochem Biophys Res Commun* 359(3), 729-734 (2007).
163. Staples CJ, Myers KN, Beveridge RD *et al*. The centriolar satellite protein Cep131 is important for genome stability. *J Cell Sci* 125(Pt 20), 4770-4779 (2012).
164. Shimizu S, Matsuzaki S, Hattori T *et al*. DISC1-kendrin interaction is involved in centrosomal microtubule network formation. *Biochem Biophys Res Commun* 377(4), 1051-1056 (2008).
165. Chen CT, Hehnly H, Yu Q *et al*. A unique set of centrosome proteins requires pericentrin for spindle-pole localization and spindle orientation. *Curr Biol* 24(19), 2327-2334 (2014).
166. Chang F, Re F, Sebastian S, Sazer S, Luban J. HIV-1 Vpr induces defects in mitosis, cytokinesis, nuclear structure, and centrosomes. *Mol Biol Cell* 15(4), 1793-1801 (2004).
167. Sancak Y, Bar-Peled L, Zoncu R, Markhard AL, Nada S, Sabatini DM. Ragulator-Rag complex targets mTORC1 to the lysosomal surface and is necessary for its activation by amino acids. *Cell* 141(2), 290-303 (2010).
168. Schroder B, Wrocklage C, Pan C *et al*. Integral and associated lysosomal membrane proteins. *Traffic* 8(12), 1676-1686 (2007).
169. Kronja I, Kruljac-Letunic A, Caudron-Herger M, Bieling P, Karsenti E. XMAP215-EB1 interaction is required for proper spindle assembly and chromosome segregation in Xenopus egg extract. *Mol Biol Cell* 20(11), 2684-2696 (2009).
170. Nakamura M, Zhou XZ, Kishi S, Lu KP. Involvement of the telomeric protein Pin2/TRF1 in the regulation of the mitotic spindle. *FEBS Lett* 514(2-3), 193-198 (2002).
171. Bouguenina H, Salaun D, Mangon A *et al*. EB1-binding-myomegalin protein complex promotes centrosomal microtubules functions. *Proc Natl Acad Sci U S A* 114(50), E10687-E10696 (2017).
172. Mimori-Kiyosue Y, Grigoriev I, Lansbergen G *et al*. CLASP1 and CLASP2 bind to EB1

and regulate microtubule plus-end dynamics at the cell cortex. *J Cell Biol* 168(1), 141-153 (2005).
173. Stehbens SJ, Paszek M, Pemble H, Ettinger A, Gierke S, Wittmann T. CLASPs link focal-adhesion-associated microtubule capture to localized exocytosis and adhesion site turnover. *Nat Cell Biol* 16(6), 561-573 (2014).
174. Setty SR, Tenza D, Truschel ST *et al*. BLOC-1 is required for cargo-specific sorting from vacuolar early endosomes toward lysosome-related organelles. *Mol Biol Cell* 18(3), 768-780 (2007).
175. Asiedu M, Wu D, Matsumura F, Wei Q. Centrosome/spindle pole-associated protein regulates cytokinesis via promoting the recruitment of MyoGEF to the central spindle. *Mol Biol Cell* 20(5), 1428-1440 (2009).
176. Firestone AJ, Weinger JS, Maldonado M *et al*. Small-molecule inhibitors of the AAA+ ATPase motor cytoplasmic dynein. *Nature* 484(7392), 125-129 (2012).
177. Opazo T, Garces A, Tapia D *et al*. Functional Evidence of the Involvement of the Dynein Light Chain DYNLRB2 in Murine Leukemia Virus Infection. *J Virol* 91(10), (2017).
178. Stuurman N, Haner M, Sasse B, Hubner W, Suter B, Aebi U. Interactions between coiled-coil proteins: Drosophila lamin Dm0 binds to the bicaudal-D protein. *Eur J Cell Biol* 78(4), 278-287 (1999).
179. Short B, Preisinger C, Schaletzky J, Kopajtich R, Barr FA. The Rab6 GTPase regulates recruitment of the dynactin complex to Golgi membranes. *Curr Biol* 12(20), 1792-1795 (2002).
180. Matanis T, Akhmanova A, Wulf P *et al*. Bicaudal-D regulates COPI-independent Golgi-ER transport by recruiting the dynein-dynactin motor complex. *Nat Cell Biol* 4(12), 986-992 (2002).
181. Terawaki S, Yoshikane A, Higuchi Y, Wakamatsu K. Structural basis for cargo binding and autoinhibition of Bicaudal-D1 by a parallel coiled-coil with homotypic registry. *Biochem Biophys Res Commun* 460(2), 451-456 (2015).
182. Liu Y, Salter HK, Holding AN *et al*. Bicaudal-D uses a parallel, homodimeric coiled coil with heterotypic registry to coordinate recruitment of cargos to dynein. *Genes Dev* 27(11), 1233-1246 (2013).
183. Grigoriev I, Splinter D, Keijzer N *et al*. Rab6 regulates transport and targeting of exocytotic carriers. *Dev Cell* 13(2), 305-314 (2007).
184. Reck-Peterson SL, Yildiz A, Carter AP, Gennerich A, Zhang N, Vale RD. Single-molecule analysis of dynein processivity and stepping behavior. *Cell* 126(2), 335-348 (2006).
185. Campbell EM, Perez O, Melar M, Hope TJ. Labeling HIV-1 virions with two fluorescent proteins allows identification of virions that have productively entered the target cell. *Virology* 360(2), 286-293 (2007).
186. Matsuto M, Kano F, Murata M. Reconstitution of the targeting of Rab6A to the Golgi apparatus in semi-intact HeLa cells: A role of BICD2 in stabilizing Rab6A on Golgi membranes and a concerted role of Rab6A/BICD2 interactions in Golgi-to-ER retrograde transport. *Biochim Biophys Acta* 1853(10 Pt A), 2592-2609 (2015).
187. Hulme AE, Kelley Z, Foley D, Hope TJ. Complementary Assays Reveal a Low Level of CA Associated with Viral Complexes in the Nuclei of HIV-1-Infected Cells. *J Virol* 89(10), 5350-5361 (2015).
188. Francis AC, Marin M, Shi J, Aiken C, Melikyan GB. Time-Resolved Imaging of Single

HIV-1 Uncoating In Vitro and in Living Cells. *PLoS Pathog* 12(6), e1005709 (2016).
189. Yee JK, Friedmann T, Burns JC. Generation of high-titer pseudotyped retroviral vectors with very broad host range. *Methods Cell Biol* 43 Pt A 99-112 (1994).
190. Zhang YJ, Hatziioannou T, Zang T *et al*. Envelope-dependent, cyclophilin-independent effects of glycosaminoglycans on human immunodeficiency virus type 1 attachment and infection. *J Virol* 76(12), 6332-6343 (2002).
191. Miyoshi H, Takahashi M, Gage FH, Verma IM. Stable and efficient gene transfer into the retina using an HIV-based lentiviral vector. *Proc Natl Acad Sci U S A* 94(19), 10319-10323 (1997).
192. Morgenstern JP, Land H. Advanced mammalian gene transfer: high titre retroviral vectors with multiple drug selection markers and a complementary helper-free packaging cell line. *Nucleic Acids Res* 18(12), 3587-3596 (1990).
193. Du S, Betts L, Yang R *et al*. Structure of the HIV-1 full-length capsid protein in a conformationally trapped unassembled state induced by small-molecule binding. *J Mol Biol* 406(3), 371-386 (2011).
194. Wei X, Decker JM, Liu H *et al*. Emergence of resistant human immunodeficiency virus type 1 in patients receiving fusion inhibitor (T-20) monotherapy. *Antimicrob Agents Chemother* 46(6), 1896-1905 (2002).
195. Platt EJ, Bilska M, Kozak SL, Kabat D, Montefiori DC. Evidence that ecotropic murine leukemia virus contamination in TZM-bl cells does not affect the outcome of neutralizing antibody assays with human immunodeficiency virus type 1. *J Virol* 83(16), 8289-8292 (2009).
196. Takeuchi Y, Mcclure MO, Pizzato M. Identification of gammaretroviruses constitutively released from cell lines used for human immunodeficiency virus research. *J Virol* 82(24), 12585-12588 (2008).
197. Derdeyn CA, Decker JM, Sfakianos JN *et al*. Sensitivity of human immunodeficiency virus type 1 to the fusion inhibitor T-20 is modulated by coreceptor specificity defined by the V3 loop of gp120. *J Virol* 74(18), 8358-8367 (2000).
198. Platt EJ, Wehrly K, Kuhmann SE, Chesebro B, Kabat D. Effects of CCR5 and CD4 cell surface concentrations on infections by macrophagetropic isolates of human immunodeficiency virus type 1. *J Virol* 72(4), 2855-2864 (1998).
199. Weiss A, Wiskocil RL, Stobo JD. The role of T3 surface molecules in the activation of human T cells: a two-stimulus requirement for IL 2 production reflects events occurring at a pre-translational level. *J Immunol* 133(1), 123-128 (1984).
200. Morner A, Bjorndal A, Albert J *et al*. Primary human immunodeficiency virus type 2 (HIV-2) isolates, like HIV-1 isolates, frequently use CCR5 but show promiscuity in coreceptor usage. *J Virol* 73(3), 2343-2349 (1999).
201. Schindelin J, Arganda-Carreras I, Frise E *et al*. Fiji: an open-source platform for biological-image analysis. *Nat Methods* 9(7), 676-682 (2012).
202. Tinevez JY, Perry N, Schindelin J *et al*. TrackMate: An open and extensible platform for single-particle tracking. *Methods* 115 80-90 (2017).
203. Burse M, Shi J, Aiken C. Cyclophilin A potentiates TRIM5alpha inhibition of HIV-1 nuclear import without promoting TRIM5alpha binding to the viral capsid. *PLoS One* 12(8), e0182298 (2017).
204. Goychuk I, Kharchenko VO, Metzler R. How molecular motors work in the crowded environment of living cells: coexistence and efficiency of normal and anomalous

transport. *PLoS One* 9(3), e91700 (2014).
205. Ellis RJ, Minton AP. Cell biology: join the crowd. *Nature* 425(6953), 27-28 (2003).
206. Mcguffee SR, Elcock AH. Diffusion, crowding & protein stability in a dynamic molecular model of the bacterial cytoplasm. *PLoS Comput Biol* 6(3), e1000694 (2010).
207. Yoder A, Guo J, Yu D, Cui Z, Zhang XE, Wu Y. Effects of microtubule modulators on HIV-1 infection of transformed and resting CD4 T cells. *J Virol* 85(6), 3020-3024 (2011).
208. Naghavi MH. Stable microtubule subsets facilitate early HIV-1 infection. *AIDS Res Hum Retroviruses* 30(3), 211-212 (2014).
209. Akhmanova A, Steinmetz MO. Microtubule +TIPs at a glance. *J Cell Sci* 123(Pt 20), 3415-3419 (2010).
210. Wloga D, Gaertig J. Post-translational modifications of microtubules. *J Cell Sci* 123(Pt 20), 3447-3455 (2010).
211. Halpain S, Dehmelt L. The MAP1 family of microtubule-associated proteins. *Genome Biol* 7(6), 224 (2006).
212. Forshey BM, Von Schwedler U, Sundquist WI, Aiken C. Formation of a human immunodeficiency virus type 1 core of optimal stability is crucial for viral replication. *J Virol* 76(11), 5667-5677 (2002).
213. Da Silva Santos C, Tartour K, Cimarelli A. A Novel Entry/Uncoating Assay Reveals the Presence of at Least Two Species of Viral Capsids During Synchronized HIV-1 Infection. *PLoS Pathog* 12(9), e1005897 (2016).
214. Stremlau M, Perron M, Lee M *et al*. Specific recognition and accelerated uncoating of retroviral capsids by the TRIM5alpha restriction factor. *Proc Natl Acad Sci U S A* 103(14), 5514-5519 (2006).
215. Hulme AE, Hope TJ. The cyclosporin A washout assay to detect HIV-1 uncoating in infected cells. *Methods Mol Biol* 1087 37-46 (2014).
216. Hendricks AG, Holzbaur EL, Goldman YE. Force measurements on cargoes in living cells reveal collective dynamics of microtubule motors. *Proc Natl Acad Sci U S A* 109(45), 18447-18452 (2012).
217. Blehm BH, Schroer TA, Trybus KM, Chemla YR, Selvin PR. In vivo optical trapping indicates kinesin's stall force is reduced by dynein during intracellular transport. *Proc Natl Acad Sci U S A* 110(9), 3381-3386 (2013).
218. Rai AK, Rai A, Ramaiya AJ, Jha R, Mallik R. Molecular adaptations allow dynein to generate large collective forces inside cells. *Cell* 152(1-2), 172-182 (2013).
219. Strunze S, Engelke MF, Wang IH *et al*. Kinesin-1-mediated capsid disassembly and disruption of the nuclear pore complex promote virus infection. *Cell Host Microbe* 10(3), 210-223 (2011).
220. Hulme AE, Perez O, Hope TJ. Complementary assays reveal a relationship between HIV-1 uncoating and reverse transcription. *Proc Natl Acad Sci U S A* 108(24), 9975-9980 (2011).
221. Rankovic S, Varadarajan J, Ramalho R, Aiken C, Rousso I. Reverse Transcription Mechanically Initiates HIV-1 Capsid Disassembly. *J Virol* 91(12), (2017).
222. Ramalho R, Rankovic S, Zhou J, Aiken C, Rousso I. Analysis of the mechanical properties of wild type and hyperstable mutants of the HIV-1 capsid. *Retrovirology* 13 17 (2016).
223. Arfi V, Lienard J, Nguyen XN *et al*. Characterization of the behavior of functional viral genomes during the early steps of human immunodeficiency virus type 1 infection. *J*

Virol 83(15), 7524-7535 (2009).
224. Cosnefroy O, Murray PJ, Bishop KN. HIV-1 capsid uncoating initiates after the first strand transfer of reverse transcription. *Retrovirology* 13(1), 58 (2016).
225. Freed EO. HIV-1 assembly, release and maturation. *Nat Rev Microbiol* 13(8), 484-496 (2015).
226. Rihn SJ, Wilson SJ, Loman NJ *et al*. Extreme genetic fragility of the HIV-1 capsid. *PLoS Pathog* 9(6), e1003461 (2013).
227. Li G, Verheyen J, Rhee SY, Voet A, Vandamme AM, Theys K. Functional conservation of HIV-1 Gag: implications for rational drug design. *Retrovirology* 10 126 (2013).
228. Fricke T, Brandariz-Nunez A, Wang X, Smith AB, 3rd, Diaz-Griffero F. Human cytosolic extracts stabilize the HIV-1 core. *J Virol* 87(19), 10587-10597 (2013).
229. Tang C, Loeliger E, Kinde I *et al*. Antiviral inhibition of the HIV-1 capsid protein. *J Mol Biol* 327(5), 1013-1020 (2003).
230. Blair WS, Isaacson J, Li X *et al*. A novel HIV-1 antiviral high throughput screening approach for the discovery of HIV-1 inhibitors. *Antiviral Res* 65(2), 107-116 (2005).
231. Rasaiyaah J, Tan CP, Fletcher AJ *et al*. HIV-1 evades innate immune recognition through specific cofactor recruitment. *Nature* 503(7476), 402-405 (2013).
232. Blair WS, Pickford C, Irving SL *et al*. HIV capsid is a tractable target for small molecule therapeutic intervention. *PLoS Pathog* 6(12), e1001220 (2010).
233. Shi J, Zhou J, Shah VB, Aiken C, Whitby K. Small-molecule inhibition of human immunodeficiency virus type 1 infection by virus capsid destabilization. *J Virol* 85(1), 542-549 (2011).
234. Fricke T, Buffone C, Opp S, Valle-Casuso J, Diaz-Griffero F. BI-2 destabilizes HIV-1 cores during infection and Prevents Binding of CPSF6 to the HIV-1 Capsid. *Retrovirology* 11 120 (2014).
235. Lad L, Clancy S, Koditek D *et al*. Functional label-free assays for characterizing the in vitro mechanism of action of small molecule modulators of capsid assembly. *Biochemistry* 54(13), 2240-2248 (2015).
236. Saito A, Ferhadian D, Sowd GA *et al*. Roles of Capsid-Interacting Host Factors in Multimodal Inhibition of HIV-1 by PF74. *J Virol* 90(12), 5808-5823 (2016).
237. Peng K, Muranyi W, Glass B *et al*. Quantitative microscopy of functional HIV post-entry complexes reveals association of replication with the viral capsid. *Elife* 3 e04114 (2014).
238. Matreyek KA, Yucel SS, Li X, Engelman A. Nucleoporin NUP153 phenylalanine-glycine motifs engage a common binding pocket within the HIV-1 capsid protein to mediate lentiviral infectivity. *PLoS Pathog* 9(10), e1003693 (2013).
239. Bhattacharya A, Alam SL, Fricke T *et al*. Structural basis of HIV-1 capsid recognition by PF74 and CPSF6. *Proc Natl Acad Sci U S A* 111(52), 18625-18630 (2014).
240. Price AJ, Jacques DA, Mcewan WA *et al*. Host cofactors and pharmacologic ligands share an essential interface in HIV-1 capsid that is lost upon disassembly. *PLoS Pathog* 10(10), e1004459 (2014).
241. Yamashita M, Engelman AN. Capsid-Dependent Host Factors in HIV-1 Infection. *Trends Microbiol* 25(9), 741-755 (2017).
242. Shi J, Zhou J, Halambage UD *et al*. Compensatory substitutions in the HIV-1 capsid reduce the fitness cost associated with resistance to a capsid-targeting small-molecule inhibitor. *J Virol* 89(1), 208-219 (2015).
243. Zhou J, Price AJ, Halambage UD, James LC, Aiken C. HIV-1 Resistance to the Capsid-

Targeting Inhibitor PF74 Results in Altered Dependence on Host Factors Required for Virus Nuclear Entry. *J Virol* 89(17), 9068-9079 (2015).
244. Lamorte L, Titolo S, Lemke CT *et al*. Discovery of novel small-molecule HIV-1 replication inhibitors that stabilize capsid complexes. *Antimicrob Agents Chemother* 57(10), 4622-4631 (2013).
245. Sticht J, Humbert M, Findlow S *et al*. A peptide inhibitor of HIV-1 assembly in vitro. *Nat Struct Mol Biol* 12(8), 671-677 (2005).
246. Barklis E, Alfadhli A, Mcquaw C *et al*. Characterization of the in vitro HIV-1 capsid assembly pathway. *J Mol Biol* 387(2), 376-389 (2009).
247. Zhang H, Zhao Q, Bhattacharya S *et al*. A cell-penetrating helical peptide as a potential HIV-1 inhibitor. *J Mol Biol* 378(3), 565-580 (2008).
248. Bocanegra R, Nevot M, Domenech R *et al*. Rationally designed interfacial peptides are efficient in vitro inhibitors of HIV-1 capsid assembly with antiviral activity. *PLoS One* 6(9), e23877 (2011).
249. Garzon MT, Lidon-Moya MC, Barrera FN *et al*. The dimerization domain of the HIV-1 capsid protein binds a capsid protein-derived peptide: a biophysical characterization. *Protein Sci* 13(6), 1512-1523 (2004).
250. Zhang H, Curreli F, Zhang X *et al*. Antiviral activity of alpha-helical stapled peptides designed from the HIV-1 capsid dimerization domain. *Retrovirology* 8 28 (2011).
251. Chen NY, Zhou L, Gane PJ *et al*. HIV-1 capsid is involved in post-nuclear entry steps. *Retrovirology* 13 28 (2016).
252. Vozzolo L, Loh B, Gane PJ *et al*. Gyrase B inhibitor impairs HIV-1 replication by targeting Hsp90 and the capsid protein. *J Biol Chem* 285(50), 39314-39328 (2010).
253. Kortagere S, Madani N, Mankowski MK *et al*. Inhibiting early-stage events in HIV-1 replication by small-molecule targeting of the HIV-1 capsid. *J Virol* 86(16), 8472-8481 (2012).
254. Kortagere S, Xu JP, Mankowski MK, Ptak RG, Cocklin S. Structure-activity relationships of a novel capsid targeted inhibitor of HIV-1 replication. *J Chem Inf Model* 54(11), 3080-3090 (2014).
255. Lemke CT, Titolo S, Goudreau N, Faucher AM, Mason SW, Bonneau P. A novel inhibitor-binding site on the HIV-1 capsid N-terminal domain leads to improved crystallization via compound-mediated dimerization. *Acta Crystallogr D Biol Crystallogr* 69(Pt 6), 1115-1123 (2013).
256. Wang W, Zhou J, Halambage UD *et al*. Inhibition of HIV-1 Maturation via Small-Molecule Targeting of the Amino-Terminal Domain in the Viral Capsid Protein. *J Virol* 91(9), (2017).
257. Thenin-Houssier S, De Vera IM, Pedro-Rosa L *et al*. Ebselen, a Small-Molecule Capsid Inhibitor of HIV-1 Replication. *Antimicrob Agents Chemother* 60(4), 2195-2208 (2016).
258. Ali SA, Teow SY, Omar TC, Khoo AS, Choon TS, Yusoff NM. A Cell Internalizing Antibody Targeting Capsid Protein (p24) Inhibits the Replication of HIV-1 in T Cells Lines and PBMCs: A Proof of Concept Study. *PLoS One* 11(1), e0145986 (2016).
259. Perrier M, Bertine M, Le Hingrat Q *et al*. Prevalence of gag mutations associated with in vitro resistance to capsid inhibitor GS-CA1 in HIV-1 antiretroviral-naive patients. *J Antimicrob Chemother* 72(10), 2954-2955 (2017).
260. Winston C. Tse JOL, Andrew Mulato, Anita Niedziela-Majka, William Rowe, John R. Somoza, Armando G. Villasenor, Stephen R. Yant, Jennifer R. Zhang, Jim Zheng

Discovery of Novel Potent HIV Capsid Inhibitors with Long-acting Potential. *Conference on Retroviruses and Opportunistic Infections* 38-New HIV Drugs, Formulations, Combinations, and Resistance (2017).